Receiver Design for Multi-Carrier Transmission Systems in the Presence of Imperfections

Muhammad Asim Ali

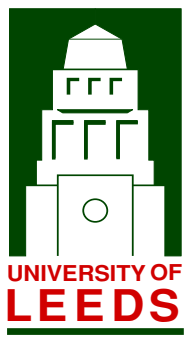

Submitted in accordance with the requirements for the degree of

Doctor of Philosophy

School of Electronic & Electrical Engineering,

University of Leeds.

19th December 2013

Declaration

The candidate confirms that the work submitted is his/her own, except where work which has formed part of jointly authored publications has been included. The contribution of the candidate and the other authors to this work has been explicitly indicated below. The candidate confirms that appropriate credit has been given within the thesis where reference has been made to the work of others. It is to assert that the candidate has contributed solely to the technical part of the joint publications under the guidance of his academic supervisors. Detailed breakdown of the publications is presented in the first chapter of this thesis.

Muhammad Asim Ali

This thesis is dedicated to my parents.

Acknowledgements

First and foremost I would like to thank Almighty Allah for the countless blessings He has bestowed upon me. I would like to thank the management of my sponsor Sukkur Institute of Business Administration for providing me the opportunity to pursue my studies. Sukkur IBA administration has supported me financially despite critical budget shortages. I would like to express my gratitude and love to my parents for their patience, unconditional love, support and encouragement. I would also like to express my deepest love and thanks to my wife and children for their understanding and patience over all these long years.

I would like to express my thanks to Dr Des McLernon for his kind mentoring and support both in an academic and personal capacity. His approach to solving complex problems through basic principles is one of the most important skills that I have acquired over these years. I would also like to thank Prof. Mounir for his constant support and guidance in refining and improving my work.

Last, but certainly not least, I would like to thank my colleagues in I3S for their wonderful company and making my stay as much fun as it possibly could be.

Abstract

Recent personal mobile communication standards have pushed for sophisticated modulation techniques which offer higher data throughput with minimal complexity in channel estimation and equalization. To achieve this objective mobile terminals require high quality performance from RF front-end devices.

Heterodyne receivers have been a widely preferred choice for RF front-ends. Although these receivers have no performance issues however they are not monolithically integratable and therefore cannot be miniaturized.

Direct conversion receivers have been around for almost a century but they have not been widely used because of their sensitivity to image problems. Further loss in the quality of RF front-ends can lead to problems like phase noise, carrier frequency offset and direct current offset. The large dynamic range of modulated signals can also be subject to the non-linear behaviour of high power amplifiers.

In the presence of all these constraints, it has been of significant research interest to explore robust techniques to jointly estimate channel and RF front-end non-idealities. The objective of this thesis is to explore low complexity schemes which take care of the imperfections present in the RF front-ends at the expanse of minimal computational complexity. The proposed schemes operate coherently to estimate the channel impulse response and other imperfections thus allowing us to reduce the constraints on analog components.

Finally, the proposed schemes are designed arround the wireless local area network standards and therefore blend seamlessly into the overall system.

Notation

$\mathbf{a}$	Small bold-faced letter defines a vector
$\mathbf{A}$	Capital bold-faced letter defines a matrix
$\mathbf{h}$	channel impulse response
$\mathbf{\Lambda}_h$	Diagonal channel frequency response matrix
$\mathbf{H}_c$	Circulant channel impulse response matrix
E_b/N_0	Energy per bit to noise ratio
E_s/N_0	Energy per symbol to noise ratio
σ_n^2	Noise variance
σ_x^2	Signal variance
σ_h^2	Sub-carrier channel variance
$\mathbf{\Pi}/\mathbf{\Pi}^{-1}$	Cyclic prefix insertion / removal matrix
L_h	Channel impulse response length
L_g	Mismatch filter impulse response length
N	OFDM symbol size
M	Bits per data symbol
N_g	Length of cyclic prefix (Guard interval)
T	OFDM symbol duration
T_s	Sampling interval
$\mathbf{F}$	DFT matrix of size $N \times N$
$\mathbf{Q}$	Permutation matrix of size $N \times N$ ($\mathbf{Q}$=$\mathbf{F}\mathbf{F}^T$)
$\mathbf{I}_N$	Identity matrix of size $N \times N$
$[\mathbf{W}\|\mathbf{V}]$	Subcomponents of DFT matrix of size $N \times L$ and $N \times (N-L)$ respectively
$\mathbf{s}$	OFDM transmitted data
$\mathbf{x}$	OFDM transmitted modulated signal
$\mathbf{r}$	OFDM received signal at RF front-end
$\mathbf{y}$	OFDM received signal before demodulation
$\mathbf{y}_f$	OFDM received signal after demodulation
$\hat{a}$	Estimate of a
$\underline{\mathbf{a}}$	$[\mathbf{a}^{I^T}; \mathbf{a}^{Q^T}]^T$
$\bar{\mathbf{a}}$	$[\mathbf{a}^{(1)^T}; \mathbf{a}^{(2)^T}]^T$
ϵ	Normalized carrier frequency offset

Δf	Actual carrier frequency offset (Hz)
p_j	j-th harmonic of PN interference
d_0	Direct current offset
η	Amplitude imbalance coefficient
θ	Phase imbalance coefficient
β_0	LO 3dB phase noise BW
p	Amplifier non-linearity coefficient
CL	Clipping Level
$g_T(t)$	Transmit pulse shape filter
$g_R(t)$	Receive low pass filter
$h^{D/I}(t)$	Desired / Interfering CIR in presence IQ imbalance
$\underrightarrow{\mathbf{h}}_{\mu/\nu}$	Modified desired / interfering CIR in presence of IQ imbalance and CFO
A_{Max}	Maximum unclipped amplitude of transmitted signal
$f(\cdot)$	Amplitude distortion function of amplifier nonlinearity
$\mathbf{\Phi}(\cdot)$	Phase distortion function of amplifier non-linearity
$g(\cdot)$	Overall transfer function of amplifier non-linearity
$\mathbf{E}$	PN or CFO process matrix
$\mathbf{P}$	Frequency domain equivalent circulant matrix associated with PN or CFO process
$\mathbf{\Theta}$	Linear interpolation matrix
$\odot$	Kronecker product
$\otimes$	Continuous time convolution
$(\cdot)^{I/Q}$	Real or imaginary component of a complex variable
$\Re\{\cdot\}/\Im\{\cdot\}$	Real or imaginary component of a complex variable
$(\cdot)^H$	Hermition operator
$(\cdot)^*$	Complex Conjugate operator
$(\cdot)^T$	Transpose operator
diag$(\cdot)$	Converts a vector into a diagonal matrix

Note: This is a set of basic variables, etc., used through this thesis. Notations specific to an individual chapter are defined inside the chapter.

Abbreviations

A/D	Analog to digital
AWGN	Additive white Gaussian noise
BER	Bit error rate
CFO	Carrier frequency offset
CFR	Channel frequency response
CIR	Channel impulse response
CL	Clipping level
CLFE	Closed form expression
CP	Cyclic prefix
CPR	Common phase rotation
D/A	Digital to analog
DC	Direct conversion structure
DCO	Direct current offset
DCR	Direction conversion receiver
FF	Frequency flat
FI	Frequency independent
FIR	Finite impulse response
FFT	Fast Fourier Transform
FS	Frequency selective
GS	Grid search
HPA	High power amplifier
IFFT	Inverse Fast Fourier Transform
ICI	Inter carrier interference
IIR	Infinite impulse response
IRF	Image reject filter
IRR	Image rejection ratio
ISI	Inter symbol interference
LMS	Least mean squares
LNA	Low noise amplifier
LO	Local oscillator
LS	Least squares
LTI	Linear time-invariant
LTV	Linear time-variant

LTS	Long training sequences
MIMO	Multi-input multi-out
ML	Maximum likelihood
MMSE	Minimum mean square error
MSE	Mean square error
NL	Non-linearity
NLLS	Non-linear least squares
OFDM	Orthogonal frequency division multiplexing
PAPR	Peak-to-average-power ratio
PLL	Phase locked loop
PN	Phase noise
QAM	Quadrature amplitude modulation
RCS	Reduced complexity scheme
RF	Radio frequency
RLS	Recursive least squares
Rx	Receiver
SCCP	Single carrier cyclic prefix
SCFDE	Single carrier frequency domain equalization
SCUW	Single carrier unique word
SL	Soft limiter
SNR	Single to noise ratio
SSPA	Solid state power amplifier
TWTA	Travelling wave tube amplifier
Tx	Transmitter
WLAN	Wireless local area network
Z-IF	Zero intermediate frequency structure
ZF	Zero forcing equalizer

Contents

List of Figures

1 Introduction

The advent of mobile communication systems has revolutionized the lives of billions of people world-wide. The ever increasing demand for higher data rates has pushed the technology for sophisticated modulation techniques which support simplified channel estimation and equalization. It is imperative that the hardware cost be kept to a minimum and this is only possible when the system can tolerate the non-ideal effects originating from lower quality analog components such as the local oscillator (LO), mixers, analog filters and high power amplifiers (HPA).

From the study of contemporary literature it is well known that the most costly section of digital transmitter and receiver systems is the set of analog components such as the LO, quadrature mixers, analog filters and HPA systems. The conventional transmitter/receiver module is based on the heterodyne architecture which uses multi-stage mixers to transfer the baseband signal to the radio frequency (RF) domain and vice versa. These systems effectively avoid the interfering image signal. However these structures require several mixing stages in addition to analog bandpass filters. These analog components have a sizeable foot print on the printed circuit board which cannot be conveniently miniaturized. Another important issue pertaining to heterodyne receivers is the power consumed by these analog components which puts pressure on the precious battery resources.

The direct conversion (DC) structure were first proposed in 1920's [3]. These structures are monolithically integratable on printed circuit boards. Despite its simple structure with minimal analog components, this architecture has not been a preferred choice of transmission systems because of the problems with LO, non-ideal mixers, near-far effects and the HPA.

More recently, a lot of research has been directed towards designing simple and robust algorithms which can compensate the effects of the non-idealities of analog components in the digital domain. This in turn allows for a small footprint, a lesser number of analog components, lower power consumption and, most important of all, reduces the cost of mobile devices.

1.1 Scope of this Thesis

The objective of this work is to design simple yet robust signal processing techniques which can combat the imperfections present in the analog front-end devices. This problem has been an area of active research for the past several years yet robust solutions which can seamlessly encompass all of the physical limitations are still not in sight.

As illustrated in Fig. 1.1, the ultimate objective of this thesis is to estimate the channel impulse response (CIR) in conjunction to all of these imperfections. Because, when we have these imperfections, channel estimation is rendered inaccurate. Therefore a higher system throughput cannot be achieved, even in a high SNR environment.

Within the scope of this work a typical transmission system has been considered in the presence of carrier frequency offset (CFO), phase noise (PN), direct current offset (DCO), IQ imbalance (also commonly known as IQ mismatch) and amplifier non-linearity. When using DC architecture the IQ imbalance can exist in either transmitter/receiver or in both sides at the same time. The IQ imbalance can be categorized into a frequency selective (FS) or a frequency independent (FI)[1] model depending on the spectral bandwidth occupied by the system. Although this is not an exhaustive set of problems facing a digital communication system these parameters have serious implications on the overall performance of the system.

This work is limited to block multi-carrier transmissions systems, mainly because schemes like WLAN, WiMAX have found wider industrial recognition and design of smart transceivers which can operate in the presence of serious imperfections would greatly benefit this market.

Mobility is also a common problem in wireless communication systems but it has not been considered within the scope of this work, i.e. the CIR is assumed to be constant over a block of symbols.

[1] In literature the term frequency independent is also referred to as frequency flat(FF)

There exist several types of LO classified mainly on the basis of presence or absence of a phase lock loop (PLL). The model of the LO without PLL, also known as a free-running oscillator, is considered to study the effects of PN. As illustrated in Fig.1.1 this thesis considers the effects of IQ mismatch present in both the transmitter and the receiver. This thesis also distinguishes between FS or FI models of IQ imbalance. As previously stated, the frequency selectivity of the IQ imbalance depends upon the bandwidth of the system. Fig. 1.1 is used to illustrate the scope of work in the subsequent chapters. The set of imperfections considered in each chapter are marked with black shade.

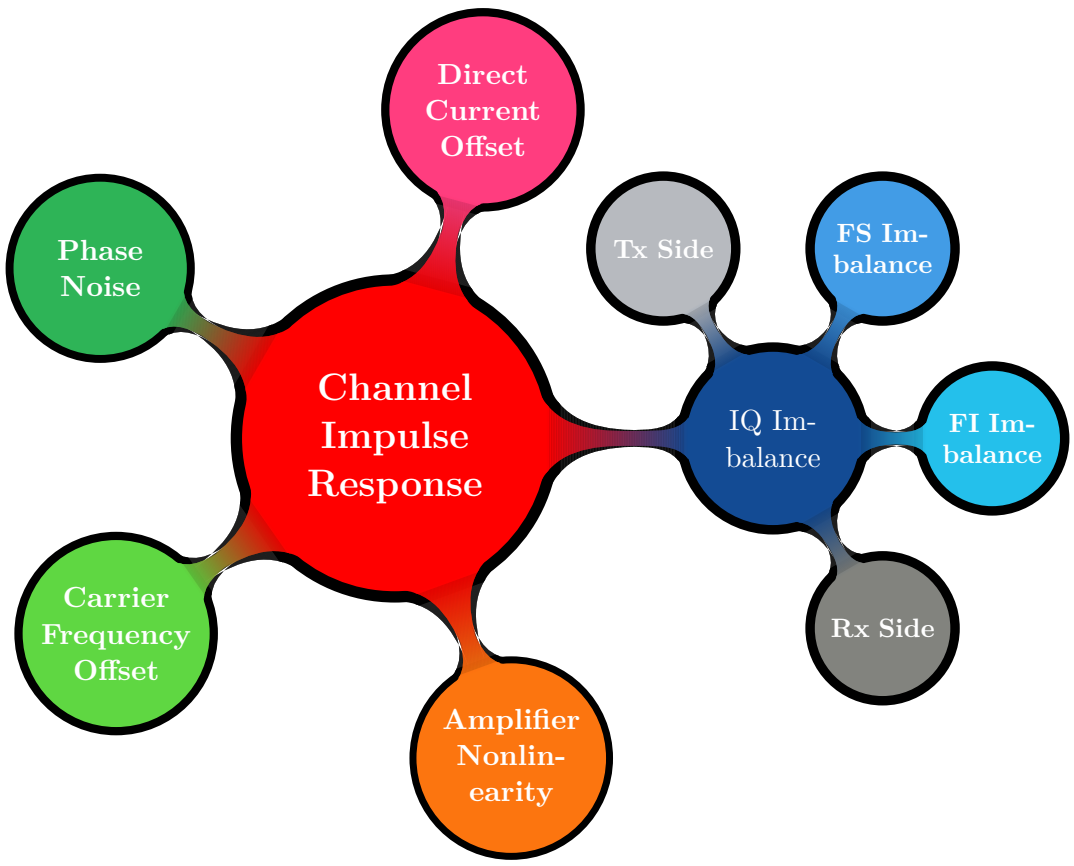

Figure 1.1: Typical (not exhaustive) set of problems encountered at direct conversion transmitter/receiver.

All the results presented in this work are based on simulation results and further investigation is required to assess the performance of these proposed schemes on a suitable hardware platform.

The main objective of this research has been to propose scalable techniques which can jointly estimate multiple parameters from both transmitter and/or receiver in conjunction with channel impulse response with minimal complexity and training. To neutralize these non-ideal effects from the received signal, some low complexity equalization techniques have also been proposed which can compensate for multiple parameters in a single solution.

The estimation of unknown parameters can be performed by transmitting a known pilot signal (training based estimation), through the received signal (blind estimation) or a combination of both techniques. This thesis is mainly focused on pilot based schemes mainly because they are robust in comparison to blind techniques as discussed in Section 2.4.

It is well known that use of channel coding techniques (such as Turbo and LDPC codes) can improve the error correction capability of the transmission system. Here such techniques have not been considered as the primary objective here is to evaluate the performance of proposed estimation and data detection techniques.

1.2 Outline of the Thesis

This thesis deals with a wide spectrum of problems. Several estimation techniques have been studied considering different sets of problems. The chapter-wise composition of this thesis is illustrated in Fig. 1.2.

Chapter 2 provides the preliminary models considered for simulation of transmission system. The detailed mathematical model of the analog front-end imperfections is provided in Section 2.3. A selective review of the solutions available in literature is provided in Section 2.4.

Chapter 3 introduces a simple iterative estimation of channel and FI Tx/Rx IQ imbalance. The system model is defined in 3.2 and the iterative estimation scheme is discussed in Section 3.3. The simulation results are provided in Section 3.5.

Chapter 4 presents a simple closed form expression (CLFE) estimation of CIR, CFO and FI/FS Rx IQ imbalance. The system model is defined in 4.2 and the CFO and modified CIR estimation schemes are discussed in Section 4.3. A simple single stage CFO, CIR and FI/FS IQ imbalance compensation scheme is proposed in Section 4.4. A simple CLFE solution for the system in the presence of DCO in addition to previously considered problems is provided in Section 4.5.

The performance of the proposed scheme is extended to MIMO systems in Section 4.6. The simulation results are provided in Section 4.7.

Chapter 5 extends the model of Chapter 3 to estimate the CIR and the FI Tx/Rx IQ imbalance in the presence of CFO. The system model is defined in 5.2 and the CFO and the modified CIR estimation schemes are discussed in Section 5.3. The simulation results are provided in Section 5.5.

Chapter 6 considers the estimation of the CIR in the presence of an HPA non-linearity at the transmitter and FI IQ imbalance at the receiver. The system model is defined in 6.2 and the estimation schemes are discussed in the subsequent subsection. The simulation results are provided in Section 6.4.

Chapter 7 focuses on the estimation of CIR in the presence of strong PN. The proposed scheme is based on single carrier cyclic prefix (SCCP) type of block transmission system where a fixed and known prefix is used to obtain a better estimate of the PN process. The system model is defined in 7.2 and the estimation schemes are discussed in the subsequent subsection. The simulation results are provided in Section 7.4.

1.3 Contributions of the Thesis

This thesis has touched upon a wide range of problems which are related to the operation of the DC structure. The contributions of this work are listed below.

1. In Section 3.3 a simple iterative FI Tx/Rx IQ imbalance estimation scheme is proposed. The proposed scheme requires only one pilot symbol to obtain reliable estimates of CIR and FI Tx/Rx IQ imbalance coefficients.

2. In Section 4.3.1 and 4.3.2 two scalable solutions to CFO estimation in the presence of FS/FI Rx IQ imbalance and FS CIR are discussed. These solutions provide a performance which is proportionate to the complexity of the receiver. Although numerous solutions have been proposed in the literature, to the best of our knowledge, the complexity and convergence time of the proposed scheme is better than the current state of the art schemes. The scope of this work is extended further by considering DCO in addition to the previously considered set of problems. To equalize the effects of CFO, FI/FS Rx IQ imbalance and FS CIR a low complexity equalizer is also proposed in Section 4.4.

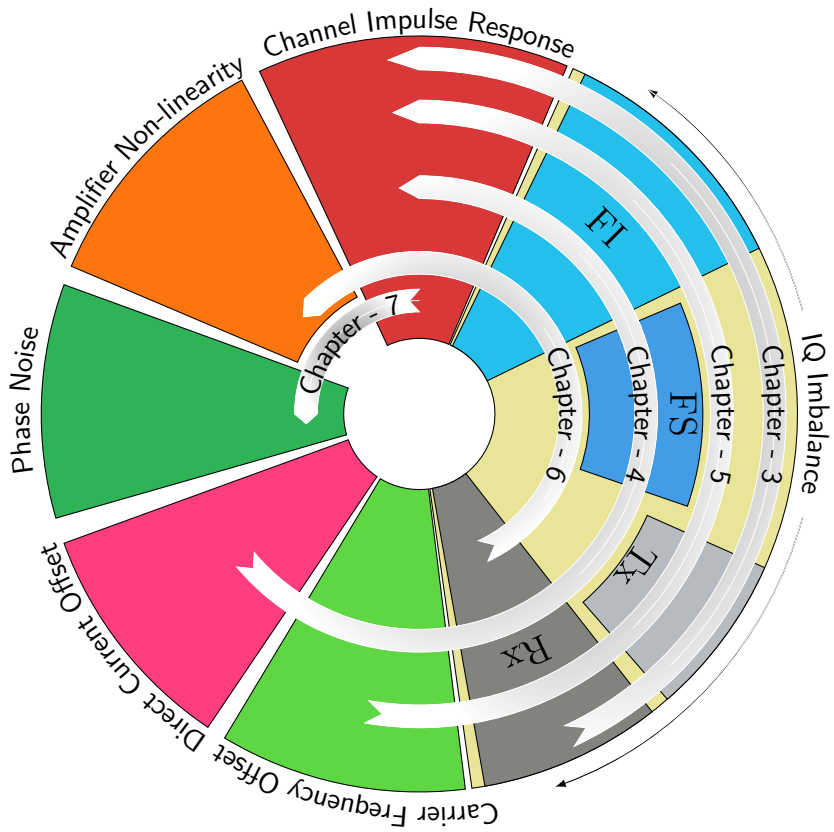

Figure 1.2: The composition of the thesis chapter by chapter.

This solution is extended to a (spatially multiplexed) MIMO transmission model and this implementation and the corresponding data detection solutions are presented in Sections 4.6 and 4.7 respectively.

3. Section 5.3 presents a simple iterative scheme (based on the model presented in Chapter 3 and 4) to estimate FI Tx/Rx IQ imbalance in the presence of CFO and FS CIR. Using the simple schemes proposed in Sections 4.3.1 and 4.3.2 accurate estimates of all the parameters can be easily obtained.

4. Section 6.2 provides a low complexity joint FS CIR, FI Rx IQ mismatch estimation in the presence of a HPA non-linearity. Unlike the existing works available in the literature the proposed solution assumes that the channel and non-linearity coefficients are unknown at the receiver and estimates them using special pilot sequences.

5. Finally in Chapter 7 a simple FS CIR estimation technique has been proposed for SCCP systems. To improve the phase rotation tracking capabilities in the receiver a uniquely known cyclic prefix is adopted and the PN process is compensated using different interpolation techniques.

1.4 List of Publications and Awards

- Muhammad Asim, Mounir Ghogho and Des McLernon, "Mitigation of Phase Noise in Single Carrier Frequency Domain Equalization Systems ", April 1-4, 2012, IEEE WCNC 2012, Paris.

- Muhammad Asim, Des McLernon and Mounir Ghogho, "Receiver Design for OFDM in the Presence of I/Q Imbalance and Amplifier Non-linearity ", September 25-27, 2012, SSPD 2012, London.

- Muhammad Asim, Mounir Ghogho and Des McLernon, "OFDM Receiver Design in the Presence of Frequency Selective IQ Imbalance and CFO", September 9-13, 2013, EUSIPCO 2013, Marrakesch.
  (Nominated for best paper award)

- Muhammad Asim, Des McLernon and Mounir Ghogho, "OFDM Receiver Design in the Presence of both Tx and Rx IQ Imbalance over Frequency Selective Channel", submitted to IEEE Communication Letters.

- Muhammad Asim, Mounir Ghogho and Des McLernon, "OFDM Receiver Design in the Presence of both Tx,Rx IQ Imbalance, Carrier Frequency Offset and Frequency Selective Channel", in preparation (to be submitted to) IEEE Transactions on Vehicular Technology.

2 System Model and Literature Review

As motivated in the previous chapter, the DC architecture is a very attractive choice but it gives rise to serious challenges. In this chapter the problems facing a DC device are discussed one by one and a detailed context is provided in addition to the mathematical model of these problems.

2.1 Transmission System

This section briefly visits the baseband multipath propagation models used for computer simulation. Later on a concise summary of block transmission systems like OFDM and SCCP systems is provided and a basic set of notations are established which are used within the framework of this thesis.

2.1.1 Channel Model

The mobile channel between the transmitter and receiver can be modelled as a linear filter. Different multipath waves have different propagation delays and the length of channel impulse response is determined by the maximum delay spread. The equivalent time-varying baseband channel impulse response is defined as [4]

$$h(t,\tau) = \sum_{v=0}^{V-1} \alpha_v(t) e^{j\theta_v(t)} \delta(\tau - \tau_v(t)) \tag{2.1}$$

where V is the total number of propagation paths; $\alpha_v(t)$ and $\theta_v(t)$ represent amplitude and phase shifts due to the propagation path and $\tau_v(t)$ is the delay spread corresponding to the $t-$th time instance, $\tau = lT_s$, $l=0,\ldots,L_h-1$ and $(L_h-1)T_s=\tau_{V-1}$; where L_h is the maximum delay spread of the multipath signal.

Throughout this thesis an equivalent complex, baseband, discrete-time channel model has been used. This complex equivalent representation allows us to employ a simplified mathematical modelling and analysis of digital communication systems. The detailed description of channel modelling can be found in [4,5]. Within the scope of this thesis only a stationary linear time-invariant (LTI) channel model has been considered.

$$h[l] = \sum_{v=0}^{V-1} \alpha_v e^{j\theta_v} \delta(l - l_v) \qquad l_v = 0, \cdots, L_h - 1 \tag{2.2}$$

For the small scale channel modelling, the power delay profile is determined through the statistical characteristics of the environment. In implementation, the power delay profile of the equivalent baseband channel is assumed to be exponential. The received signal in the presence of a frequency selective channel and additive noise is defined as

$$y[n] = \sum_{l=0}^{L_h-1} h[l]x[n-l] + n[n] \quad n = 0, \cdots, N-1 \tag{2.3}$$

where $n[n]$ is the additive white Gaussian noise which is complex and circulantly symmetric i.e. $n[n] \sim \mathcal{CN}(0, \sigma_n^2)$. For general block transmission system the SNR is defined as

$$\text{SNR} = \frac{MN_D}{N + N_g} \cdot \frac{E_b}{N_0} \tag{2.4}$$

where M is the modulation index ($M = \log_2 \mathcal{S}$) $\mathcal{S}$ being the size of constellation; N, N_D, N_g are respectively the number of total subcarriers, data subcarriers and the length of guard samples. If the symbol energy is assumed to be normalized such that $E_s = ME_b = 1$ then the noise variance can be calculated as

$$\sigma_n^2 = 10^{-\left(\frac{\text{SNR}_{\text{dB}}}{10}\right)} \tag{2.5}$$

where SNR_{dB} is the logarithmic value of the SNR as defined in (2.4) and $\sigma_n^2 = N_0 \cdot N_D/N + N_g$. In the following subsections a brief introduction to the block transmission systems is provided and the basic notation is introduced which will be followed throughout the thesis.

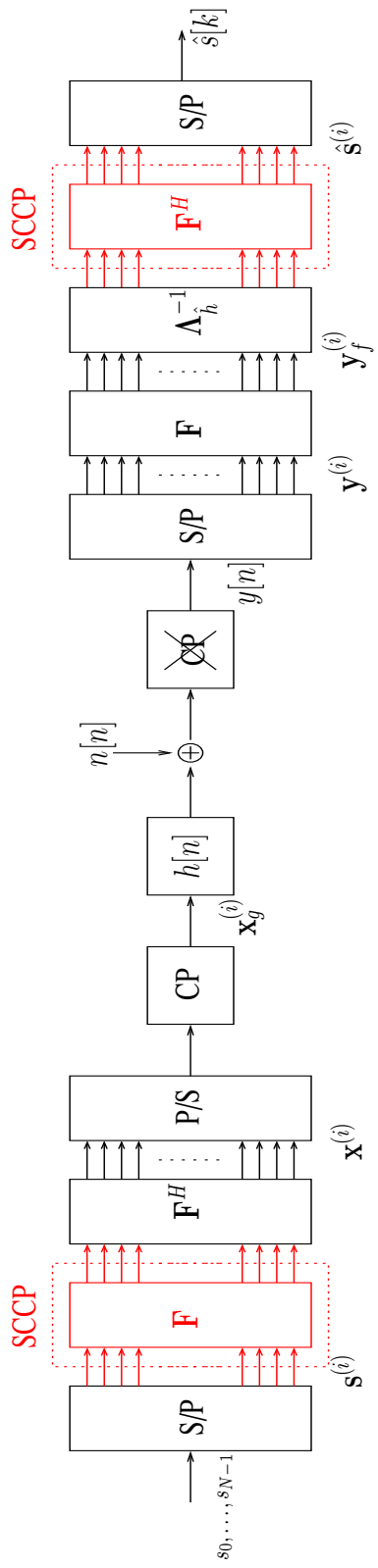

Figure 2.1: Simplified structure of block transmission systems (OFDM and SCCP), with the assumption that the dimensions of additional DFT/IDFT operators is exactly the same. The components in red are specific to only SCCP systems.

2.1.2 OFDM Transmission System

OFDM systems [6–8] have found wide acceptance in all facets of the digital communication systems. This modulation technique has been applied from high speed wire-line networks to digital audio and video broadcasts. More recently, WLAN (which employs OFDM) has gathered significant attention as a de-facto wireless transmission standard for small area networks, despite the fact that OFDM is very sensitive to problems arising from transmitter/receiver non-idealities (discussed later), timing and frequency synchronization issues. It has found application mainly because of cost effective hardware implementation. OFDM and other structured transmission systems operate on fixed number of data samples chosen from the QAM constellation, commonly referred to as a *symbol*. The equivalent, continuous-time OFDM modulated signal is defined as

$$x(t) = \sum_{i} \sum_{k=0}^{N-1} s^{(i)}[k] g_k(t - iT) \tag{2.6}$$

where $s^{(i)}[k]$ is the data symbol corresponding to the $k-$th subcarrier of the i-th OFDM symbol and $g_k(t)$ is the pulse shaping filter corresponding the k-th subcarrier which is defined as

$$g_k(t) = e^{j\frac{2\pi kt}{T}} \text{rect}(t/T). \tag{2.7}$$

The data modulated on each subcarrier is orthogonal since

$$\frac{1}{T} \int_0^T g_k(t) \cdot g_m^*(t) dt = \delta[k - m]. \tag{2.8}$$

The modulation process can also be described in compact vector notation. The vector symbol corresponding to i-th OFDM symbol is defined as

$$\mathbf{s}^{(i)} = [s^{(i)}[0], s^{(i)}[1], \cdots, s^{(i)}[N-1]]^T. \tag{2.9}$$

This vector could also contain several null (*unloaded*) subcarriers. The data samples now modulated on an orthogonal set of subcarriers. The modulation operation is essentially performed via inverse IDFT. The computationally efficient way of doing this is the inverse fast Fourier transform (IFFT),

$$\mathbf{x}^{(i)} = \mathbf{F}^H \mathbf{s}^{(i)} \tag{2.10}$$

where $\mathbf{F}^H$ is the IDFT matrix and $\mathbf{F}[j,k]{=}1/\sqrt{N}e^{-\frac{2\pi}{N}jk}$ with $j,k{=}0,\cdots,N-1$. This signal can then be up converted to RF domain and transmitted over the air interface. In the presence of a frequency selective channel the i-th OFDM symbol would interfere with $i{+}1$-th OFDM symbol. To avoid this situation a certain number of guard-samples are inserted at the start of each OFDM symbol. They are commonly known as the *guard interval* or *cyclic prefix* (CP). A CP is actually the insertion of the last N_g samples of the OFDM symbol at the beginning of the symbol,

$$\mathbf{x}_g^{(i)} = \left[x^{(i)}[N{-}N_g], x^{(i)}[N{-}N_g{-}1], \ldots, x^{(i)}[N{-}1], x^{(i)}[0], \ldots, x^{(i)}[N{-}1]\right]^T. \tag{2.11}$$

From now on OFDM symbol index (i) is ignored when no confusion can be caused. In the presence of an appropriate cyclic prefix the convolution of the OFDM symbol with the channel impulse response can be considered as a circulant convolution when CP is removed at the receiver. The input/output model of the OFDM system with a frequency selective channel and additive white Gaussian noise is defined in matrix notation as

$$\begin{bmatrix} y[0] \\ y[1] \\ y[2] \\ \vdots \\ \vdots \\ \vdots \\ y[N{-}1] \end{bmatrix} = \begin{bmatrix} h[0] & 0 & \cdots & h[L_h{-}1] & h[L_h{-}2] & \cdots & h[1] \\ h[1] & h[0] & \ddots & 0 & h[L_h{-}1] & \ddots & h[2] \\ \vdots & \ddots & \ddots & & & \ddots & \vdots \\ \vdots & \ddots & \ddots & & & & h[L_h{-}1] \\ h[L_h{-}1] & \ddots & \ddots & & & & 0 \\ 0 & 0 & \ddots & & & \ddots & \vdots \\ 0 & 0 & \ddots & & & h[0] & 0 \\ 0 & 0 & \cdots & & \ldots & & h[0] \end{bmatrix} \cdot \begin{bmatrix} x[0] \\ x[1] \\ x[2] \\ \vdots \\ x[N{-}1] \end{bmatrix} + \begin{bmatrix} n[0] \\ n[1] \\ n[2] \\ \vdots \\ n[N{-}1] \end{bmatrix}. \tag{2.12}$$

(2.12) can be compactly written as

$$\mathbf{y} = \mathbf{H}_c\mathbf{x} + \mathbf{n} \tag{2.13}$$

where $\mathbf{H}_c$ is an $N\times N$ column circulant matrix (as defined in (2.12)). From [9] (Ch.6 pg. 298) it is known that any circulant matrix can be diagonalized by left and right multiplication with DFT and IDFT matrices,

$$\mathbf{\Lambda}_h := \mathbf{F}\mathbf{H}_c\mathbf{F}^H \tag{2.14}$$

where $\mathbf{\Lambda}_h$ is the diagonal matrix created from channel frequency response (CFR) $\mathbf{\Lambda}_h = \text{diag}(H[0],\ldots,H[N-1])$ with $H[k]$ being CFR on the k-th subcarrier. Now, the overall received signal can be written as

$$\mathbf{y}_f = \mathbf{F}(\mathbf{H_c}\mathbf{F}^H\mathbf{s} + \mathbf{n}). \tag{2.15}$$

The complete transmission scheme of the OFDM system is illustrated in Fig. 2.1. The channel estimation is an important part of the receiver system. In literature the simplest solution is to estimate the unknown channel by transmitting a known pilot sequence. The channel coefficients are obtained using a simple least squares (LS) solution as

$$\hat{\mathbf{h}} = \left(\mathbf{X}^H\mathbf{X}\right)^{-1}\mathbf{X}^H\mathbf{y}_f \tag{2.16}$$

where $\mathbf{h}$ is the CIR vector of size $L_h\times 1$, $\mathbf{X}$:=$\mathbf{SW}$ with $\mathbf{S}$ is the $N\times N$ diagonal matrix of the known pilot symbol and $\mathbf{W}$ is the $N\times L_h$ component of the DFT matrix (i.e. $\mathbf{W}[k,l]$=$1/\sqrt{N}e^{-j\frac{2\pi kl}{N}}$). This solution provides an accurate estimation of the LTI channel (in time domain) but may suffer from noise amplification in low SNR conditions. However many works in the literature have also proposed to use comb-pilot structure for estimation of the channel coefficients.

The modulation of data on orthogonal subcarriers (as illustrated in Fig. 2.2) allows us to pack data samples close together without interfering with each other, but in the case when this orthogonality is lost the performance of the OFDM system is severely degraded. The biggest advantage of OFDM system is the higher data-rate and simplicity of equalization, unlike the Viterbi decoder used for maximum likelihood sequence estimation in time domain for single carrier systems which requires exhaustive search over all possible scenarios. For an OFDM system a simple one-tap equalizer is the optimal equalizer in the maximum likelihood sense.

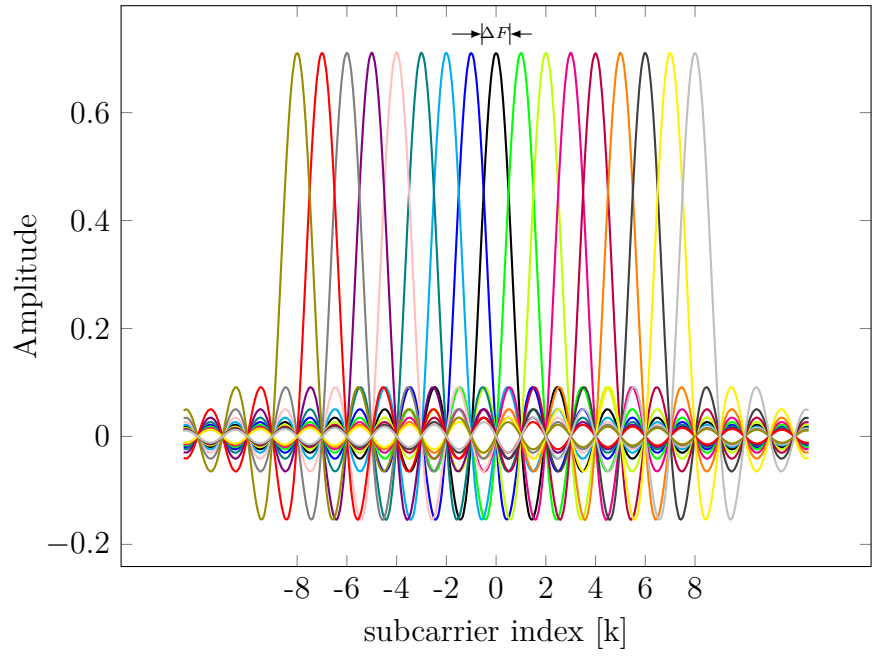

Figure 2.2: The spectral representation of the OFDM signal.

2.1.3 SCCP Transmission System

OFDM transmission systems offer a simple modulation, demodulation with efficient implementation using the FFT/IFFT. However, this system may suffer from serious performance degradation because of the dynamic range of the transmitted signal. The system is also very sensitive to other non-idealities of the transceiver architecture in addition to time and frequency synchronization issues. A very interesting solution proposed in the literature which has gained a lot of attention lately is the *single carrier cyclic prefix* (SCCP) transmission scheme [10–12]. In the literature the SCCP scheme is also known as the *single-carrier frequency domain equalization* (SC-FDE) transmission scheme. A simplified block diagram implementation of this scheme is illustrated in Fig. 2.1. The additional components which are associated with SCCP are highlighted in red. For simplicity, this work assumes that the size of all DFT and IDFT operations is of the same dimension (this is generally not the case in practice). The SCCP system offers several features in comparison to OFDM systems. For example it suffers from high dynamic range problem to a lesser extent, SCCP is also relatively less sensitive to IQ mismatch and carrier frequency offset [13]. More recently this scheme has been standardized in LTE as an uplink transmission scheme.

Unlike OFDM systems no modulation is performed on the transmitter side and each block of data symbols is appended with the CP and transmitted to the receiver. The receiver converts the signal into the frequency domain and the equalization is performed in the frequency domain and then the signal is converted back into time domain. This process is illustrated in Fig. 2.1.

The *zero-forcing* ZF equalization of the received signal (for the case when IFFT and FFT sizes in the transmitter are same) is described as follows [14].

$$\hat{\mathbf{s}} = \mathbf{F}^H \mathbf{\Lambda}_h^{-1} \mathbf{F} \mathbf{y}. \tag{2.17}$$

2.2 Up/Down Conversion Structures

The up and down conversion of the transmitted and the received signal is performed using dedicated RF front-end devices. In the literature these devices are categorized into two types based on the number of conversion stages involved in the process. The *hetero-dyne* structures involve two or more stages in conversion while *homodyne* structures perform conversion within a single stage. The heterodyne structures (as shown in Fig.2.3(a)) have been widely adapted as a preferred choice of RF front-end because of their better *selectivity* and *sensitivity* characteristics [2]. The hetero-dyne structures are not sensitive to IQ-imbalance because the LO operating at the second stage is 2 magnitudes less and while the desired signal is being amplified the interfering image signal is suppressed at each stage.

A typical homodyne structure is illustrated in Fig.2.3(b). A direct conversion structure extends the intermediate frequency to zero frequency. It is for this reason these structures do not require an image reject filter (IRF). Since IRFs are not needed, this architecture is more suitable to monolithic integration.

The graphical illustration of the image problem caused by the direct conversion receiver is presented in Fig. 2.4. The undesired/interfering image signal $r_f^*[\cdot]$ present at the image frequency $-f_c$ is also down-converted to the baseband. In the case of perfectly balanced quadrature mixer this image signal can be filtered-out completely. However, in the presence of IQ imbalance a residue image signal will be present at the output of a direct conversion receiver (more detail is provided in section 2.3.3).

In the literature several single stage devices have been proposed, namely the Weaver and the Hartley architectures [2], but as pointed out in the reference all these devices suffer from image problems.

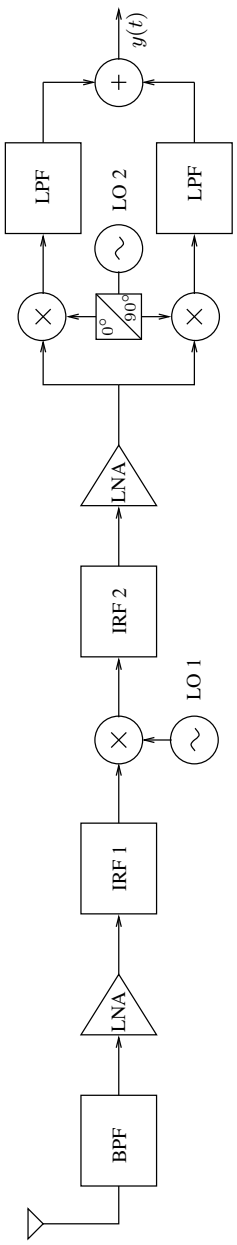

(a) The heterodyne receiver structure

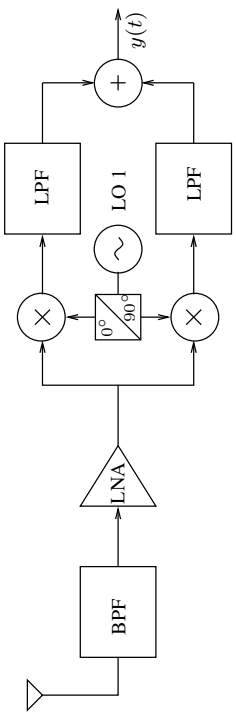

(b) The homodyne receiver structure

Figure 2.3: Simplified block diagram of receiver structures.

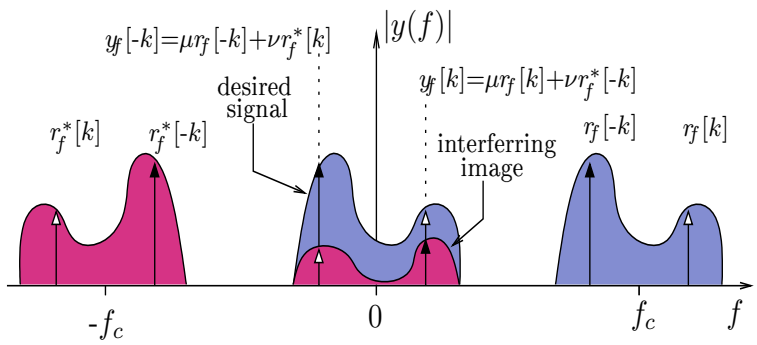

Figure 2.4: The effect of image interference in a direct conversion receiver [1].

Now that a basic frame-work of block transmission system has been established in the next section a detailed account of a limited (selected) set of analog imperfections is provided. These imperfections inflict serious problems on the performance of the transmission systems and are primarily associated with DC structures.

2.3 Transmitter and Receiver Imperfections

In [2, 15], the authors have highlighted the challenges and the opportunities presented by DC architecture. Although heterodyne structures are a reliable choice for transmission and reception, however the sizeable number of analog components required in the design of these blocks means that their foot print cannot be reduced and all this performance comes at a cost which cannot be minimized further. Direct conversion receivers were proposed in 1920's [3] but their sensitivity to the characteristics of the analog components have prevented them from being used widely. More recently, with the advent of powerful signal processing capabilities at the disposal of receiver, it has become possible to deal with these problems using sophisticated signal processing techniques.

The typical system model considered within the scope of this work is illustrated in Fig. 2.5. The transmit and receive IQ imbalance occurs due to amplitude and phase imbalance in the quadrature mixers. If the transmit pulse shaping filters and/or receiver low pass filters in the quadrature arms of the transceiver are not balanced, this gives rise to frequency selective IQ imbalance. The phase noise can also exist in both transmitter and receiver sides. As demonstrated in [16] the transmit and receiver phase noise can be combined as an equivalent

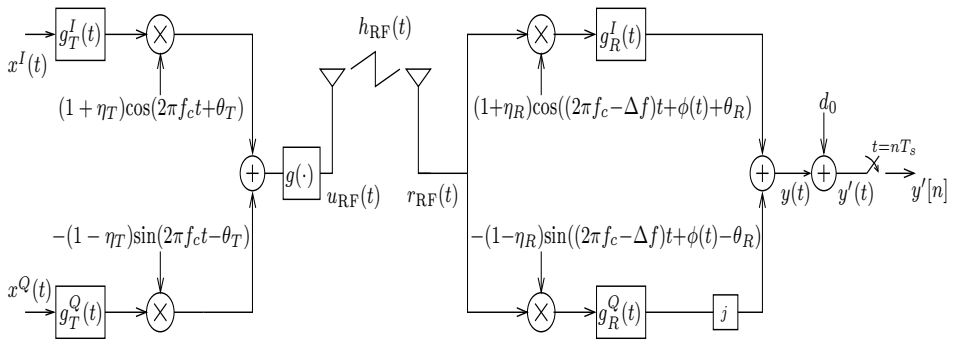

Figure 2.5: Transmission system in the presence of transmitter and receiver imperfections.

(approximate) PN process at the receiver. However, only receiver phase noise is considered here. The direct current offset is also assumed to be effecting only the receiver side. Although the effects of non-linear amplification do exist both at the transmitter and the receiver, it is assumed to be present at the transmitter side only.

The following subsections provide a concise description of these problems and illustrate their effects on multi-carrier transmission systems. Although it is of immense importance to study the precise electrical structures of all these devices, these studies are limited only to the equivalent mathematical models of the problems under consideration.

2.3.1 Phase Noise

Phase noise (PN) appears because of the instability of the LO. PN is a random walk of the phase ($\phi(t)$) of the LO output signal, often modelled by Brownian motion or a Weiner process. The spectrum of an LO with phase jitter is modelled as a Lorentzian power spectrum. The PSD of this spectral leakage has been parameterized in [17]. The PN model discussed here is specific to a free-running oscillator only and is not valid for a phase locked loop (PLL) based model. Although PLL base LO are used widely and are prone to PN problem to a lesser extent but free-running oscillator have been considered in this work mainly because of their simple mathematical model. In the equivalent discrete-time domain the n^{th} PN sample is related to the previous sample via

$$\phi[n] = \phi[n-1] + w[n] \tag{2.18}$$

where $\phi[n]$ is the equivalent, baseband, discrete-time representation of the continuous PN process illustrated in Fig. 2.5, $w[n] \sim \mathcal{N}(0, \sigma_w^2)$, with $\sigma_w^2 = 2\pi\beta_0 T_s$, T_s is the sampling interval and β_0 is defined as the two-sided 3-dB bandwidth of the PN process. The equivalent discrete-time realization of the PN process is illustrated in Fig. 2.6(a).

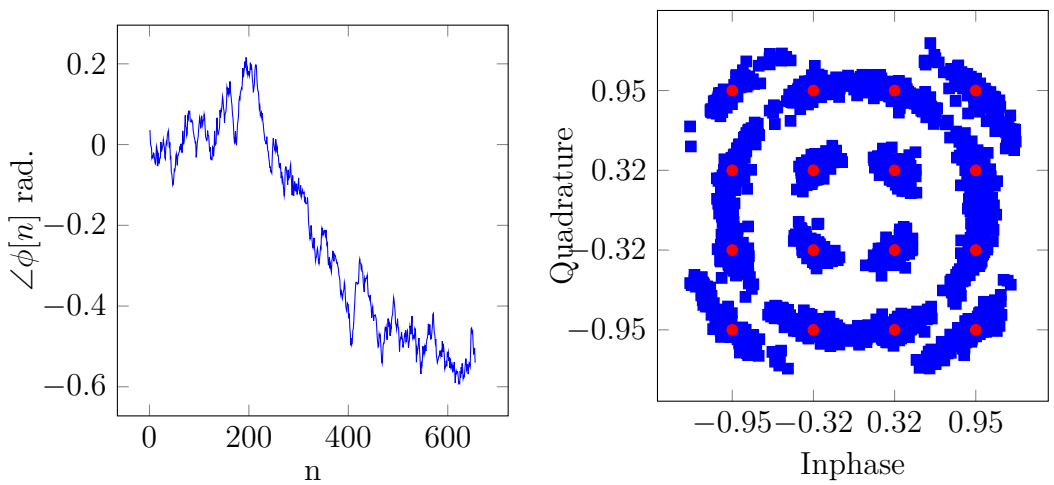

(a) PN process in discrete-time representation (b) Effects of PN process on OFDM (16 QAM) in noiseless case

Figure 2.6: The PN process and its effects on an OFDM system with β_0=1kHz.

The PN process has been studied widely. The statistical characteristics of the PN process for free running and PLL based oscillators have been defined in [18]. Further details of PN process have been provided in [19–21]. PN is a serious problem and it has also been studied in the context of optical communication systems. The PN process is generally associated with the ratio of energy at the carrier frequency to the energy leaked to the adjacent spectrum. The properties of PN process have been associated with the structure of the LO. In the next we describe the effects of PN on an OFDM system.

Let $y[n]$ be the received discrete-time signal in the presence of a PN process.

$$y[n] = r[n]e^{j\phi[n]} \tag{2.19}$$

where $r[n]$ is the equivalent discrete-time representation of the baseband equivalent of the received RF signal (see Fig. 2.5). In compact matrix notation the

received signal can be expressed as

$$\mathbf{y} = \mathbf{E}\mathbf{H}_c\mathbf{x} + \mathbf{n} \tag{2.20}$$

where $\mathbf{E}$ is a diagonal matrix of the PN process. The received signal after demodulation (while ignoring the additive noise) can be defined as [22]

$$\begin{aligned} y_f[k] &= \frac{1}{\sqrt{N}} \sum_{n=0}^{N-1} y[n] e^{-j\frac{2\pi}{N}kn} \\ &= \left(\frac{1}{\sqrt{N}}\right)^2 \sum_{n=0}^{N-1} e^{j\phi[n]} \sum_{r=0}^{N-1} s[r]H[r] e^{j\frac{2\pi}{N}rn} e^{-j\frac{2\pi}{N}kn} \\ &= \frac{1}{N} \sum_{n=0}^{N-1} e^{j\phi[n]} \sum_{r=0}^{N-1} s[r]H[r] e^{j\frac{2\pi}{N}(r-k)n}. \end{aligned}$$

Now by distinguishing between the two instances when (r=k) and (r≠k) the received signal can be decomposed as

$$y_f[k] = \frac{1}{N}\left(s[k]H[k] \sum_{n=0}^{N-1} e^{j\phi[n]} + \sum_{\substack{r=0 \\ r\neq k}}^{N-1} s[r]H[r] \sum_{n=0}^{N-1} e^{j\phi[n]} e^{j\frac{2\pi}{N}(r-k)n} \right) \tag{2.21}$$

$$= s[k]H[k] \underbrace{\sum_{n=0}^{N-1} e^{j\phi[n]}}_{p_0} + \frac{1}{N} \sum_{\substack{r=0 \\ r\neq k}}^{N-1} s[r]H[r] \underbrace{\sum_{n=0}^{N-1} e^{j\frac{2\pi}{N}(r-k)n} e^{j\phi[n]}}_{p_{(r-k)}} \tag{2.22}$$

$$= s[k]H[k]p_0 + \frac{1}{N} \sum_{\substack{r=0 \\ r\neq k}}^{N-1} s[r]H[r]p_{(r-k)} \tag{2.23}$$

where $s[k]$ and $H[k]$ are respectively the transmitted data and the CFR on the k-th subcarrier, with p_0 the mean of the PN process over a symbol duration, also known as the common phase rotation (CPR). As observed from (2.23), p_{r-k} with $r-k$=$1,\ldots,N-1$ are the higher order harmonics of the PN process spectrum. The second component of (2.23) is the data dependent interference which is commonly known as intercarrier interference (ICI). The effects of PN on OFDM transmission are illustrated in Fig. 2.6(b). In compact matrix notation (2.23) after demodulation can be written as

$$\mathbf{y}_f = \mathbf{P}\mathbf{\Lambda}_h\mathbf{s} + \mathbf{z} \tag{2.24}$$

where $\mathbf{z}$ is the equivalent complex white Gaussian additive noise, $\mathbf{P}$ is a circulant matrix constructed from the column vector $[p_0, p_1, \cdots, p_{N-1}]^T$ and $\mathbf{\Lambda}_h$ is a diagonal matrix obtained from the CFR (i.e. diag($\mathbf{Wh}$)).

The estimation and compensation of the PN process in the multicarrier system is a very sensitive problem because as illustrated in the Fig 2.6(a), PN is a rapidly time-varying process. In practice it is not possible to completely eliminate the PN process as it requires knowledge of all the PN samples (i.e. $\phi[n]$, n=$0, \ldots, N-1$) effecting the OFDM symbol.

Most of the solutions proposed in literature suggest estimating and compensate for only the CPR while ignoring the ICI. More recently [23] has proposed estimating the PN process using linear interpolation of the PN values obtained from the known pilot samples. In [24] and [25] they have illustrated that by linear interpolation between CPR estimates obtained from subsequent OFDM symbols the PN process can compensated effectively.

2.3.2 Carrier Frequency Offset

Carrier frequency offset (CFO) occurs due to Doppler shift and/or mismatch between the operating frequency of the transmit and receive LOs. An LO is an analog component and uses high quality components that can significantly increase the cost of the transceiver.

The received OFDM signal in the presence of a CFO is defined as

$$y(t) = r(t) \cdot e^{j2\pi\Delta f t}. \tag{2.25}$$

In contemporary literature of OFDM systems the CFO is typically measured on a normalized scale, i.e. relative to the subcarrier spacing in OFDM systems (i.e. $1/T$ with T=NT_s).

$$\epsilon = T\Delta f. \tag{2.26}$$

In practice, ϵ could take any arbitrary value and it is often divided into the integer and fractional components, (ϵ=τ+ϕ) with τ, ϕ being the integer and fractional components of ϵ. This thesis is concerned with only the fractional component of the CFO[1]. Now using this definition the received OFDM signal in the presence

[1] In practice coarse CFO estimation is performed using short training sequences and thus it is fair to assume that the residual CFO left in the system is only fractional.

of CFO can be defined as

$$\begin{bmatrix} y_{[0]} \\ y_{[1]} \\ \vdots \\ y_{[N-1]} \end{bmatrix} = \begin{bmatrix} e^{j2\pi\epsilon\frac{0}{N}} & 0 & \cdots & 0 \\ 0 & e^{j2\pi\epsilon\frac{1}{N}} & \ddots & 0 \\ 0 & 0 & \ddots & 0 \\ 0 & 0 & \ddots & 0 \\ 0 & 0 & \cdots & e^{j2\pi\epsilon\frac{N-1}{N}} \end{bmatrix} \begin{bmatrix} h[0] & 0 & \cdots & \cdots & h[1] \\ h[1] & h[0] & \ddots & \ddots & h[2] \\ \vdots & \ddots & \ddots & \ddots & \vdots \\ h[L_h-1] & 0 & \ddots & \ddots & h[L_h-1] \\ \vdots & 0 & \ddots & \ddots & \vdots \\ \vdots & 0 & \ddots & \ddots & 0 \\ 0 & 0 & \cdots & \cdots & h[0] \end{bmatrix} \begin{bmatrix} x_{[0]} \\ x_{[1]} \\ \vdots \\ \vdots \\ x_{[N-1]} \end{bmatrix} + \begin{bmatrix} n_{[0]} \\ n_{[1]} \\ \vdots \\ \vdots \\ n_{[N-1]} \end{bmatrix}. \tag{2.27}$$

Now (2.27) can be expressed in matrix notation as

$$\mathbf{y} = \mathbf{E}\mathbf{H}_c\mathbf{x} + \mathbf{n}. \tag{2.28}$$

The effect of CFO on the k-th subcarrier can be described as

$$\begin{aligned} y_f[k] &= \frac{1}{\sqrt{N}} \sum_{n=0}^{N-1} e^{j\frac{2\pi}{N}kn\epsilon} \sum_{r=0}^{N-1} s[r]H[r]e^{-j\frac{2\pi}{N}(r-k)n} \\ &= \frac{1}{N} s[k]H[k] \underbrace{\sum_{n=0}^{N-1} e^{j\frac{2\pi}{N}kn\epsilon}}_{p_0} + \frac{1}{N} \sum_{\substack{r=0 \\ r\neq k}}^{N-1} s[r]H[r] \underbrace{\sum_{n=0}^{N-1} e^{j\frac{2\pi}{N}(r-k)n} e^{j\frac{2\pi}{N}kn\epsilon}}_{p_{(r-k)}} \end{aligned} \tag{2.29}$$

In compact matrix notation the (2.29) can be expressed as

$$\mathbf{y}_f = \mathbf{P}\mathbf{\Lambda}_h\mathbf{s} + \mathbf{z}. \tag{2.30}$$

From (2.29) it is evident that CFO is a serious problem because the orthogonality between the subcarriers is lost[2]. The received signal suffers from CPR and ICI

[2]The notation $\mathbf{P}$ is interchangeably used to denote either the circulant frequency domain

as in the case of PN. The data dependent nature of the ICI implies that the performance of the system cannot be improved even in a high SNR situation. The value of the CFO present in typical devices operating in 5 GHz band is 20 ppm (parts per million) which means the signal performs a 2π rotation every 10μs [26] and without CFO compensation it is not possible to use OFDM system for transmission.

2.3.3 IQ Imbalance

IQ imbalance is one of the common problems faced by DC transmitters and receivers. This problem arises due to the amplitude and phase mismatch between the in-phase and quadrature-phase arms of the (de)modulator as illustrated in Fig. 2.5. In the literature this problem is modelled as an asymmetric and a symmetric problem. The corresponding diagrams (only for receiver devices) are illustrated in Fig. 2.7. For the asymmetric model of IQ imbalance as illustrated

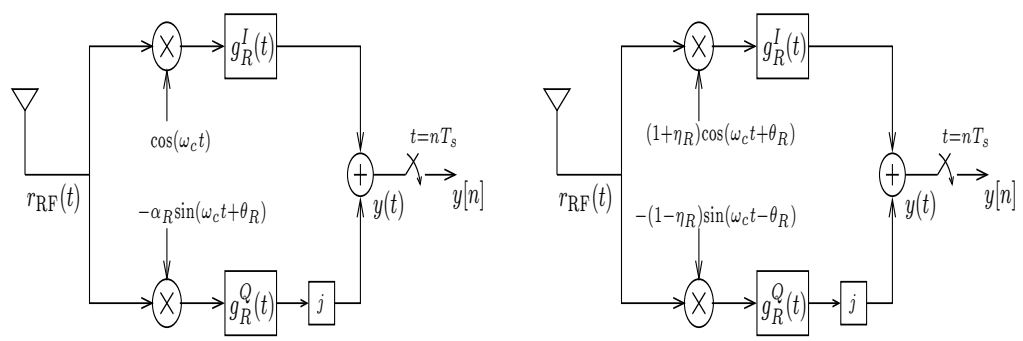

(a) Asymmetric model of IQ imbalance in DC receiver

(b) Symmetric model of IQ imbalance in DC receiver

Figure 2.7: Typical models of direct conversion (Zero-IF) receiver.

in Fig. 2.7(a) the gains of the desired and the interfering(mirror) signals for a DC receiver (see (2.34)) are defined in [27–29] as

$$\begin{aligned} \mu_R &= \frac{1+\alpha_R e^{-j\theta_R}}{2} \\ \nu_R &= \frac{1-\alpha_R e^{j\theta_R}}{2} \end{aligned} \tag{2.31}$$

representation of PN or a CFO process

where α_R and θ_R are respectively the amplitude and phase imbalances. Likewise for the symmetric model of IQ imbalance as illustrated in Fig.2.7(b), these gains are defined as

$$\begin{aligned}\mu_R &= \cos\theta_R - j\eta_R \sin\theta_R \\ \nu_R &= \eta_R \cos\theta_R + j\sin\theta_R.\end{aligned} \tag{2.32}$$

where α_R=$1 + \eta_R$ (η_R is the amplitude imbalance typically measured as a percentage). The effect of these models on the received signal is equivalent. Only a symmetric IQ imbalance model has been considered within the scope of this work. Since the DC modulator can be deployed at the transmitter the equivalent baseband output signal in the presence of FI IQ imbalance is defined as

$$u(t) = \mu_T x(t) + \nu_T x^*(t) \tag{2.33}$$

where $x(t)$ is the OFDM modulated signal as defined in (2.6), μ_T is the gain of the useful transmit signal while ν_T is the gain of the interfering signal, which is simply the complex conjugate of the original signal. Similarly, the received signal in the presence of only FI Rx IQ imbalance is defined as

$$y(t) = \mu_R r(t) + \nu_R r^*(t). \tag{2.34}$$

where $r(t)$ is the baseband equivalent signal at the input of RF front-end. The problem of IQ imbalance is not limited only to the transmitter or receiver RF front-ends but both sides can suffer from IQ imbalance simultaneously. The received signal in the presence of FI Tx/Rx IQ imbalance can be compactly written in vector notation (assuming an AWGN channel) as

$$\mathbf{y} = \mu_R \mathbf{r} + \nu_R \mathbf{r}^* + \mathbf{n}.$$

Using (2.33) in (2.34) and ignoring the fading channel we get

$$\mathbf{y} = \mu_R \mu_T \mathbf{x} + \mu_R \nu_T \mathbf{x}^* + \nu_R \mu_T^* \mathbf{x}^* + \nu_R \nu_T^* \mathbf{x} + \mathbf{n}. \tag{2.35}$$

In the absence of Tx IQ imbalance, (2.35) reduces to (2.34). In the presence of the slightest mismatch between the in-phase and quadrature-phase arms of the DC receivers it is not possible to remove this interference (caused by the image).

Typically the effect of IQ imbalance is more serious in low cost receiver devices, i.e., they suffer from a low pass filter (LPF) mismatch in addition to the amplitude and phase imbalance coefficients.

The effect of IQ imbalance on SCCP scheme (only for the simplistic case when IFFT and FFT operations at transmitter are of same size) is illustrated in Fig. 2.8(a). It is evident that the effect of FI IQ imbalance on SCCP systems is very uncomplicated. It can be seen that the constellation is skewed. This is acceptable as long as the constellation diagram is not distorted significantly. However it is hard to deduce any conclusions for the case when different dimensions of Fourier matrices are used.

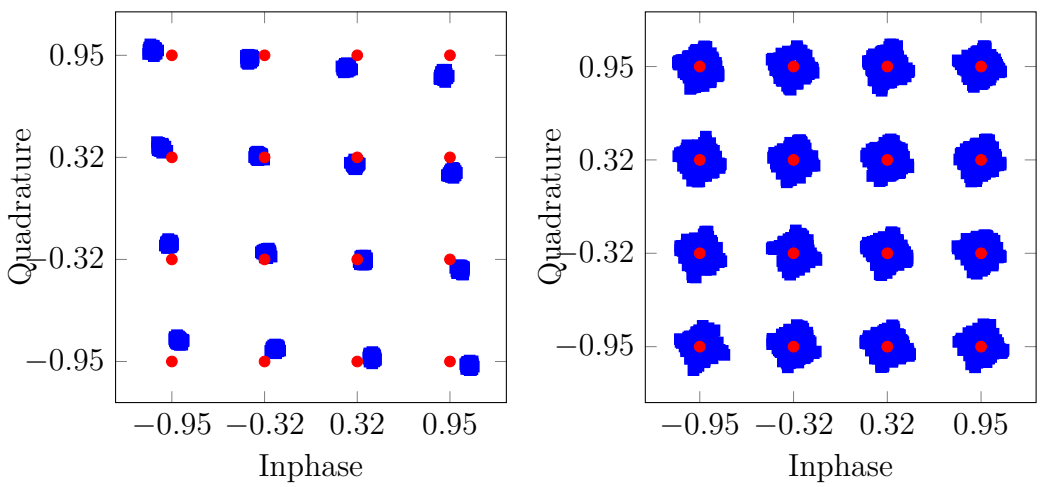

(a) Effects of IQ imbalance on a single carrier cyclic prefix system

(b) Effects of IQ imbalance on an OFDM system

Figure 2.8: The effects of IQ imbalance on SCCP and OFDM schemes with 16-QAM, $\eta = 5\%$, $\theta = 5^\circ$ in AWGN channel with E_b/N_0=30dB.

Now for an OFDM transmission system the received signal (after demodulation) can be expressed in terms of the multi-path channel and the transmitted signal as

$$\mathbf{y}_f = \mu_R \mathbf{F}\mathbf{H}_c\mathbf{F}^H\mathbf{s} + \nu_R \mathbf{F}\mathbf{H}_c^*\mathbf{F}^T\mathbf{s}^*.$$

And after further simplification

$$\mathbf{y}_f = \mu_R \mathbf{\Lambda}_h \mathbf{s} + \nu_R \bar{\mathbf{\Lambda}}_h^* \mathbf{Q} \mathbf{s}^* \tag{2.36}$$

where $\mathbf{\Lambda}_h$ is the CFR matrix associated with the multi-path FS channel as defined in (2.14). Similarly, the matrix $\bar{\mathbf{\Lambda}}_h^* := \text{diag}(\mathbf{W}\mathbf{h}^*)$ and $\mathbf{Q}{=}\mathbf{F}\mathbf{F}^T$ is defined as the permutation matrix. For a data vector $\mathbf{s} = [s[0], s[1], \cdots, s[N{-}2], s[N{-}1]]^T$ its mirror image is defined as $\mathbf{Q}\mathbf{s}^*{=}[s^*[0], s^*[N{-}1], s^*[N{-}2], \cdots, s^*[3], s^*[2], s^*[1]]^T$, mirror image of the CFR can also be defined similarly.

For multi-carrier systems like OFDM the received demodulated signal $y_f[k]$ is the sum of actual received sample $r_f[k]$ ($r_f[k] := H[k]s[k]$) and its complex conjugate mirror image $r_f^*[\text{-}k]$ (i.e. $r_f^*[\text{-}k] := H^*[\text{-}k]s^*[\text{-}k]$) as illustrated in Fig. 2.4. If the complex gain of the useful signal and the interfering image ($\mu_{T/R}$ and $\nu_{T/R}$) is same for all subcarriers then IQ imbalance is considered to be frequency independent (FI), and it is frequency selective (FS) otherwise. A detailed formulation of the system in the presence of FS IQ imbalance is provided in subsequent paragraphs.

Another way of looking at (2.36) is that the data symbol on every subcarrier suffers from cross-talk with its mirror image sub-carriers. If the IQ imbalance coefficients are known at the receiver then the desired(useful) signal can be decoupled from its interfering image using a set of linear equations. The effects of FI Rx IQ imbalance on (16-QAM) OFDM transmission systems are illustrated in Fig. 2.8(b).

The impact of this interference is commonly measured in terms of image rejection ratio (IRR) and is defined as

$$\begin{aligned} \text{IRR} &= \frac{P_{\text{interference}}}{P_{\text{signal}}} = \frac{|\nu|^2}{|\mu|^2} \\ &= \frac{\eta^2 \cos^2\theta + \sin^2\theta}{\cos^2\theta + \eta^2 \sin^2\theta}. \end{aligned} \tag{2.37}$$

IRR is an important figure of merit for DC devices and is often referred to in the literature.

For multicarrier systems like OFDM in the presence of non-ideal components like A/D and D/A convertors, filters etc., the IQ imbalance problem becomes frequency selective. This is because the gains of interference experienced by

each subcarrier is related to the mismatch between the in-phase and quadrature-phase branches. The frequency selectivity is not a critical issue in narrow band transmission systems, but it becomes much more relevant for higher bandwidth systems (such as WLAN, WiMAX and LTE). The overall transmission model in the presence of the FS IQ imbalance is illustrated in Fig. 2.5 where $g_T^I(t)$ and $g_T^Q(t)$ are appropriate LPFs at the transmitter, and similarly $g_R^I(t)$ and $g_R^Q(t)$ are the LPFs at the receiver. In the literature the behaviour of the LPFs is modelled in two different ways. The authors in [27, 29, 30] have modelled the mismatch filters (i.e. $(g_T^I(t) \pm g_T^Q(t))/2$ and $(g_R^I(t) \pm g_R^Q(t))/2$) as an infinite impulse response (IIR) filter, while [31–33] have assumed it to be a non-causal FIR filter.

In the subsequent paragraph the system model for a transmission system in the presence of FS Tx/Rx IQ mismatch is defined.

The equivalent baseband transmitted signal at the output of the RF front-end is defined as $u(t)$=LPF$\{u_{RF}(t)e^{-j\omega_c t}\}$ [34]. The equivalent baseband signal in the presence of FS IQ mismatch is defined as

$$u(t) = \Big[(1+\eta_T)\Big(x^I(t)\otimes g_T^I(t)\Big)\cos(\omega_c t+\theta_T) - (1-\eta_T)(x^Q(t)\otimes g_T^Q(t)\sin(\omega_c t-\theta_T))\Big] \cdot(\cos\omega_c t - j\sin\omega_c t). \tag{2.38}$$

The real and imaginary components of the transmitted equivalent baseband signal are defined as

$$\begin{aligned} u^I(t) &= (1+\eta_T)(x^I(t)\otimes g_T^I(t))\cos(\theta_T) + (1-\eta_T)(x^Q(t)\otimes g_T^Q(t))\sin(\theta_T) \\ u^Q(t) &= (1+\eta_T)(x^I(t)\otimes g_T^Q(t))\sin(\theta_T) + (1-\eta_T)(x^Q(t)\otimes g_T^Q(t))\cos(\theta_T). \end{aligned} \tag{2.39}$$

Combining these components together and simplifying the expressions further the transmitted baseband signal can be expressed as

$$\begin{aligned} u(t) = &\left[(\cos\theta_T + j\eta_T\sin\theta_T)\left(\frac{g_T^I(t)+g_T^Q(t)}{2}\right) + (\eta_T\cos\theta_T + j\sin\theta_T)\left(\frac{g_T^I(t)-g_T^Q(t)}{2}\right)\right]\otimes x(t) \\ &+\left[(\eta_T\cos\theta_T + j\sin\theta_T)\left(\frac{g_T^I(t)+g_T^Q(t)}{2}\right) + (\cos\theta_T + j\eta_T\sin\theta_T)\left(\frac{g_T^I(t)-g_T^Q(t)}{2}\right)\right]\otimes x^*(t). \end{aligned} \tag{2.40}$$

In short-hand notation the expression of (2.40) can be written as

$$u(t) = (\mu_T k_T^1(t) + \nu_T k_T^2(t)) \otimes x(t) + (\nu_T k_T^1(t) + \mu_T k_T^2(t)) \otimes x^*(t) \tag{2.41}$$

which can be further simplified as

$$u(t) = h^{(T,D)}(t) \otimes x(t) + h^{(T,I)}(t) \otimes x^*(t) \tag{2.42}$$

where $h^{(T,D)}(t)$ and $h^{(T,I)}(t)$ are the equivalent (modified) CIRs pertaining to the desired and interfering(image) channels at transmitter. Extending this idea further we define the equivalent baseband representation of the received signal after down-conversion by a DC receiver in the presence of FS IQ mismatch. The received signal after down conversion can be defined as

$$\begin{aligned} y^I(t) &= (1+\eta_R)\Big((r^I(t)\cos\omega_c t - r^Q(t)\sin\omega_c t)\cos(\omega_c t + \theta_R)\Big) \otimes g_R^I(t) \\ y^Q(t) &= -(1-\eta_R)\Big((r^I(t)\cos\omega_c t - r^Q(t)\sin\omega_c t)\sin(\omega_c t - \theta_R)\Big) \otimes g_R^Q(t). \end{aligned} \tag{2.43}$$

After some straight forward calculation the equivalent baseband received signal can be defined as

$$\begin{aligned} y(t) = &\left[(\cos\theta_R - j\eta_R\sin\theta_R)\left(\frac{g_R^I(t)+g_R^Q(t)}{2}\right) + (\eta_R\cos\theta_R - j\sin\theta_R)\left(\frac{g_R^I(t)-g_R^Q(t)}{2}\right)\right] \otimes r(t) \\ &+ \left[(\cos\theta_R + j\eta_R\sin\theta_R)\left(\frac{g_R^I(t)-g_R^Q(t)}{2}\right) + (\eta_R\cos\theta_R + j\sin\theta_R)\left(\frac{g_R^I(t)+g_R^Q(t)}{2}\right)\right] \otimes r^*(t) \end{aligned} \tag{2.44}$$

which can be written in short-hand notation as

$$y(t) = (\mu_R k_R^1(t) + \nu_R^* k_R^2(t)) \otimes r(t) + (\nu_R k_R^1(t) + \mu_R^* k_R^2(t)) \otimes r^*(t) \tag{2.45}$$

which can be further simplified as

$$y(t) = h^{(R,D)}(t) \otimes r(t) + h^{(R,I)}(t) \otimes r^*(t) \tag{2.46}$$

here $h^{(R,D)}(t)$ and $h^{(R,I)}(t)$ are the equivalent (modified) CIRs pertaining to desired and interfering channels at the receiver. Since the equivalent received base-

band signal in the presence of a FS CIR can be expressed as

$$r(t) = h(t) \otimes u(t) \tag{2.47}$$

therefore using the definition of the Tx signal from (2.42) in (2.47), (2.46) can be finally redefined as

$$\begin{aligned} y(t) &= h^{(R,D)}(t) \otimes r(t) + h^{(R,I)} \otimes r^*(t) \\ &= h^{(R,D)}(t) \otimes (h^{(T,D)}(t) \otimes h(t) \otimes x(t) + h^{(T,I)}(t) \otimes h(t) \otimes x^*(t)) \\ &\quad + h^{(R,I)}(t) \otimes (h^{(T,D)}(t) \otimes h(t) \otimes x(t) + h^{(T,I)}(t) \otimes h(t) \otimes x^*(t))^*. \end{aligned}$$

Re-arranging the desired and interfering components of the received signal we can write

$$\begin{aligned} y(t) = &\left(h^{(R,D)}(t) \otimes h^{(T,D)}(t) \otimes h(t) + h^{(R,I)}(t) \otimes h^{*(T,I)}(t) \otimes h^*(t)\right) \otimes x(t) \\ &+ \left(h^{(R,D)}(t) \otimes h^{(T,I)}(t) \otimes h(t) + h^{(R,I)}(t) \otimes h^{*(T,D)}(t) \otimes h^*(t)\right) \otimes x^*(t). \end{aligned} \tag{2.48}$$

The effect of the IQ imbalance in a multi-carrier transmission system is illustrated in Fig. 2.8(b). It is obvious from the figure that the effect of IQ imbalance on multi-carrier systems is more profound and complicated in comparison with single carrier systems. From the simulation results it is evident that the even a small imbalance ($\theta = 5^\circ$ and $\eta = 5\%$) can limit the system performance even in high SNR.

2.3.4 Direct Current Offset

There are several reasons for occurrence of direct current offset (DCO). Firstly, the isolation between the LO port and the inputs of the mixer and the LNA is not perfect -i.e., a finite amount of feed-through exists from the LO port to the input of the LNA and mixer. This so called '*LO leakage*' stems from the capacitative and substrate coupling. The leakage signal appearing at the inputs of the LNA and the mixer is now mixed with the LO signal and produces a *dc* component. This phenomena is called *self-mixing*. This problem may also arise if a large interferer leaks from the LNA or mixer input to the LO port and is multiplied by itself. The graphical illustration of both scenarios is in Fig. 2.9.

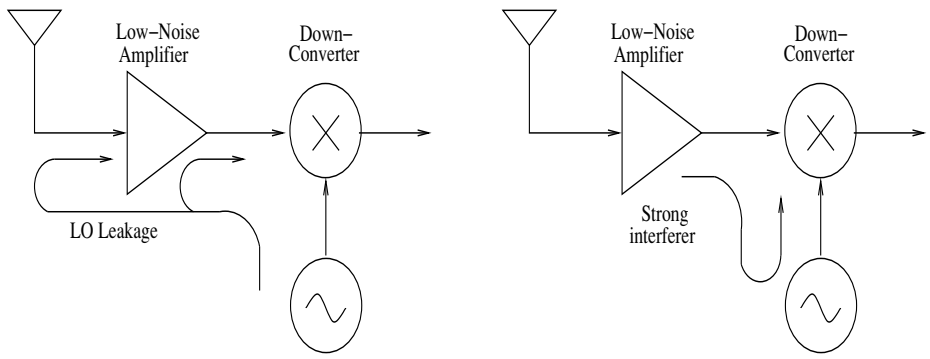

(a) LO leakage effects (b) Self-mixing effects

Figure 2.9: Effects of signal leakage on direct conversion receiver [2].

In practice the effects of DCO vary much slowly than the CIR, it is for this reason it is commonly modelled as an additive complex constant d_0 at the output of the device [35–37] as illustrated in Fig. 2.5.

2.3.5 High Power Amplifier

Amplifier non-linearity problem emanates from the non-linear behaviour of transmit/receive amplifier at the analog front-end of the system. The effect of this problem is not critical on the constant modulus single carrier transmission system. However the effect of this distortion is very significant on systems where the signals have a large dynamic range. The OFDM transmission system is unfortunately very sensitive to the effects of amplifier non-linearity because of the large variations in the modulated signal. The variation of the signal is measured as peak to average power ratio (PAPR)[3], which is defined as

$$\text{PAPR} = \frac{\max\{x^2[n]\}}{E\{x^2[n]\}}. \tag{2.49}$$

The amplifier non-linearity has serious effects not only on the transmitted signal but also on the signals of the adjacent carriers. The distortion caused to the transmitted signal is known as in-band distortion while the distortion to the adjacent users is more commonly known as out-of-band distortion. Although the out-of-band radiation can be curtailed using a bandpass filter, the self-inflicted

[3] in practice crest factor (CF) is a more suitable measure of the dynamic range of the signal and the distribution of dynamic range is defined as a complementary cumulative distribution function (CCDF).

interference cannot be filtered out from the signal. This interference limits the achievable SNR in the receiver. The Federal Communication Commission requires an out of band emission on WLAN in the range of -51 to -60 dB , while OFcom requires that it be less than -55 dB outside the allowable spectral range.

The effects of the HPA are analyzed in terms of the effect of input amplitude to output amplitude and input amplitude to the output phase. These are referred to as the AM/AM and AM/PM characteristics. The most common way to limit the dynamic range of transmit signal is to use a clipper. The AM/AM and AM/PM characteristics of an ideal clipper (also known as soft limiter (SL)) are defined as

$$g(x[n]) = \begin{cases} x[n] & , \quad |x[n]| \leq A_{\max} \\ |A_{\max}|e^{j\phi[n]} & , \quad |x[n]| > A_{\max} \end{cases} \tag{2.50}$$

where $A_{\max}$ is the maximum unclipped signal amplitude. This is idealized behaviour and is not found in practice.

In the literature two of the most popular amplifiers which have found a wider application in the telecommunication industry are namely the solid state power amplifiers (SSPA) and the travelling wave tube amplifiers (TWTA). The mathematical models most commonly used to describe the behaviour of these amplifiers are respectively Rapp's model [38] and Saleh's model [39] several other variants are available in [40]. Since Rapp's model accurately describes the behaviour of the HPA's used in mobile communication devices, only these amplifiers will be considered in further discussion. If the input to HPA is defined in polar co-ordinates as $x[n] := |x[n]|\exp(j\phi[n])$, then the magnitude and phase transfer functions of the SSPA can be modelled as

$$\begin{aligned} f(|x[n]|) &= \frac{|x[n]|}{\left[1 + \left(\frac{|x[n]|}{A_{\max}}\right)^{2p}\right]^{1/2p}}, \\ \Phi(x[n]) &\simeq 0. \end{aligned} \tag{2.51}$$

where $f(\cdot)$ and $\Phi(\cdot)$ are the AM/AM and AM/PM transfer functions and p is the non-linearity factor and as $p \to \infty$, this model approaches a soft limiter characteristics. By combining the magnitude and phase dependent components the output function of an HPA is defined as $g(x[n]) := f(|x[n]|)\exp(j\Phi(x[n]) + \phi[n])$.

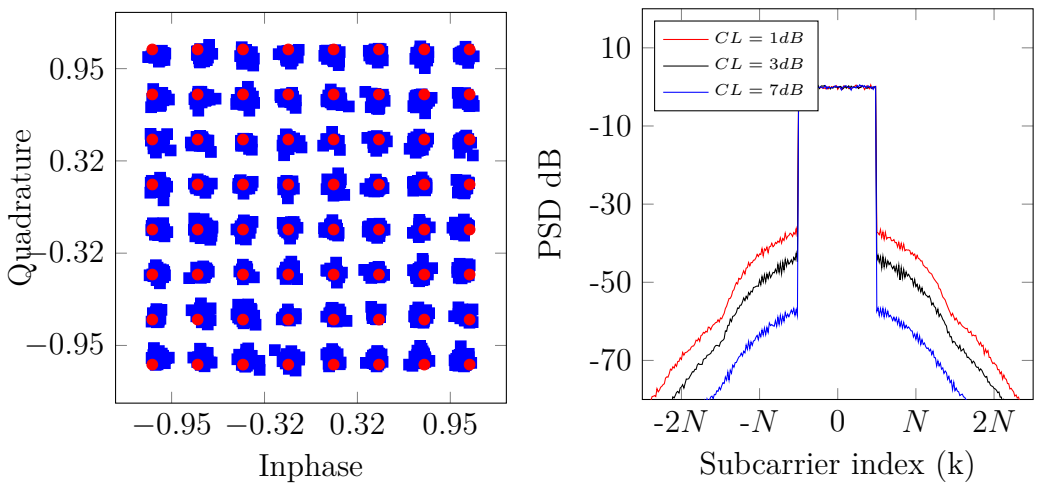

(a) Effects of clipping with CL=5dB

(b) Leakage effects of AN on OFDM spectrum

Figure 2.10: The effects of amplifier non-linearity on OFDM with $N = 64$, $p = 2$ and SNR=40dB.

The effects of amplifier non-linearity on OFDM system have been presented in Fig 2.10. It is obvious from Fig. 2.10(a) and 2.10(b) that non-linearity leads to degradation of constellation and speactral leakage. The effect of non-linearity is associated with clipping level (CL) which is defined in (6.18). In the literature there exists an extensive review of the effects of the memory of amplifier non-linearity. However, within the scope of this thesis only memoryless amplifiers are considered.

In multi-carrier transmission systems, the effects of non-linearity are directly related to the number of subcarriers. Several solutions have been purposed to mitigate these effects on the transmission side, such as subcarrier loading, predistortion and adjusting the input power of the amplifier to move the operating point of the amplifier in the linear region. The simplest way to reduce the dynamic range of the transmitted sequence is to clip the signal at transmitter. This is done widely in practice and it causes a loss in BER performance in addition to out-of-band radiation.

Signal processing at the transmitter side is the most widely used method to mitigate the effects of non-linearity. But in this thesis we have focused on development of techniques which can jointly mitigate the effects of CIR in conjunction with amplifier non-linearity.

In the next section a review of techniques available in the literature to estimate any subset of these problems is provided. This review is not an exhaustive one but it outlines the research trend and cites a selection of different techniques proposed over the past decade.

2.4 Literature Review

DC architecture is also commonly known as homodyne and zero intermediate frequency (Zero-IF) structure. These structures are the simplest receivers and have been around since the early 1920's [3]. They have not found application because of their instability and sensitivity. The interest in these simple devices was reinvigorated by [15]. The biggest drawback of the DC architecture is the presence of inherent problems such as PN, CFO, IQ mismatch and DCO. In the presence of these imperfections it is not possible to estimate channel accurately even in high SNR conditions. This situation curtails the achievable performance of the transmission system.

In contrast to homodyne transceivers, the heterodyne devices have been more popular. Because of their multi-stage design they avoid image interference problems using costly analog bandpass filters on each stage. An equally important drawback of the heterodyne structures is that because of the additional analog components it is not possible to minimize the cost of the hetrodyne transceivers and it is also not possible to integrate these structures on the printed circuit board.

Lately the research trend has been to estimate the above mentioned non-idealities jointly using minimal training samples and/or adaptation time.

The following section provides a detailed account of numerous solutions proposed in the literature to mitigate these problems. The literature has been grouped together based on the set of parameters estimated together. Different articles have been sub-grouped together to compare and contrast the performance of the solutions focusing on similar problems.

CIR, IQ imbalance, CFO and DCO estimation

The authors in [15] in his review of DC architecture has proposed an analog circuit to allow off-line calibration of the IQ imbalance present in the device. This dedicated calibration mechanism can increase the cost of the receiver. Now due to recent advances in semi-conductor electronics more sophisticated signal

processing capabilities are available at the receiver and system designers can rely on signal processing techniques to mitigate these effects through efficient signal processing techniques.

The earliest paper looking to estimate FI IQ imbalance using pilot-symbols can be found in [41]. These authors have proposed to transmit a known pilot symbol where half of the subcarrier bins are left empty (unloaded) so that the effects of the corresponding image subcarriers (as described in (2.36)) can be determined. A good estimate of IQ mismatch can be obtained through averaging over available (pilot) observation samples. Another scheme which performs joint CIR and FI Rx IQ imbalance estimation has been proposed in [42]. The authors have proposed a special set of scattered pilots to estimate FI IQ imbalance coefficients using pilot subcarriers from two consecutive symbols. The scheme is specific to the WLAN standard. Both these schemes are very simple but they are also very limited in their application.

The earliest work found in the literature for joint estimation of FI/FS Rx IQ mismatch is [27]. The authors have proposed an adaptive least mean square (LMS) estimation of CIR and FI/FS IQ mismatch using pilots with either symmetric or asymmetric samples on image subcarriers. The convergence speed of this scheme is related to the choice of adaptation parameters. This scheme requires several training symbols to obtain reliable estimates. Another adaptive scheme proposed in [43] suggests to use pilot symbols with corresponding image subcarriers set to zero. This scheme using the pairs of signal and image subcarriers can jointly estimate the CFR and FI Rx IQ-imbalance coefficients. The authors in [44] have extended their work to the case of FI Tx/Rx IQ imbalance. More recently another low complexity adaptive FS IQ mismatch estimation in the presence of CFO (which is assumed to be known perfectly) using LMS technique appeared in [45].

Another work on the joint estimation of CFR and FI/FS Rx IQ imbalance has been proposed by [32]. These authors proposed a recursive least square (RLS) solution, and have extended their work to estimate FI/FS Tx/Rx IQ imbalance and CFO using similar adaptive schemes in [46].

Another solution found in literature [29] has extended the problem to jointly estimate FI/FS, Tx/Rx IQ imbalance for MIMO-OFDM systems using an RLS scheme.

It can be observed from all these solutions that the adaptation process is slow to converge and several pilot symbols are required for convergence. These schemes estimate CFR in conjunction with, FI/FS Tx/Rx IQ imbalance. The

convergence performance of these estimators is not acceptable because wireless channels are time-varying and it is not realistic to assume that the adaptive process can keep track of the albeit slowly time varying channel process. The number of unknowns to be estimated (when estimating the combined CFR and IQ mismatch process) can be large. The schemes in [27, 29, 32, 44] also do not exploit the fact that the complexity of the receiver can be minimized by reducing the number of parameters to be estimated.

More recently [31] have proposed estimation of the CIR and FI/FS Rx IQ imbalance in time-domain using an optimal training sequence. This scheme estimates combined CIR and FS IQ imbalance as a CLFE. The overall channel is estimated as the impulse response associated with the desired and the interfering components of the received signal as defined in (2.36). In [34] these authors have extended the closed form estimation solution to FI/FS Tx/Rx IQ imbalance and CIR estimation.

A maximum likelihood estimation of the CIR, CFO, IQ mismatch and DCO has been proposed by [36]. This scheme considers only the FI type of IQ mismatch and estimation of these parameters is performed through a multi-dimensional grid search. Although this scheme is very effective, it is too complex to be used in practice. Some other schemes estimating DCO in addition to CIR and FI IQ imbalance through LS solution can be found in [35, 37].

The problem of joint CIR, FI Rx IQ mismatch and CFO estimation has been studied widely. In [47] authors have proposed an IQ imbalance and CFO estimation scheme with grid search cost minimization using known pilot subcarriers. In [28] the authors have proposed the estimation of FI/FS IQ imbalance and CFO processes using a pilot symbol which is made up from the periodic repetition of a smaller pilot sequences. The estimates of CFO are obtained using a one dimensional search and then by fixing these estimates in a least squares problem the estimates of IQ mismatch are obtained. Both these techniques do not estimate the CIR. Another simple solution [48] found in the literature exploits the fact that the CFR does not change rapidly over adjacent subcarriers and abrupt fluctuations are induced in CFR by IQ imbalance. The estimates of CFO are obtained through the two consecutive pilot symbols. More recently the authors in [49] have proposed a CLFE for estimation of FS CIR, FI Rx IQ imbalance and CFO using the time-domain model of the system. These authors have also proposed to use the repetition of smaller blocks within a pilot symbol which allows for estimation of a large CFO variation. The authors have extended this work to MIMO-OFDM systems in [50]. This solution is elegant but does not work in the case of FS IQ

mismatch. Authors in [46, 51] have proposed an adaptive estimation of Tx/Rx IQ imbalance in the presence of CFO but they have not devised any strategy for CFO estimation within their framework.

More recently [50, 52–54] have used OFDM symbols with periodic training blocks within a pilot symbol for estimation of a wide range CFO. The authors in [50, 52] have proposed to use the repeated periodic sequences for CFO and FI IQ mismatch, whereas [53, 54] have provided a good solution for CFO and FS IQ mismatch. These solutions are good in the general sense but it is not so obvious how they may be adopted to the model of WLAN (IEEE 802.11).

The joint estimation of CIR, FI/FS Rx IQ mismatch and CFO is studied in the presence of timing offset and has been considered in [33]. The estimation of CFO resorts to a highly complex GS scheme.

In literature many blind FI/FS IQ mismatch estimation techniques have been proposed in [55–58]. In [55–57] the authors have estimated the FI/FS IQ mismatch in general transmission system using the second-order statistics through adaptive (LMS) techniques. These articles argue that IQ mismatch can be effectively estimated regardless of the additive noise, FS CIR and CFO. However, the slow nature of the proposed low complexity adaptation leads to convergence delays. The authors in [58] have proposed estimating the FS Tx/Rx IQ mismatch in the presence of DCO and FS CIR. However this solution too requires an unpractically large data size to be of any use.

Joint PN, IQ mismatch and CIR Estimation

PN has been an area of active research for quite some time. The performance of coded-OFDM systems in the presence of PN has been assessed in [17]. In [22] the authors have quantified the degradation in the operating SNR in the presence of PN. Detailed analysis of SNR degradation in multi-carrier systems has also been provided by [59]. The mitigation of PN is a complicated problem. The simplest solution to this problem is to use high quality oscillators. Most typical solution proposed in literature [17, 22] estimate CPR through the pilot samples inserted within the OFDM symbols. In [60], the authors have proposed to estimate CPR using known pilot samples and then do data detection and use the estimated data samples as pilots to perform a second stage estimation of CPR. In [61], the authors have studied the effects of PN on coded-OFDM system. In [62] the authors have used a Kalman filter to track the PN process.

In [63,64] the authors have demonstrated that the PN process can be combated using coded systems with deep interleaver blocks. The authors have also proposed to estimate the PN process in frequency domain (i.e. after demodulation). At the first step only the CPR p_0 (as defined in (2.23)) is estimated and used to mitigate the PN. The hard decisions are then fed back to estimate the 1st harmonic of intercarrier interference (p_1) and then this process is iterated and a fixed number of harmonics is estimated. Although this solution does work but it is not practical. Since the interleaved code is spread over multiple symbols the computational overhead is very high; Further more, this solution does not consider any other imperfections that may be present in the system.

A set of individual solutions to all of the above problems have been proposed in [65]. However, in this work every problem is considered in isolation and so this leaves much room for improvement.

More recently the authors in [18] have proposed joint estimation of CIR, FI Rx IQ mismatch and PN process. The authors have suggested that instead of estimating only the CPR, it may be possible to estimate an interpolated version of the entire PN process effecting an OFDM symbol. The proposed scheme approximates the N PN process samples with just M' samples. The CIR, PN and FI Rx IQ mismatch estimates are obtained through a multi-dimensional grid search algorithm. The number of unknowns is minimized to reduce the complexity of the estimator.

Another good solution found in literature [66] can jointly estimate the CIR and FI Rx IQ imbalance in the presence of PN with a CLFE. Since the PN is a rapidly time varying process as illustrated in Fig. 2.6, therefore it is essential to estimate the CPR coefficient p_0 for every OFDM system and it has been demonstrated in [67] that by interpolating between two subsequent CPR's (i.e. $p_0^{(i)}$ and $p_0^{(i+1)}$) the effects of PN process can be significantly reduced.

Amplifier Non-linearity and CIR Estimation

As established in section 2.3.5 the HPA non-linearity is a serious issue. The spectral leakage caused by a non-linear system is illustrated in the Fig. 2.10(b). The simplest way to avoid this problem as proposed in literature [68–70] is to clip the signal. If the clipping occurs rarely the transmitted signal is not effected. However, in the case of severe clipping the transmitted signal creates interference to itself and adjacent carriers. Another possibility is to operate the amplifier in the linear region of operation; of course this yields a loss of amplifier efficiency

which is defined by its class. It has been suggested in the literature [71] that error correction codes can improve the performance of the system in the presence of non-linear behaviour. Another very common technique to combat these effects is to modify (pre-distort) the transmitted signal in such a way that the signal is restored after passing through the non-linearity [72–74]. Although a predistorter is a very good solution it requires a feedback loop (at least for the adaptation process). From the literature [74] it is known that every data sample requires complex multiplication operations which are directly related to the order of the non-linearity. This results in a computational overhead which may not be desirable.

In the literature several schemes have been considered to mitigate the effects of clipping and non-linearity [70, 75, 76], they have used a pre-transmission *intentional clipping* and filtering to mitigate the effects of clipping.

Another common solution cited in the literature [68] allows for distortion to take place at the transmitter and estimates it as a data dependent interference in the receiver in an iterative fashion. This scheme assumes that the CIR and non-linearity parameters are perfectly known at the receiver. An exhaustive review reveals that no scheme exists in the literature which can estimate the CIR in addition to other front-end non-idealities, when the transmitted signal is affected by amplifier non-linearity.

An approximate comparison of different well-cited techniques (in terms of computational complexity and training data required for estimation) has been illustrated in Fig. 2.11. Fig. 2.11 does not stem from an exact complexity analysis but is merely for illustrative purpose only. The parameters have been grouped together on the basis of how commonly they have been considered together. The scope of each solution is clearly identified. The schemes have been broadly categorized into three different types namely (i) Adaptive schemes (ii) GS schemes (iii) CLFE and/or iterative techniques. Adaptive estimation techniques (such as LMS and RLS) are of low complexity but they require several pilot symbols for convergence. Several multi-dimensional GS solutions have been proposed to jointly obtain optimal estimates of multiple parameter. But these schemes are computationally intensive and may not be practical if the dimension of GS is more than a few coefficients. The CLFE solutions are more elegant because of their simplicity and fixed complexity. In the recent past several CLFE solutions have been proposed to estimate multiple parameters jointly.

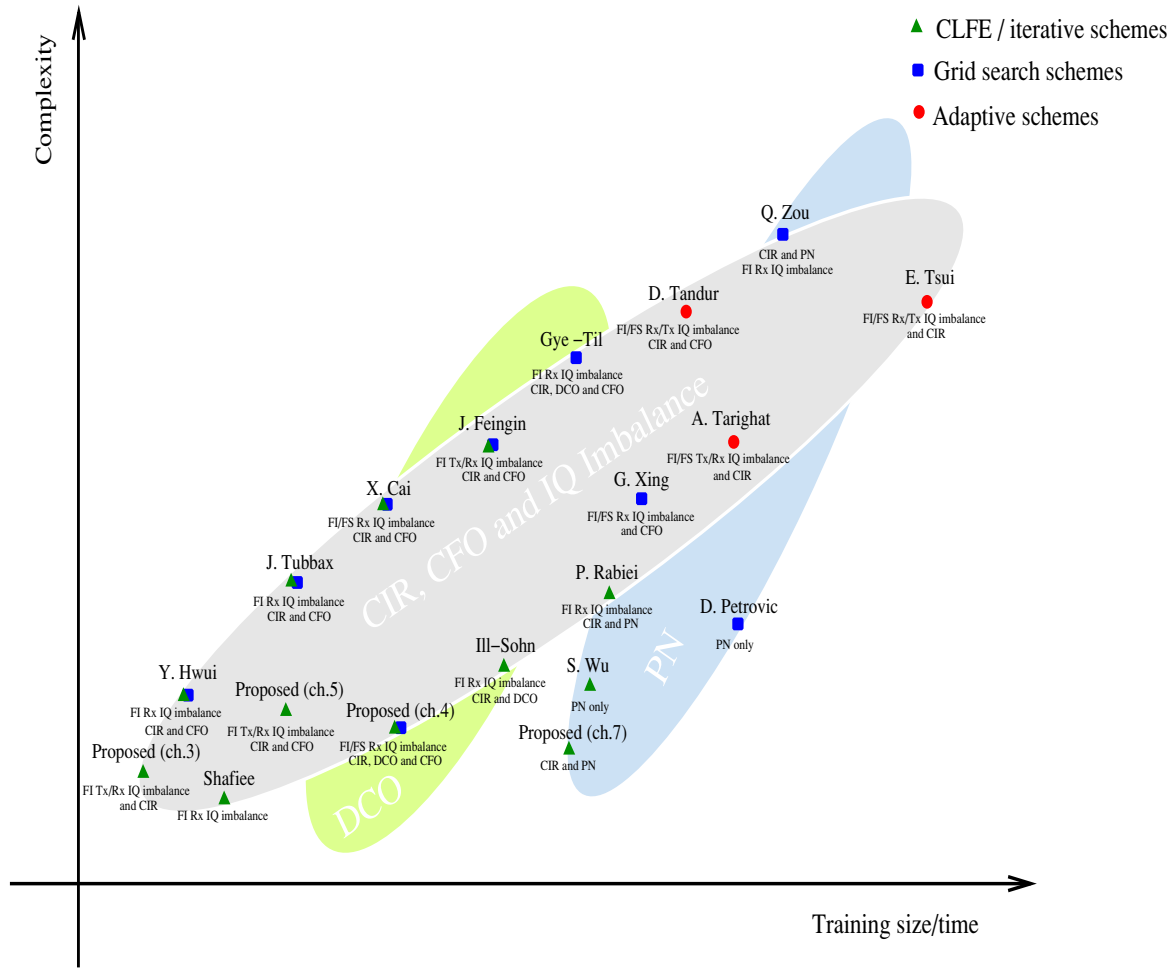

Figure 2.11: Complexity/training-size comparison of different schemes proposed in the literature.

It must be said that it is hard to compare different techniques which consider different sets of parameters and scenarios. Fig. 2.11 provides an approximate comparison between different techniques.

The CLFE solutions have a fixed complexity and training size thus they are located at the bottom left corner. The multi-dimensional GS schemes are computationally intensive and thus they are located at the top right corner of the figure. The adaptive schemes tread a balance between computational complexity and data size required for convergence.

3

Joint CIR and FI Tx/Rx IQ Imbalance Estimation

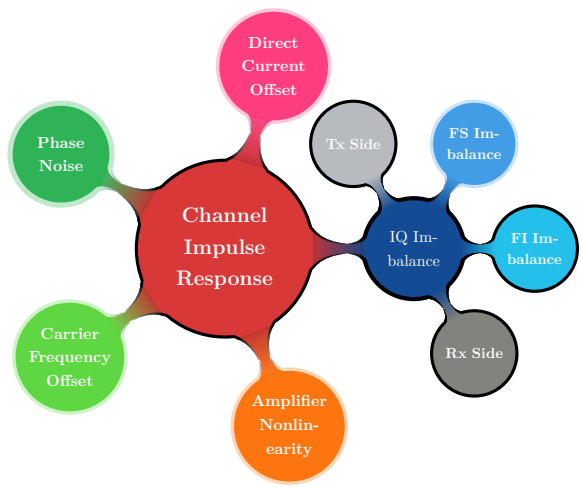

Abstract

In this chapter a low complexity iterative joint CIR, FI Tx/Rx IQ imbalance estimation technique is proposed. The proposed scheme is based on a simple doubly linear model of the transmission system in the presence of FS CIR and FI Tx/Rx non-idealities.

In contrast to existing schemes available in the literature this scheme does not take an adaptive approach to the estimation of unknown parameters. The proposed scheme requires only one pilot symbol for the estimation of all unknown parameters. The proposed scheme works equally effectively when IQ imbalance is present at either the transmitter and/or receiver.

The proposed scheme conforms to the IEEE 802.11 standard but can be adapted to any blocked OFDM transmission system. Despite its slightly high complexity the proposed scheme provides an excellent complexity/convergence trade-off.

3.1 Introduction

OFDM systems are becoming widely accepted in all modern communication standards. They find application in WiMAX (IEEE 802.16), WLAN (IEEE 802.11n) and LTE cellular technology. Their biggest advantage is in being more spectrally efficient and maximizing the system throughput. The simple and low cost DC transceiver is a preferred choice because it keeps the hardware cost to minimum but this transceiver suffers from problems like IQ imbalance, CFO, DCO and PN. Therefore it is essential that the transceiver can handle the effects of these practical limitations in the digital domain. The traditional approach is to transmit certain training sequences and then do joint estimation of both the CIR and the non-ideal behaviour parameters. From the literature it is known that these schemes require multiple long training symbols (LTS) to achieve acceptable CIR estimates.

The authors in [41] have proposed a simple FI Rx IQ imbalance estimation technique. If a known set of pilots is transmitted while leaving the corresponding image subcarriers empty, then IQ imbalance coefficients can be estimated through a simple cross-coupled relation which exists between the actual and the interfering subcarrier (see Fig. 2.4 and (2.36)). Another simple technique proposed in [77] exploits the fact that the smoothness of CFR is lost in the presence of IQ imbalance. Therefore by transmitting a known pilot symbol IQ imbalance and CFR can be estimated. Both [41, 77] are low complexity schemes operating with only one pilot symbol, but they both are specific to systems where IQ imbalance is present only in the receiver.

Several adaptive methods have been proposed to estimate Tx/Rx IQ imbalance parameters in OFDM systems. An LMS based scheme is proposed in [27] to estimate FI/FS Rx IQ imbalance. However this scheme requires several pilot symbols and is slow to converge. In [43] the authors have proposed to transmit a set of known pilots while leaving the corresponding image subcarriers empty. The authors have proposed to exploit the linear cross-coupling relation which exists between the desired and image subcarriers. This scheme jointly estimates the CFR and FI Rx IQ imbalance using the fact that in an OFDM (with IQ imbalance) system each subcarrier interferes with its (frequency domain) mirror image, this idea has been extended to the FI Tx/Rx IQ imbalance scenario in [44]. Another adaptive scheme has been proposed in [32] for joint estimation of FI Tx/Rx IQ imbalance and CIR.

The main drawback of all these schemes is that they all require several OFDM symbols to adaptively estimate both IQ imbalance and the CIR. Another disadvantage of all these schemes is that all these schemes tend to estimate the CFR instead of the CIR which can be estimated more accurately with fewer pilot samples.

Several blind Tx/Rx IQ imbalance estimation techniques have been proposed in the literature [57, 58] but these schemes require large numbers of data samples to acquire reliable estimates.

The aim of this chapter is to study a low complexity joint FS CIR and FI Tx/Rx IQ imbalance estimation technique for an OFDM system. In contrast to other works proposed in the literature which require many training symbols, the proposed scheme in this thesis can estimate the FS CIR and the FI Tx/Rx IQ imbalance using only the training sequences which are already part of WLAN standards. The proposed joint estimation scheme is iterative and can estimate the CIR and FI Tx/Rx IQ imbalance parameters within a few iterations.

The rest of the chapter is now organized as follows. Section 3.2 presents a typical transmission system based on DC architecture in the presence of non-idealities. The proposed iterative solution for joint FS CIR and FI Tx/Rx IQ imbalance estimation is presented in section 3.3. A simple joint FI Tx/Rx IQ imbalance compensation and CIR equalization is presented in section 3.4. Section 3.5 presents the BER performance of the proposed scheme and finally section 3.6 concludes this chapter.

3.2 Signal Model

The diagram of a typical system in the presence of Tx/Rx IQ imbalance is illustrated in Fig. 3.1. It is evident that in the case of lack of orthogonality in the in-phase and quadrature-phase arms of the quadrature mixer the system will suffer from the image problem (as illustrated in section 2.3.3). The transmit and receive filters (i.e. $g_T^{I/Q}(t)$ and $g_R^{I/Q}(t)$) are assumed to be matched perfectly and therefore only FI IQ imbalance is present in the transmitter and receiver. This can severely degrade the performance of the system and effectively limit the achievable SNR.

As already explained in section 2.3.3 there are several ways of representing IQ imbalance in the literature. Throughout this work only the model presented in [26, 31, 34] is employed.

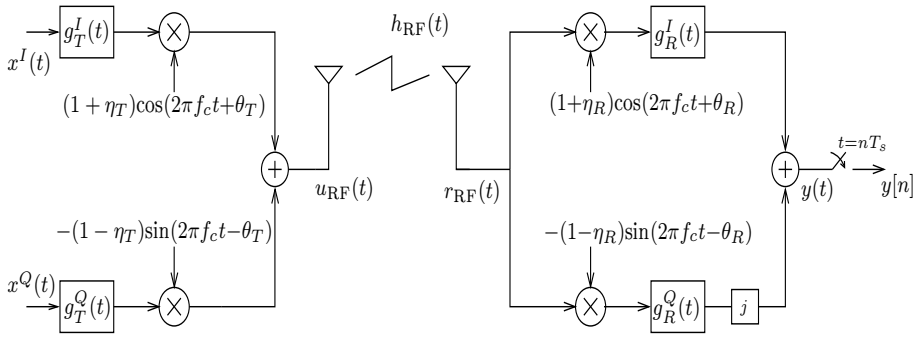

Figure 3.1: The equivalent model of a DC transmitter and receiver in the presence of Tx/Rx IQ imbalance.

The equivalent baseband transmitted signal at the RF front-end is defined as $u(t)$=LPF$\{u_{RF}(t)e^{-j\omega_c t}\}$ where ω_c is the carrier frequency and $u(t)$ is the equivalent complex baseband signal. By simplifying (2.41) to consider only the FI IQ imbalance $u(t)$ can be expressed as

$$u(t) = \mu_T x(t) + \nu_T x^*(t) \tag{3.1}$$

with

$$\begin{aligned} \mu_T &:= \cos\theta_T + j\eta_T \sin\theta_T \\ \nu_T &:= \eta_T \cos\theta_T + j\sin\theta_T \end{aligned} \tag{3.2}$$

where $x(t)$ is the modulated OFDM signal; η_T and θ_T respectively represent the amplitude and phase imbalances present on the transmitter side. From (2.45), the equivalent baseband received signal in the presence of FI Rx IQ imbalance, a FS CIR and additive noise is defined as

$$\begin{aligned} y(t) = \mu_R\Big(\mu_T x(t) + \nu_T x^*(t)\Big) \otimes h(t) \\ + \nu_R\bigg(\Big(\mu_T x(t) + \nu_T x^*(t)\Big) \otimes h(t)\bigg)^* + n(t) \end{aligned} \tag{3.3}$$

where $h(t)$ is the complex baseband equivalent CIR and $n(t)$ is the equivalent complex circularly symmetric additive white Gaussian noise. After baud-rate sampling and removing the cyclic prefix this equation can be rewritten in the matrix notation

$$\mathbf{y} = \underbrace{\mu_R\mu_T}_{\alpha}\mathbf{X}\mathbf{h} + \underbrace{\nu_R\nu_T^*}_{\beta}\mathbf{X}\mathbf{h}^* + \underbrace{\mu_R\nu_T}_{\gamma}\mathbf{X}^*\mathbf{h} + \underbrace{\nu_R\mu_T^*}_{\delta}\mathbf{X}^*\mathbf{h}^* + \mathbf{n} \tag{3.4}$$

where $\mathbf{X}$=circ($\mathbf{F}^H\mathbf{s}$) is the $N\times L_h$ circulant matrix constructed from the transmitted pilot vector $\mathbf{s}$; $\mathbf{h}$ is the $L_h\times 1$ equivalent discrete-time channel impulse response; $\mathbf{n}$ is $N\times 1$ vector of complex additive noise $\mathbf{n} \sim \mathcal{CN}(\mathbf{0}, \sigma_n^2\mathbf{I}_N)$; α, β, γ and δ are complex variables which fully represent the FI Tx/Rx IQ imbalance process. The aim of this work is to estimate these parameters instead of the corresponding amplitude and phase imbalance (i.e. $\theta_{\mathrm{T/R}}, \eta_{\mathrm{T/R}}$). This model completely represents the system input/output relation in the presence of CIR and FI Tx/Rx IQ imbalance. The second term on the right-hand side of the equality is very small in magnitude and so this component can be ignored while estimating the channel and imbalance parameters. The equivalent model used in implementation is thus

$$\mathbf{y} \quad = \alpha\mathbf{X}\mathbf{h} + \gamma\mathbf{X}^*\mathbf{h} + \delta\mathbf{X}^*\mathbf{h}^* + \mathbf{n}. \tag{3.5}$$

The equivalent frequency domain model of (3.5) can be written as

$$\mathbf{y}_f = \mathbf{F}\mathbf{y} = \alpha\mathbf{\Lambda}_h\mathbf{s} + \gamma\mathbf{\Lambda}_h\mathbf{Q}\mathbf{s}^* + \delta\bar{\mathbf{\Lambda}}_h^*\mathbf{Q}\mathbf{s}^* + \mathbf{z} \tag{3.6}$$

where $\mathbf{\Lambda}_h$ is the diagonal CFR matrix (i.e. $\mathbf{\Lambda}_h$=diag($\mathbf{W}\mathbf{h}$)). $\bar{\mathbf{\Lambda}}_h^*$ is also a CFR matrix but conjugated and mirror imaged (i.e. $\bar{\mathbf{\Lambda}}_h^*$=diag($\mathbf{W}\mathbf{h}^*$)) and $\mathbf{z}$ is the equivalent additive noise in the frequency domain.

Now rewriting (3.5) in terms of real and imaginary components

$$\begin{bmatrix} \mathbf{y}^I \\ \mathbf{y}^Q \end{bmatrix} = \begin{bmatrix} \mathbf{X}^I & \mathbf{X}^I & \mathbf{X}^I & -\mathbf{X}^Q & \mathbf{X}^Q & -\mathbf{X}^Q \\ \mathbf{X}^Q & -\mathbf{X}^Q & -\mathbf{X}^Q & \mathbf{X}^I & \mathbf{X}^I & -\mathbf{X}^I \end{bmatrix} \cdot \left(\begin{bmatrix} \alpha^I & -\alpha^Q \\ \gamma^I & -\gamma^Q \\ \delta^I & \delta^Q \\ \alpha^Q & \alpha^I \\ \gamma^Q & \gamma^I \\ -\delta^Q & \delta^I \end{bmatrix} \odot \mathbf{I}_{L_h} \right) \begin{bmatrix} \mathbf{h}^I \\ \mathbf{h}^Q \end{bmatrix} + \begin{bmatrix} \mathbf{n}^I \\ \mathbf{n}^Q \end{bmatrix} \tag{3.7}$$

where superscripts 'I' and 'Q' represent respectively the real and imaginary components of a particular complex variable. So (3.7) can be compactly written as

$$\underline{\mathbf{y}} = \mathbf{X}_1\Big(\mathbf{\Theta}_1 \odot \mathbf{I}_{L_h}\Big)\underline{\mathbf{h}} + \underline{\mathbf{n}} \tag{3.8}$$

where $\mathbf{X}_1$ is the matrix pertaining to the transmitted pilot sequence, $\mathbf{\Theta}_1$ is the matrix pertaining to the effects of the overall IQ imbalance process and $\underline{\mathbf{h}}$ is the real-valued vector of CIR. The expression (3.5) can also be equivalently rewritten as

$$\begin{bmatrix} \mathbf{y}^I \\ \mathbf{y}^Q \end{bmatrix} = \begin{bmatrix} \mathbf{X}^I & \mathbf{X}^I & \text{-}\mathbf{X}^I & \text{-}\mathbf{X}^I & \text{-}\mathbf{X}^Q & \mathbf{X}^Q & \mathbf{X}^Q & \text{-}\mathbf{X}^Q \\ \mathbf{X}^Q & \text{-}\mathbf{X}^Q & \text{-}\mathbf{X}^Q & \mathbf{X}^Q & \mathbf{X}^I & \text{-}\mathbf{X}^I & \mathbf{X}^I & \text{-}\mathbf{X}^I \end{bmatrix} \cdot \begin{bmatrix} \mathbf{h}^I & \mathbf{0} & \mathbf{0} & \mathbf{0} & \mathbf{0} & \mathbf{0} \\ \mathbf{0} & \mathbf{0} & \mathbf{h}^I & \mathbf{0} & \mathbf{h}^I & \mathbf{h}^Q \\ \mathbf{0} & \mathbf{h}^Q & \mathbf{0} & \mathbf{0} & \mathbf{0} & \mathbf{0} \\ \mathbf{0} & \mathbf{0} & \mathbf{0} & \mathbf{h}^Q & \mathbf{0} & \mathbf{0} \\ \mathbf{h}^Q & \mathbf{h}^I & \mathbf{0} & \mathbf{0} & \mathbf{0} & \mathbf{0} \\ \mathbf{0} & \mathbf{0} & \mathbf{0} & \mathbf{0} & \mathbf{0} & \mathbf{0} \\ \mathbf{0} & \mathbf{0} & \mathbf{h}^Q & \mathbf{h}^I & \mathbf{0} & \mathbf{h}^I \\ \mathbf{0} & \mathbf{0} & \mathbf{0} & \mathbf{0} & \mathbf{h}^Q & \mathbf{0} \end{bmatrix} \begin{bmatrix} \alpha^I \\ \alpha^Q \\ \gamma^I \\ \gamma^Q \\ \delta^I \\ \delta^Q \end{bmatrix} + \begin{bmatrix} \mathbf{n}^I \\ \mathbf{n}^Q \end{bmatrix} \tag{3.9}$$

and this can also be compactly written as

$$\underline{\mathbf{y}} = \mathbf{X}_2 \mathbf{A}_{\boldsymbol{h}} \boldsymbol{\theta} + \underline{\mathbf{n}} \tag{3.10}$$

where $\mathbf{0}$ is a zero column vector of appropriate dimensions, $\mathbf{X}_2$ is an alternative representation of the transmitted pilot sequence, $\mathbf{A}_{\boldsymbol{h}}$ is the corresponding matrix pertaining to the CIR and $\boldsymbol{\theta}$=$[\alpha^{\mathrm{I}}\ \alpha^{\mathrm{Q}}\ \gamma^{\mathrm{I}}\ \gamma^{\mathrm{Q}}\ \delta^{\mathrm{I}}\ \delta^{\mathrm{Q}}]^T$. Since the total transmission model of (3.5) can be expressed in two different (but equivalent) set of linear equations (3.8) and (3.10), these equations are termed as a *doubly linear* model of the transmission system. The next section presents an iterative joint FI Tx/Rx IQ imbalance and CIR estimation scheme.

3.3 Channel and IQ Imbalance Estimation

In this section an iterative scheme is discussed which uses the linear models presented in (3.8) and (3.10) to iteratively estimate the CIR and FI Tx/Rx IQ imbalance coefficients α, γ and δ. Using (3.8) the CIR can be estimated as, assuming no IQ imbalance is present in the system,

$$\hat{\underline{\mathbf{h}}} = \left(\mathbf{X}_{\boldsymbol{\theta}}^T \mathbf{X}_{\boldsymbol{\theta}}\right)^{-1} \mathbf{X}_{\boldsymbol{\theta}}^T \underline{\mathbf{y}} \tag{3.11}$$

where $\mathbf{X}_{\boldsymbol{\theta}}=\mathbf{X}_1\left(\boldsymbol{\Theta}_1 \odot \mathbf{I}_{L_h}\right)$. Now that an initial estimation of CIR is available it is possible to find the estimates of the IQ imbalance using (3.10) with the help of the following model

$$\hat{\boldsymbol{\theta}} = \left(\mathbf{X}_{\boldsymbol{h}}^T \mathbf{X}_{\boldsymbol{h}}\right)^{-1} \mathbf{X}_{\boldsymbol{h}}^T \underline{\mathbf{y}} \tag{3.12}$$

where $\mathbf{X}_{\boldsymbol{h}}=\mathbf{X}_2\mathbf{A}_{\boldsymbol{h}}$. The overall scheme is organized in algorithm 1.

Algorithm 1 Joint FI Tx/Rx IQ Imbalance and CIR Estimation. An iterative algorithm for estimating the IQ imbalance and channel using pilot symbols.

1: **input:** $\underline{\mathbf{y}}$
2: **output:** $\underline{\hat{\mathbf{h}}}$ and $\hat{\boldsymbol{\theta}}$
3: **intialization:** $\boldsymbol{\theta}^{(0)} = [1\ 0\ 0\ 0\ 0\ 0]^T$,
which corresponds to the no FI Tx/Rx IQ imbalance case.
4: **calculate:** $\underline{\hat{\mathbf{h}}}^{(0)} = \left(\mathbf{X}_{\hat{\theta}^{(0)}}^T \mathbf{X}_{\hat{\theta}^{(0)}}\right)^{-1} \mathbf{X}_{\hat{\theta}^{(0)}}^T \underline{\mathbf{y}}$ assuming no Tx/Rx IQ imbalance and calculate $\mathbf{X}_{\hat{\boldsymbol{h}}^{(0)}}$ using the model in (3.10)
5: **repeat**
6: calculate

$$\hat{\boldsymbol{\theta}}^{(k)} = \left(\mathbf{X}_{\hat{\boldsymbol{h}}^{(k-1)}}^T \mathbf{X}_{\hat{\boldsymbol{h}}^{(k-1)}}\right)^{-1} \mathbf{X}_{\hat{\boldsymbol{h}}^{(k-1)}}^T \underline{\mathbf{y}} \tag{3.13}$$

7: calculate $\mathbf{X}_{\theta}$ using the estimates of $\boldsymbol{\theta}^{(k)}$ in model of (3.8)
8: LS estimates of CIR

$$\underline{\hat{\mathbf{h}}}^{(k)} = \left(\mathbf{X}_{\hat{\boldsymbol{\theta}}^{(k)}}^T \mathbf{X}_{\hat{\boldsymbol{\theta}}^{(k)}}\right)^{-1} \mathbf{X}_{\hat{\boldsymbol{\theta}}^{(k)}}^T \underline{\mathbf{y}} \tag{3.14}$$

9: calculate $\mathbf{X}_{\hat{\boldsymbol{\theta}}^{(k)}}$ using the model in (3.10) with estimates $\underline{\hat{\mathbf{h}}}^{(k)}$
10: k=k+1
11: **until** No significant improvement in cost function
i.e., $\left\| \underline{\mathbf{y}} - \mathbf{X}_1\left(\hat{\boldsymbol{\Theta}}_1^{(k)} \odot \mathbf{I}_{L_h}\right)\underline{\hat{\mathbf{h}}}^{(k)} \right\| < e$
or maximum numbers of iterations reached.

This is a heuristic approach and it is not easy to show analytically that the these estimates do in fact converge. The proposed estimator is suitable for the scenario when the coherence-time is larger then the symbol duration. For rapidly time-varying channels other frequency domain approaches may be considered.

3.4 Channel and IQ Imbalance Equalization

Using the system model defined in (3.6) it is possible to reformulate the system as

$$\begin{bmatrix} \mathbf{y}_f^I \\ \mathbf{y}_f^I \end{bmatrix} = \begin{bmatrix} \mathbf{\Lambda}_h^I & \mathbf{\Lambda}_h^I\mathbf{Q} & \bar{\mathbf{\Lambda}}_h^I\mathbf{Q} & -\mathbf{\Lambda}_h^Q & \mathbf{\Lambda}_h^Q\mathbf{Q} & -\bar{\mathbf{\Lambda}}_h^Q\mathbf{Q} \\ \mathbf{\Lambda}_h^Q & \mathbf{\Lambda}_h^Q\mathbf{Q} & -\bar{\mathbf{\Lambda}}_h^Q\mathbf{Q} & \mathbf{\Lambda}_h^I & -\mathbf{\Lambda}_h^I\mathbf{Q} & -\bar{\mathbf{\Lambda}}_h^I\mathbf{Q} \end{bmatrix} \cdot \left(\begin{bmatrix} \alpha^I & -\alpha^Q \\ \gamma^I & \gamma^Q \\ \delta^I & \delta^Q \\ \alpha^Q & \alpha^I \\ -\gamma^Q & \gamma^I \\ -\delta^Q & \delta^I \end{bmatrix} \odot \mathbf{I}_N \right) \begin{bmatrix} \mathbf{s}^I \\ \mathbf{s}^Q \end{bmatrix} + \begin{bmatrix} \mathbf{z}^I \\ \mathbf{z}^Q \end{bmatrix}. \tag{3.15}$$

In compact notation this can be expressed as

$$\underline{\mathbf{y}}_f = \mathbb{\Lambda}_{\boldsymbol{h}} \Big(\mathbf{\Theta}_2 \odot \mathbf{I}_N \Big) \underline{\mathbf{s}} + \underline{\mathbf{z}}. \tag{3.16}$$

If we define the overall effect of CIR and FI Tx/Rx IQ imbalance as $\hat{\mathbf{H}} = \mathbb{\Lambda}_{\hat{h}} \Big(\hat{\mathbf{\Theta}}_2 \odot \mathbf{I}_N \Big)$ using the estimates obtained through (3.13) and (3.14) then these effects can be compensated using a simple MMSE equalizer as follows

$$\underline{\mathbf{s}} = \left(\hat{\mathbf{H}}^H \hat{\mathbf{H}} + \sigma_z^2 \mathbf{I}_{2N} \right)^{-1} \hat{\mathbf{H}}^H \underline{\mathbf{y}}_f. \tag{3.17}$$

The BER performance of the proposed equalization is presented in the next section.

3.5 Simulation Results

This chapter is concerned with a typical SISO OFDM system like a WLAN/WiMAX transmission system. The number of subcarriers in each OFDM symbol is N=64. The system bandwidth is assumed to be 20 MHz and the sampling rate is defined as (T_s=0.05μs). The subcarrier spacing is assumed to be ΔF=312.5 kHz. The simulations are based on Rayleigh fading process with a channel memory of L_h=6 taps and an exponential power delay profile $e^{-\underline{\gamma} l}$ with $\underline{\gamma}$=0.2 and l=0, 1, . . . , L_h−1 is considered. To mitigate the effects of inter symbol interference (ISI), the guard

interval is assumed to be longer than the CIR, i.e. N_g=10. The transmitted data is assumed to be taken from a 16 QAM constellation and no channel coding is used in these simulations. Each OFDM block contains 10 OFDM symbols. The first symbol of each block is a known training sequence chosen from a BPSK constellation according to the criterion presented in [31]. The IQ imbalance process defined in (3.2) is assumed to be a random variable with uniformly distributed amplitude imbalance, $\eta_{T/R} \sim \mathcal{U}$[-0.05, 0.05], and phase imbalance, $\theta_{T/R} \sim \mathcal{U}[-5^\circ, 5^\circ]$. Similar models have been used in [31, 34, 44]. An independent realization of CIR and FI Tx/Rx IQ imbalance coefficients is generated for every OFDM block.

The BER performance for the uncoded 16 QAM modulation scheme using our proposed solution is presented in Fig. 3.2. It can be seen that in the case of ignoring IQ imbalance the BER performance of the system suffers a BER floor in the moderate and high SNR region. For further comparison a simple scheme based on algorithm 1 is implemented where only FI RX IQ imbalance is assumed (to be present and compensated for) in the system . The simulation results show that this system also suffers from a performance floor when Tx IQ imbalance is not taken into account. The BER performance of the proposed iterative scheme is within a 1 dB range of the ideal case for the system under consideration. From the simulation results it is evident that even in the case of severe IQ imbalance, near ideal BER performance can be obtained within a few iterations of the estimation process.

The proposed method provides near optimal BER performance after only one iteration of estimation process. Each iteration requires inversion of two real square matrices of dimension $2L_h$ and 6 respectively.

3.6 Conclusions

In this chapter a joint estimation of CIR and FI Tx/Rx IQ imbalance has been studied specifically for OFDM systems. A simple iterative process has been devised using a doubly linear model of the transmission system in the presence of FI Tx/Rx IQ imbalance and FS CIR. The proposed scheme can effectively estimate the CIR and the FI Tx/Rx IQ imbalance with a few iterations. Simulation results show that the proposed scheme performs equally well when IQ imbalance exists on either one or both sides of the system. The proposed scheme blends seamlessly with the WLAN standard but it can be adapted to any other OFDM transmission standard. The proposed scheme uses ordinary training sequences already defined in the WLAN standards. Simulation results show that the proposed scheme is

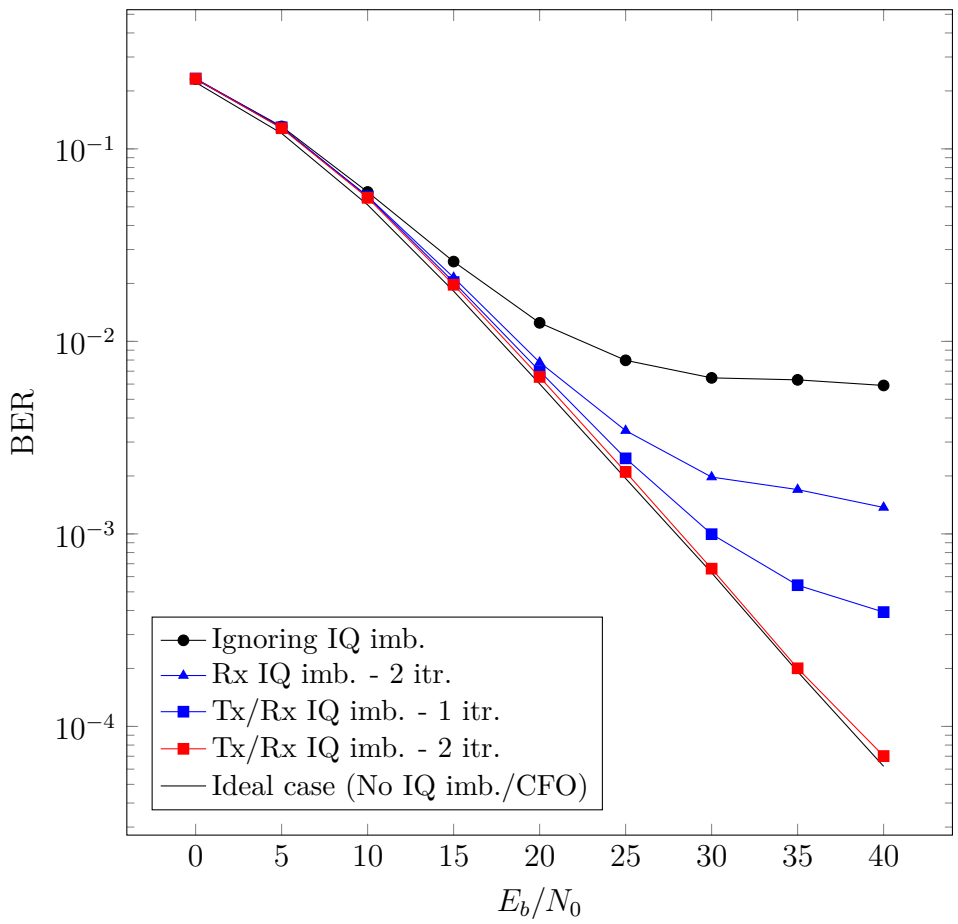

Figure 3.2: BER performance of the proposed scheme (3.17) using CIR and FI Tx/Rx IQ imbalance estimation schemes of (3.11) and (3.12), 16 QAM, N=64, $\eta_{\mathrm{T/R}} \sim \mathcal{U}[-0.05, 0.05]$, $\theta_{\mathrm{T/R}} \sim \mathcal{U}[-5^\circ, 5^\circ]$, Rayleigh channel with L_h=6 taps and 5,000 Monte-Carlo realizations.

equally effective not only in the case of severe FI Tx/Rx IQ imbalance but also in higher-order constellation schemes.

We have also proposed a low complexity single stage joint Tx/Rx IQ imbalance compensation and CIR equalization scheme which can effectively deal with IQ imbalance and a FS CIR. The simulation results show that the proposed schemes provide an excellent performance/complexity trade-off.

4 Joint CIR, CFO, DCO and FI/FS Rx IQ Imbalance Estimation

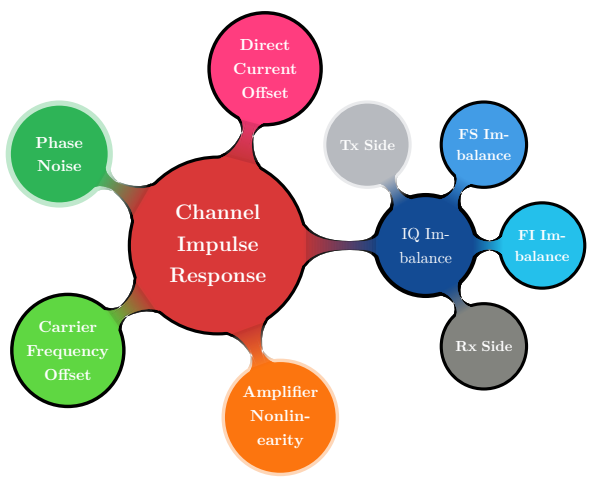

Abstract

The objective of this chapter is to design a receiver architecture which can jointly estimate the FS CIR, FI/FS Rx IQ imbalance, CFO and DCO using long training sequences. All of these problems are typical for low cost RF front-ends. This chapter proposes a set of two scalable solutions to estimate CFO whereas FS CIR and FI/FS Rx IQ imbalance are estimated in tandem through a closed form expression.

A low complexity single stage equalizer is also proposed which can mitigate the effects of CFO and equalize the CIR along with FI/FS IQ imbalance in a single step. The proposed solutions are also extended to MIMO-OFDM systems.

The simulation results illustrate that solutions proposed in this chapter provide an excellent performance/complexity trade-off.

4.1 Introduction

As previously stated, direct conversion RF front-ends are ideally suited for low cost devices. Unfortunately these low cost front-ends suffer from problems like IQ imbalance, CFO, DCO and PN.

The problem of IQ imbalance becomes much more sensitive when dealing with broad bandwidth systems (such as WLAN, WiMAX and LTE). As already explained in Chapter 2, FS IQ imbalance and FS CIR are closely intertwined. It is possible to decouple these problems and estimate them one by one, but commonly these parameters are estimated simultaneously.

Several methods have been proposed to estimate Tx/Rx IQ imbalance in OFDM systems and [27] presented an LMS scheme which estimates FI/FS Rx IQ imbalance. The convergence performance of this scheme depends on the choice of adaptation step-size. The estimate of FI IQ imbalance and CIR for OFDM systems has been considered using pre- and post-FFT processing [43]. The authors have used the frequency domain model of channel and IQ imbalance to create a set of linear equations with the help of special training symbols. This scheme exploits the fact that in the presence of IQ imbalance in an OFDM system each subcarrier effects its (frequency domain) mirror image. The main drawback of this scheme is that it requires several (ten or more) OFDM symbols to adaptively estimate both IQ imbalance and the channel coefficients. In addition, these symbols are non-standard and so may not be useful in estimating other system parameters such as timing offset, PN or CFO. Another adaptive scheme has been proposed by [32] for joint estimation of CFO, FI Tx/Rx IQ imbalance and CIR. However, all of these schemes are computationally complex and require several training sequences to converge to a reliable estimate. These schemes also do not exploit the fact that by reducing the number of unknowns the complexity of the receiver can be minimized.

The idea of joint IQ imbalance and CIR estimation for an OFDM system has been considered in [31] where the authors have designed an optimal training sequence to jointly estimate FS IQ imbalance and the channel (as a set of two independent channels related to the useful and the interfering signal). A non-linear least square (NLLS) estimation of CFO and FS IQ imbalance has been proposed by [28]. More recently [50], some authors have proposed a simple and robust joint CIR, FI Rx IQ imbalance and CFO estimation for MIMO-OFDM systems. This scheme also uses the LTS sequences available in WLAN standards. But this scheme too is limited to FI IQ imbalance and does not consider the FS

imbalance model which is essential in broad bandwidth systems such as WLAN and WiMax.

The joint estimation of FS CIR, IQ imbalance and DCO has been studied by [35, 37]. Both these authors have used a simple LS solution to estimate FS CIR, FI Rx IQ imbalance and DCO.

This chapter concerns a low complexity joint CIR, CFO, DCO and IQ imbalance estimation for an OFDM system. In contrast to other works proposed in the literature which require many training symbols, this scheme can estimate the CIR and the IQ imbalance using only the training sequences which are already part of WLAN standards. The proposed joint estimation scheme is very simple and robust. Another advantage of the proposed system is that it can perform CIR estimation for FI/FS IQ imbalance in the presence of FS CIR regardless of the delay spread of the LPF impulse responses (see Fig. 4.1) as long as a sufficiently long guard interval is ensured and an appropriate CIR length is considered for estimation.

The rest of the chapter is now organized as follows. Section 4.2 presents the model of a typical DC receiver in the presence of non-ideal behaviour. The proposed optimal and reduced complexity solutions for joint FS IQ imbalance, CIR and CFO estimation are presented in section 4.3. Section 4.4 presents the scheme for joint CFO, IQ imbalance mitigation, CIR equalization and data detection. In section 4.5 the system is reconsidered in the presence of DCO in addition to CFO, IQ imbalance and CIR. Section 4.6 provides straight-forward extension of the proposed scheme to the spatially multiplexed MIMO scenario. Section 4.7 presents the MSE and BER performance of the proposed schemes and section 4.8 concludes this chapter.

4.2 Signal Model

The typical diagram of a DC receiver front-end is illustrated in Fig. 4.1. It is obvious that in the case of lack of orthogonality in the in-phase and quadrature-phase arms of the IQ receiver the system will suffer from the image problem. This can severely degrade the performance of the receiver and effectively limit the achievable SNR. A low cost LO can also introduce a linear frequency offset to the received data sequence and so it will further degrade the performance of the receiver. These problems motivate us to design a simple yet robust receiver architecture which can handle the effects of this non-ideal behaviour and improve the operating SNR even in presence of severe IQ imbalance, CFO and DCO.

This work is organized as follows. Sections 4.2 , 4.3 and 4.4 do not consider the presence of DCO. The problem of DCO is considered specifically in section 4.5. Section 4.6 extends the proposed solutions to spatially multiplexed systems.

The IQ imbalance occurs due to unequal amplitude and phase gains in the I and Q branch of the DC device. There are several ways of representing IQ imbalance in the literature and as has already been stated in Chapter 2 only the symmetric model as defined in [26, 43] is considered here. The received signal at the RF front-end is defined as $r_{RF}(t)=\Re\{r(t)e^{j\omega_c t}\}$ where ω_c is the carrier frequency and $r(t)$ is the equivalent complex baseband signal defined as $r(t):=c(t)\otimes x(t)+n(t)$, where $x(t)$ is the baseband equivalent of transmitted RF signal, $c(t)$ is the equivalent transmission channel and $n(t)$ is the equivalent zero mean white noise. As illustrated in Fig. 4.1 the LPF gains of the I and Q branches are not matched exactly. The received signals in the I and Q branch in the presence of FS IQ imbalance are given as

$$\begin{aligned} y^I(t) =&(1+\eta)[\cos(2\pi\Delta f t-\theta)\cdot r^I(t) \\ &-\sin(2\pi\Delta f t-\theta)\cdot r^Q(t)]\otimes g^I(t) \qquad (4.1) \\ y^Q(t) =&(1-\eta)[\sin(2\pi\Delta f t+\theta)\cdot r^I(t) \\ &+\cos(2\pi\Delta f t+\theta)\cdot r^Q(t)]\otimes g^Q(t) \qquad (4.2) \end{aligned}$$

where superscript I/Q represents the real and imaginary components of a complex signal, η[1] represents the amplitude imbalance, θ is the phase imbalance, Δf is the CFO introduced by the LO, and $g^I(t)$ and $g^Q(t)$ are the impulse responses of the LPF's in the in-phase and quadrature-phase branches respectively. In the case of FI IQ imbalance then $g^I(t)=g^Q(t) = g(t)$. So from (4.1) and (4.2), the

[1]Since only Rx IQ imbalance is considered, the subscripts 'T/R' have been dropped, for the rest of this chapter.

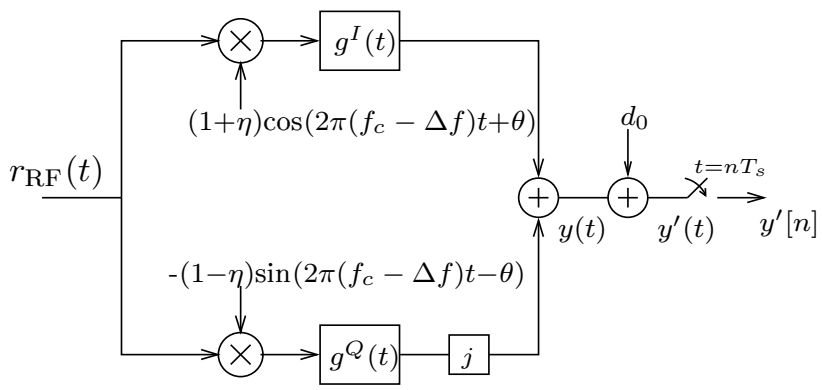

Figure 4.1: The equivalent model of a DC receiver in the presence of FS IQ mismatch, DCO and CFO.

output of the DC receiver in Fig. 4.1 is:

$$\begin{aligned} y(t) =& y^I(t) + jy^Q(t) \\ =& \Big[(\cos\theta - j\eta\sin\theta)\left(\frac{g^I(t)+g^Q(t)}{2}\right) \\ &+ (\eta\cos\theta - j\sin\theta)\left(\frac{g^I(t)-g^Q(t)}{2}\right)\Big] \otimes r(t)e^{j2\pi\Delta ft} \\ &+ \Big[(\eta\cos\theta + j\sin\theta)\left(\frac{g^I(t)+g^Q(t)}{2}\right) \\ &+ (\cos\theta + j\eta\sin\theta)\left(\frac{g^I(t)-g^Q(t)}{2}\right)\Big] \otimes r^*(t)e^{-j2\pi\Delta ft}. \end{aligned} \tag{4.3}$$

Re-writing the filter mismatch terms in (4.3) yields

$$\begin{aligned} k^1(t) &:= \frac{g^I(t)+g^Q(t)}{2} \\ k^2(t) &:= \frac{g^I(t)-g^Q(t)}{2}. \end{aligned} \tag{4.4}$$

Similarly, the complex amplitude and phase mismatches in (4.3) are defined as follows

$$\begin{aligned} \mu &:= \cos\theta - j\eta\sin\theta \\ \nu &:= \eta\cos\theta + j\sin\theta. \end{aligned} \tag{4.5}$$

In the absence of IQ imbalance (i.e. θ=η=0), then $\mu = 1$ and $\nu = 0$. Now, from (4.3), (4.4) and (4.5) the received signal can be defined as

$$\begin{aligned} y(t) =& h^D(t) \otimes \Big(c(t) \otimes x(t) \Big) e^{j2\pi\Delta f t} \\ &+ h^I(t) \otimes \Big(c^*(t) \otimes x^*(t) \Big) e^{\text{-}j2\pi\Delta f t} + \tilde{n}(t) \end{aligned} \tag{4.6}$$

where

$$\begin{aligned} h^D(t) &= \mu k^1(t) + \nu^* k^2(t) \\ h^I(t) &= \nu k^1(t) + \mu^* k^2(t) \end{aligned} \tag{4.7}$$

and $\tilde{n}(t)$=$\Big(h^D(t) e^{j2\pi\Delta f t} + h^I(t) e^{\text{-}j2\pi\Delta f t} \Big) \otimes n(t)$. Here $h_\mu(t)$:=$h^D(t) \otimes c(t)$ and $h_\nu(t)$:=$h^I(t) \otimes c^*(t)$ are the equivalent overall channel models pertaining to the desired and image signals respectively [28]. A detailed formulation of the desired and interfering channels was also presented in Chapter 2. A step by step derivation of the above proposition is also presented in Appendix A. The received signal after sampling at the baud rate $(1/T_s)$ and cyclic prefix removal can be written as

$$\mathbf{y}^{(i)} = \mathbf{E}^{(i)} \mathbf{X}_c \mathbf{h}_\mu + \mathbf{E}^{(i)^*} \mathbf{X}_c^* \mathbf{h}_\nu + \mathbf{n}^{(i)} \tag{4.8}$$

where 'i' is the symbol index and $\mathbf{E}^{(i)}$=diag$(\{e^{j\frac{2\pi}{N}\epsilon[(i-1)(N+N_g)+N_g+n]}\}_{n=0}^{N-1})$, is the CFO process affecting the $i-$th OFDM symbol; N and N_g are respectively the size of the OFDM symbol and the cyclic prefix; ϵ is the CFO coefficient normalized to the subcarrier spacing, i.e. ϵ=$T\Delta f$ (T=NT_s); $\mathbf{n}^{(i)} \sim \mathcal{CN}(\mathbf{0}, \sigma_n^2 \mathbf{I}_N)$ is the circularly symmetric complex additive white Gaussian noise; $\mathbf{X}_c$ is the $N \times L'$ circulant matrix constructed from the transmitted OFDM pilot symbols, i.e., $\mathbf{x}$=$\mathbf{F}^H\mathbf{s}$, where $\mathbf{s}$ is the known pilot symbol vector of size $N \times 1$; $\mathbf{h}_\mu$ and $\mathbf{h}_\nu$ are respectively the equivalent overall CIRs pertaining to the useful and the interfering signals in (4.8). The impulse response of the useful and the interfering channels can be of any arbitrary lengths. However, for simplicity these channels are assumed to be of the same length, i.e., $L' \geq L_h + L_g + 1$, where L_h and L_g are the respective lengths of the equivalent discrete-time CIR ($\mathbf{h}$) and the two LPF's in Fig. 4.1. In practice the normalized CFO can take any value of offset, which can then be decomposed into integer and fractional parts, namely ϵ=τ+ϕ, where τ and ϕ are respectively integer and fractional, i.e. $-1 \leq \phi \leq 1$. However

in practice the maximum detectable range of the CFO using a LTS is defined as $|\phi|<N/2(N+N_g)$ [78]. In the literature, several schemes are available which can estimate the integer and fractional part of the CFO process. However the scope of this work is limited to only the fractional part of the CFO.

In this next section an optimal joint IQ imbalance, FS CIR and the CFO estimation scheme is presented. Subsequently, a reduced complexity scheme (RCS) is also proposed which provides a good complexity/performance trade-off.

4.3 Parameter Estimation

In this section two estimation schemes are proposed. The first scheme is the non-linear least squares (NLLS) scheme which is the optimal scheme but it is computationally intensive. Subsequently a suboptimal joint estimation scheme is proposed which provides acceptable estimates of system parameters with much lower implementation complexity.

4.3.1 Nonlinear Least Squares Method

The devised strategy is based on (as defined in the IEEE 802.11 WLAN standard) two LTS training sequences in the first two symbols of an OFDM block (i.e. $i=1,2$). So (4.8) becomes

$$\underbrace{\begin{bmatrix}\mathbf{y}^{(1)}\\ \mathbf{y}^{(2)}\end{bmatrix}}_{\bar{\mathbf{y}}} = \underbrace{\begin{bmatrix}\hat{\mathbf{E}}^{(1)}\mathbf{X}_c & (\hat{\mathbf{E}}^{(1)}\mathbf{X}_c)^*\\ \hat{\mathbf{E}}^{(2)}\mathbf{X}_c & (\hat{\mathbf{E}}^{(2)}\mathbf{X}_c)^*\end{bmatrix}}_{\mathbf{A}_\phi}\begin{bmatrix}\mathbf{h}_\mu\\ \mathbf{h}_\nu\end{bmatrix} + \underbrace{\begin{bmatrix}\mathbf{n}^{(1)}\\ \mathbf{n}^{(2)}\end{bmatrix}}_{\bar{\mathbf{n}}} \tag{4.9}$$

where $\hat{\mathbf{E}}^{(i)}$ is the estimate of $\mathbf{E}^{(i)}$ in (4.8) via (4.11) and (4.18). The LS channel estimates (given the CFO estimates) are:

$$\begin{bmatrix}\hat{\mathbf{h}}_\mu\\ \hat{\mathbf{h}}_\nu\end{bmatrix} = \left(\mathbf{A}_{\hat{\phi}}^H\mathbf{A}_{\hat{\phi}}\right)^{-1}\mathbf{A}_{\hat{\phi}}^H\bar{\mathbf{y}}. \tag{4.10}$$

The NLLS estimate of the CFO process can then be found from

$$\hat{\phi}_{\text{opt}} = \arg\max_{\phi} \quad \bar{\mathbf{y}}^H\mathbf{A}_\phi(\mathbf{A}_\phi^H\mathbf{A}_\phi)^{-1}\mathbf{A}_\phi^H\bar{\mathbf{y}} \tag{4.11}$$

where maximization is performed via a grid search. Using the estimates of ϕ from (4.18) as an initial search point in (4.11) the search convergence time can be

minimized. The NLLS scheme yields optimal CFO and joint channel estimates at the expense of additional complexity.

4.3.2 Reduced Complexity Scheme

In this section a simple solution is proposed for joint estimation of CFO, FI/FS IQ imbalance and FS CIR using a frequency domain model. The model of (4.8) can now be equivalently rewritten in the frequency domain notation as

$$\mathbf{y}_f^{(i)} = \mathbf{F}\mathbf{y}^{(i)} = \mathbf{P}^{(i)}\mathbf{S}\mathbf{W}\mathbf{h}_\mu + \mathbf{P}^{(i)^H}\mathbf{Q}\mathbf{S}^H\mathbf{W}^*\mathbf{h}_\nu + \mathbf{z}^{(i)} \tag{4.12}$$

where $\mathbf{S}$=diag($\mathbf{s}$) is the known pilot sequence; $\mathbf{Q}$ is the permutation matrix defined as $\mathbf{Q} = \mathbf{F}\mathbf{F}^T$; $\mathbf{z}^{(i)}$=$\mathbf{F}\mathbf{n}^{(i)}$; $\mathbf{P}^{(i)}$ is the circulant matrix of the CFO process which is defined as $\mathbf{P}^{(i)}$=$\mathbf{F}\mathbf{E}^{(i)}\mathbf{F}^H$ [18]. Decomposing this expression further we get

$$\begin{aligned}\mathbf{y}_f^{(i)} = {} & p_0^{(i)}\mathbf{S}\mathbf{W}\mathbf{h}_\mu + {p_0^{(i)}}^*\mathbf{Q}\mathbf{S}^H\mathbf{W}^*\mathbf{h}_\nu \\ & + \mathbf{P}_{\mathrm{ICI}}^{(i)}\mathbf{S}\mathbf{W}\mathbf{h}_\mu + {\mathbf{P}_{\mathrm{ICI}}^{(i)}}^*\mathbf{Q}\mathbf{S}^H\mathbf{W}^*\mathbf{h}_\nu + \mathbf{z}^{(i)}\end{aligned} \tag{4.13}$$

where $\mathbf{P}^{(i)}$=$p_0^{(i)}\mathbf{I}_N + \mathbf{P}_{\mathrm{ICI}}^{(i)}$ and $p_0^{(i)}$=$e^{j\frac{2\pi}{N}\epsilon[(i-1)(N+N_g)+N_g+\frac{N}{2}]}$ is the mean value of the CFO process (i.e. CPR), while $\mathbf{P}_{\mathrm{ICI}}^{(i)}$ is the ICI component of the CFO which is caused by the spectral leakage of adjacent subcarriers. Taking the data dependent interference and additive noise into account it is possible to re-write (4.13) as

$$\mathbf{y}_f^{(i)} = \mathbf{S}\mathbf{W}\underrightarrow{\mathbf{h}}_\mu^{(i)} + \mathbf{Q}\mathbf{S}^H\mathbf{W}^*\underrightarrow{\mathbf{h}}_\nu^{(i)} + \tilde{\mathbf{z}}^{(i)} \tag{4.14}$$

where $\underrightarrow{\mathbf{h}}_\mu^{(i)} = p_0^{(i)}\mathbf{h}_\mu$, $\underrightarrow{\mathbf{h}}_\nu = {p_0^{(i)}}^*\mathbf{h}_\nu$ and $\tilde{\mathbf{z}}^{(i)}$ is the sum of the remaining interfering terms in (4.13). So

$$\mathbf{y}_f^{(i)} = \underbrace{\begin{bmatrix}\mathbf{S}\mathbf{W} & \mathbf{Q}\mathbf{S}^H\mathbf{W}^*\end{bmatrix}}_{\mathbf{A}} \begin{bmatrix}\underrightarrow{\mathbf{h}}_\mu^{(i)} \\ \underrightarrow{\mathbf{h}}_\nu^{(i)}\end{bmatrix} + \tilde{\mathbf{z}}^{(i)}.$$

A simple least-squares estimator can determine the modified CIR as

$$\begin{bmatrix}\hat{\underrightarrow{\mathbf{h}}}_\mu^{(i)} \\ \hat{\underrightarrow{\mathbf{h}}}_\nu^{(i)}\end{bmatrix} = \left(\mathbf{A}^H\mathbf{A}\right)^{-1}\mathbf{A}^H\mathbf{y}_f^{(i)}. \tag{4.15}$$

Note that this estimator does not require any matrix inversion during run-time, as the pilot sequence is known *a-priori* at the receiver. The LS estimates of $\underset{\rightarrow}{\mathbf{h}}_{\mu}^{(i)}$ and $\underset{\rightarrow}{\mathbf{h}}_{\nu}^{(i)}$ are obtained using the two LTS sequences which are defined in the IEEE 802.11 standards. Assuming that the CIR does not change within a transmission frame and all OFDM symbols are affected by same CFO coefficient[2], it can be easily shown that we can estimate the CFO as

$$\hat{\phi} = \quad \arg\min_{\phi} \underbrace{\left\| \underset{\rightarrow}{\hat{\mathbf{h}}}_{\mu}^{(1)} - e^{j\kappa\phi} \underset{\rightarrow}{\hat{\mathbf{h}}}_{\mu}^{(2)} \right\|^2}_{L(\phi)}, \tag{4.16}$$

where $\kappa{=}2\pi(N{+}N_g)/N$. The solution of (4.16) can be found through differentiation

$$\begin{aligned} \frac{\partial L(\phi)}{\partial \phi} &= je^{-j\kappa\phi} \underset{\rightarrow}{\mathbf{h}}_{\mu}^{(1)^H} \underset{\rightarrow}{\mathbf{h}}_{\mu}^{(2)} - je^{j\kappa\phi} \underset{\rightarrow}{\mathbf{h}}_{\mu}^{(2)^H} \underset{\rightarrow}{\mathbf{h}}_{\mu}^{(1)} \\ &= 2\Re\{je^{-j\kappa\phi} \underset{\rightarrow}{\mathbf{h}}_{\mu}^{(1)^H} \underset{\rightarrow}{\mathbf{h}}_{\mu}^{(2)}\} \\ &= \sin(\kappa\phi)\Re\{\underset{\rightarrow}{\mathbf{h}}_{\mu}^{(1)^H} \underset{\rightarrow}{\mathbf{h}}_{\mu}^{(2)}\} - \cos(\kappa\phi)\Im\{\underset{\rightarrow}{\mathbf{h}}_{\mu}^{(1)^H} \underset{\rightarrow}{\mathbf{h}}_{\mu}^{(2)}\} = 0 \end{aligned} \tag{4.17}$$

where functions $\Re\{\cdot\}$ and $\Im\{\cdot\}$ respectively yield the real and imaginary component of a variable, the superscript indices represent the CIR estimate from LTS sequences i.e. $(i{=}1,2)$ respectively. The solution of (4.16) is

$$\hat{\phi} = \frac{1}{\kappa}\tan^{-1}\left(\frac{\Im\{\underset{\rightarrow}{\mathbf{h}}_{\mu}^{(1)^H} \underset{\rightarrow}{\mathbf{h}}_{\mu}^{(2)}\}}{\Re\{\underset{\rightarrow}{\mathbf{h}}_{\mu}^{(1)^H} \underset{\rightarrow}{\mathbf{h}}_{\mu}^{(2)}\}}\right) \quad -\frac{1}{2} \leq \phi \leq \frac{1}{2}. \tag{4.18}$$

The performance of this scheme suffers from residual interference in the high SNR region since the data dependent interference (see (4.13) and (4.14)) has been ignored. Once the CFO is known then the CIR can be estimated as in (4.10).

The next section presents a joint single step CIR and impairment mitigation scheme.

[2]This may not be true in the case of cellular uplink scenario.

4.4 Single Stage CFO, IQ Imbalance and Channel Equalization

In contrast to previously proposed schemes which compensate IQ imbalance, CFO and CFR in multiple steps, [48, 49], a single stage equalization technique is proposed to compensate IQ imbalance, CFO and equalize the channel in the frequency domain. The conventional FI IQ imbalance can be compensated from the received signal in (4.8) (as [50])

$$\mathbf{y}^{\mathrm{I/Q}} = \mu^{-1}\left[\frac{\mathbf{y} - \frac{\nu}{\mu^*}\mathbf{y}^*}{1 - \left|\frac{\nu}{\mu}\right|^2}\right] \tag{4.19}$$

where $\mathbf{y}^{\mathrm{I/Q}}$ is the time domain sequence after IQ imbalance compensation where symbol index 'i' has been dropped in (4.8). This scheme is limited to the case when IQ imbalance is FI and the equivalent base-band channel will be estimated after both IQ imbalance and CFO are compensated. However in the case of FS IQ imbalance it is possible to estimate the CIR and FS IQ imbalance jointly using (4.10) and estimate the CFO using (4.18). Therefore channel equalization, CFO and IQ imbalance compensation can be performed in a single step. Re-writing (4.8) in the frequency domain we have

$$\mathbf{y}_f = \mathbf{P}\mathbf{\Lambda}_\mu \mathbf{s} + \mathbf{P}^H \mathbf{\Lambda}_\nu \mathbf{Q}\mathbf{s}^* + \mathbf{z}. \tag{4.20}$$

where $\mathbf{\Lambda}_\mu$ and $\mathbf{\Lambda}_\nu$ are diagonal matrices of the desired and interfering CIR $(\mathbf{h}_\mu, \mathbf{h}_\nu)$ respectively. Using (4.19) with (4.20) it is not difficult to show that a joint channel, CFO and IQ imbalance equalizer can be devised as

$$\hat{\mathbf{s}} = \left(\mathbf{I}_N - \mathbf{\Lambda}_{\hat{\nu}}\mathbf{Q}\mathbf{\Lambda}_{\hat{\mu}}^{-*}\mathbf{\Lambda}_{\hat{\nu}}^{*}\mathbf{Q}\mathbf{\Lambda}_{\hat{\mu}}^{-1}\right)^{-1}\left[\mathbf{\Lambda}_{\hat{\mu}}^{-1}\hat{\mathbf{P}}^H\left(\mathbf{y}_f - \mathbf{\Lambda}_{\hat{\nu}}\mathbf{Q}\mathbf{\Lambda}_{\hat{\mu}}^{-*}\mathbf{y}_f^*\right)\right] \tag{4.21}$$

where $\mathbf{\Lambda}_{\hat{\mu}}$, $\mathbf{\Lambda}_{\hat{\nu}}$ are the estimated diagonal matrices obtained from (4.10) and $\hat{\mathbf{P}}$ is the circulant matrix constructed from the estimated CFO process obtained from (4.18).

Implementation of the above equalizer is low complexity as it does not require matrix inversion (the $(\cdot)^{-1}$ term in (4.21) is a diagonal matrix). We compare performance of these techniques with the well-cited joint channel, CFO and FS IQ imbalance estimation schemes. The complexity of the joint CFO, FI Rx IQ imbalance estimation scheme proposed in [50] is of the order of $\mathcal{O}(N)$, however the scope of this scheme is limited to FI IQ imbalance only. The adaptive estimators

(capable of estimating FI/FS IQ imbalance) proposed in the references [32, 43] require at least 10 long pilot symbols to converge to a reliable estimate. The complexity of these schemes is of the order $K\mathcal{O}(N^2)$, where K is the number of training symbols. The proposed scheme provides a closed-form expression for joint estimation of CIR, CFO and FI/FS IQ imbalance process with complexity order of $2\mathcal{O}(NL'^2)$, where L' is the length of the equivalent CIRs as defined for (4.8). In the case when $L' \ll N$, then the complexity of the proposed scheme is far less than other adaptive channel estimation schemes.

4.5 DCO Estimation

In section 4.3 and 4.4 the DCO has not been considered. In this section a simple strategy is devised to eliminate the DCO when the CFO and the FI/FS IQ imbalance are all present in the system . As explained in section 2.3.4, DCO can be modelled as a complex constant which exists at the output of the DC receiver as illustrated in Fig. 4.1. The received signal in the presence of DCO can be defined as

$$\mathbf{y}'^{(i)} = \mathbf{E}^{(i)}\mathbf{X}_c\mathbf{h}_\mu + \mathbf{E}^{(i)^*}\mathbf{X}_c^*\mathbf{h}_\nu + d_0\mathbf{1} + \mathbf{n}^{(i)} \tag{4.22}$$

where $\mathbf{1}$ is $N\times 1$ vector with all elements being one, the frequency domain equivalent of the received signal can be written as

$$\mathbf{y}_f'^{(i)} = \mathbf{P}^{(i)}\mathbf{S}\mathbf{W}\mathbf{h}_\mu + \mathbf{P}^{(i)^H}\mathbf{Q}\mathbf{S}^H\mathbf{W}^*\mathbf{h}_\nu + d_0\mathbf{e} + \mathbf{z}^{(i)} \tag{4.23}$$

where $\mathbf{e}=[\sqrt{N}, 0, \ldots, 0]^T$ is a $N\times 1$ vector with only one non-zero element. Now taking into account the DCO, the modified channel estimates can be obtained from

$$\mathbf{y}_f'^{(i)} = \underbrace{\begin{bmatrix}\mathbf{S}\mathbf{W} & \mathbf{Q}\mathbf{S}^H\mathbf{W}^* & \mathbf{e}\end{bmatrix}}_{\mathbf{A}'} \begin{bmatrix}\vec{\mathbf{h}}_\mu^{(i)} \\ \vec{\mathbf{h}}_\nu^{(i)} \\ d_0\end{bmatrix} + \tilde{\mathbf{z}}^{(i)}. \tag{4.24}$$

Using the estimates of the modified CIR ($\vec{\mathbf{h}}_\mu^{(i)}$) from two consecutive pilot symbols then the estimates of CFO can be obtained through (4.18). Now using these estimates in the modified version of (4.9), the estimates of desired and interfering CIRs and DCO can be conveniently obtained through the LS solution

of the following model

$$\underbrace{\begin{bmatrix}\mathbf{y}'^{(1)}\\ \mathbf{y}'^{(2)}\end{bmatrix}}_{\bar{\mathbf{y}}'} = \underbrace{\begin{bmatrix}\hat{\mathbf{E}}^{(1)}\mathbf{X}_c & (\hat{\mathbf{E}}^{(1)}\mathbf{X}_c)^* & \mathbf{1}\\ \hat{\mathbf{E}}^{(2)}\mathbf{X}_c & (\hat{\mathbf{E}}^{(2)}\mathbf{X}_c)^* & \mathbf{1}\end{bmatrix}}_{\mathbf{A}'_\phi}\begin{bmatrix}\mathbf{h}_\mu\\ \mathbf{h}_\nu\\ d_0\end{bmatrix} + \underbrace{\begin{bmatrix}\mathbf{n}^{(1)}\\ \mathbf{n}^{(2)}\end{bmatrix}}_{\bar{\mathbf{n}}'}. \tag{4.25}$$

The overall estimation accuracy can be improved further using the NLLS technique as defined in Section 4.3.

4.6 Extension to MIMO Systems

A low complexity FI/FS Rx IQ imbalance, CFO and FS CIR estimation technique has been established in sections 4.2 and 4.3. This section extends the previously presented models to a (spatial multiplexing) MIMO system. The extension of SISO schemes to the MIMO case is straight forward and near optimal estimation performance can be achieved for all parameters. For the MIMO system it is assumed that each receiver antenna suffers from unique IQ imbalance and CFO parameters. It is assumed that the number of receive antenna N_R is equal or more than the number of transmit antenna N_T i.e ($N_R \geq N_T$) with j=1, . . . , N_R and k=1, . . . , N_T. In this implementation the CIRs between all of the transmission links are assumed to be statistically independent without any loss of generality. Like previous sections this model is also limited only to IQ imbalance originating at the receiver side. In the case of FI IQ imbalance the received signal vector at the j-th receive antenna for the i-th OFDM symbol is defined as

$$\begin{aligned}\mathbf{y}^{\langle j\rangle,(i)} = {} & \mu^{\langle j\rangle}\mathbf{E}^{\langle j\rangle,(i)}\mathbf{X}_c^{\langle 1\rangle,(i)}\mathbf{h}^{\langle j,1\rangle} + \nu^{\langle j\rangle}\left(\mathbf{E}^{\langle j\rangle,(i)}\mathbf{X}_c^{\langle 1\rangle,(i)}\mathbf{h}^{\langle j,1\rangle}\right)^* + \\ & + \mu^{\langle j\rangle}\mathbf{E}^{\langle j\rangle,(i)}\mathbf{X}_c^{\langle 2\rangle,(i)}\mathbf{h}^{\langle j,2\rangle} + \nu^{\langle j\rangle}\left(\mathbf{E}^{\langle j\rangle,(i)}\mathbf{X}_c^{\langle 2\rangle,(i)}\mathbf{h}^{\langle j,2\rangle}\right)^* + \\ & \qquad\qquad \cdots\cdots\cdots \\ & + \mu^{\langle j\rangle}\mathbf{E}^{\langle j\rangle,(i)}\mathbf{X}_c^{\langle N_T\rangle,(i)}\mathbf{h}^{\langle j,N_T\rangle} + \nu^{\langle j\rangle}\left(\mathbf{E}^{\langle j\rangle,(i)}\mathbf{X}_c^{\langle N_T\rangle,(i)}\mathbf{h}^{\langle j,N_T\rangle}\right)^* + \mathbf{n}^{\langle j\rangle,(i)}\end{aligned} \tag{4.26}$$

where superscript index $\langle j\rangle,(i)$ represents the OFDM signal on the $j-$th receive antenna at the $i-$th time index and $\mathbf{h}^{\langle j,k\rangle}$ is the CIR vector connecting the k-th transmit antenna to the j-th receive antenna. To simplify the notation the symbol index (i) is dropped in subsequent discussion when no confusion is possible. Now,

extending the definition of a SISO system in the presence of FI/FS CIR, CFO and FS IQ imbalance from (4.8) the received signal on the j-th antenna can be defined as

$$\begin{aligned}\mathbf{y}^{\langle j\rangle} = &\mathbf{E}^{\langle j\rangle}\mathbf{X}_c^{\langle 1\rangle}\mathbf{h}_\mu^{\langle j,1\rangle} + \mathbf{E}^{\langle j\rangle^*}\mathbf{X}_c^{\langle 1\rangle^*}\mathbf{h}_\nu^{\langle j,1\rangle} + \\ &+\mathbf{E}^{\langle j\rangle}\mathbf{X}_c^{\langle 2\rangle}\mathbf{h}_\mu^{\langle j,2\rangle} + \mathbf{E}^{\langle j\rangle^*}\mathbf{X}_c^{\langle 2\rangle^*}\mathbf{h}_\nu^{\langle j,2\rangle} + \\ &\qquad\qquad\cdots\cdots\cdots \\ &+\mathbf{E}^{\langle j\rangle}\mathbf{X}_c^{\langle N_T\rangle}\mathbf{h}_\mu^{\langle j,N_T\rangle} + \mathbf{E}^{\langle j\rangle^*}\mathbf{X}_c^{\langle N_T\rangle^*}\mathbf{h}_\nu^{\langle j,N_T\rangle} + \mathbf{n}^{\langle j\rangle}\end{aligned} \tag{4.27}$$

where $\mathbf{h}_\mu^{\langle j,k\rangle}$ and $\mathbf{h}_\nu^{\langle j,k\rangle}$ are the direct and interfering channels pertaining to the channel between the k-th transmit to the j-th receive antenna as defined in (4.8). Since (4.27) presents a generalized system model encompassing both FS and FI IQ imbalance models and it is considered in further discussion. Transforming (4.27) into frequency domain gives:

$$\begin{aligned}\mathbf{y}_f^{\langle j\rangle} =&\mathbf{P}^{\langle j\rangle}\left(\mathbf{\Lambda}_\mu^{\langle j,1\rangle}\mathbf{s}^{\langle 1\rangle} + \mathbf{\Lambda}_\mu^{\langle j,2\rangle}\mathbf{s}^{\langle 2\rangle} + \cdots + \mathbf{\Lambda}_\mu^{\langle j,N_T\rangle}\mathbf{s}^{\langle N_T\rangle}\right) \\ &+\mathbf{P}^{\langle j\rangle^H}\left(\mathbf{\Lambda}_\nu^{\langle j,1\rangle}\mathbf{Q}\mathbf{s}^{\langle 1\rangle^*} + \mathbf{\Lambda}_\nu^{\langle j,2\rangle}\mathbf{Q}\mathbf{s}^{\langle 2\rangle^*} + \cdots + \mathbf{\Lambda}_\nu^{\langle j,N_T\rangle}\mathbf{Q}\mathbf{s}^{\langle N_T\rangle^*}\right) + \tilde{\mathbf{z}}^{\langle j\rangle}.\end{aligned} \tag{4.28}$$

Now (4.28) can be equivalently written in matrix notation as

$$\begin{aligned}\underbrace{\begin{bmatrix}\mathbf{y}_f^{\langle 1\rangle}\\ \vdots \\ \mathbf{y}_f^{\langle N_R\rangle}\end{bmatrix}}_{\boldsymbol{y}_f} = &\underbrace{\begin{bmatrix}\mathbf{P}^{\langle 1\rangle}\mathbf{\Lambda}_\mu^{\langle 1,1\rangle} & \cdots & \mathbf{P}^{\langle 1\rangle}\mathbf{\Lambda}_\mu^{\langle 1,N_T\rangle}\\ \mathbf{P}^{\langle 2\rangle}\mathbf{\Lambda}_\mu^{\langle 2,1\rangle} & \cdots & \mathbf{P}^{\langle 2\rangle}\mathbf{\Lambda}_\mu^{\langle 2,N_T\rangle}\\ \vdots & \cdots & \vdots \\ \mathbf{P}^{\langle N_R\rangle}\mathbf{\Lambda}_\mu^{\langle N_R,1\rangle} & \cdots & \mathbf{P}^{\langle N_R\rangle}\mathbf{\Lambda}_\mu^{\langle N_R,N_T\rangle}\end{bmatrix}}_{\mathbb{\Lambda}_\mu}\underbrace{\begin{bmatrix}\mathbf{s}^{\langle 1\rangle}\\ \vdots \\ \mathbf{s}^{\langle N_T\rangle}\end{bmatrix}}_{\boldsymbol{s}} \\ &+\underbrace{\begin{bmatrix}\mathbf{P}^{\langle 1\rangle^H}\mathbf{\Lambda}_\nu^{\langle 1,1\rangle}\mathbf{Q} & \cdots & \mathbf{P}^{\langle 1\rangle^H}\mathbf{\Lambda}_\nu^{\langle 1,N_T\rangle}\mathbf{Q}\\ \mathbf{P}^{\langle 2\rangle^H}\mathbf{\Lambda}_\nu^{\langle 2,1\rangle}\mathbf{Q} & \cdots & \mathbf{P}^{\langle 2\rangle^H}\mathbf{\Lambda}_\nu^{\langle 2,N_T\rangle}\mathbf{Q}\\ \vdots & \cdots & \vdots \\ \mathbf{P}^{\langle N_R\rangle^H}\mathbf{\Lambda}_\nu^{\langle N_R,1\rangle}\mathbf{Q} & \cdots & \mathbf{P}^{\langle N_R\rangle^H}\mathbf{\Lambda}_\nu^{\langle N_R,N_T\rangle}\mathbf{Q}\end{bmatrix}}_{\mathbb{\Lambda}_\nu}\underbrace{\begin{bmatrix}\mathbf{s}^{\langle 1\rangle^*}\\ \vdots \\ \mathbf{s}^{\langle N_T\rangle^*}\end{bmatrix}}_{\boldsymbol{s}^*} + \begin{bmatrix}\mathbf{z}^{\langle 1\rangle}\\ \mathbf{z}^{\langle 2\rangle}\\ \vdots \\ \mathbf{z}^{\langle N_R\rangle}\end{bmatrix}.\end{aligned} \tag{4.29}$$

Finally, taking the ICI component of $\mathbf{P}^{\langle j \rangle}$ as additive noise and expressing the FS CIR in time domain, then the model of (4.29) can be approximated as

$$\begin{bmatrix} \mathbf{y}_f^{\langle 1 \rangle} \\ \vdots \\ \mathbf{y}_f^{\langle N_R \rangle} \end{bmatrix} = \underbrace{\begin{bmatrix} \mathbf{S}^{\langle 1 \rangle}\mathbf{W} & \mathbf{S}^{\langle 2 \rangle}\mathbf{W} & \cdots & \mathbf{S}^{\langle N_T \rangle}\mathbf{W} \end{bmatrix}}_{\mathbf{A}_1} \begin{bmatrix} \underrightarrow{\mathbf{h}}_{\mu}^{\langle 1 \rangle} & & \underrightarrow{\mathbf{h}}_{\mu}^{\langle N_R \rangle} \\ \overbrace{\underrightarrow{\mathbf{h}}_{\mu}^{\langle 1,1 \rangle}} & \cdots & \overbrace{\underrightarrow{\mathbf{h}}_{\mu}^{\langle N_R,1 \rangle}} \\ \underrightarrow{\mathbf{h}}_{\mu}^{\langle 1,2 \rangle} & \cdots & \underrightarrow{\mathbf{h}}_{\mu}^{\langle N_R,2 \rangle} \\ & \vdots & \\ \underrightarrow{\mathbf{h}}_{\mu}^{\langle 1,N_T \rangle} & \cdots & \underrightarrow{\mathbf{h}}_{\mu}^{\langle N_R,N_T \rangle} \end{bmatrix} +$$

$$\underbrace{\begin{bmatrix} \mathbf{Q}\mathbf{S}^{H\langle 1 \rangle}\mathbf{W}^* & \mathbf{Q}\mathbf{S}^{H\langle 2 \rangle}\mathbf{W}^* & \cdots & \mathbf{Q}\mathbf{S}^{H\langle N_T \rangle}\mathbf{W}^* \end{bmatrix}}_{\mathbf{A}_2} \begin{bmatrix} \underrightarrow{\mathbf{h}}_{\nu}^{\langle 1 \rangle} & & \underrightarrow{\mathbf{h}}_{\nu}^{\langle N_R \rangle} \\ \overbrace{\underrightarrow{\mathbf{h}}_{\nu}^{\langle 1,1 \rangle}} & \cdots & \overbrace{\underrightarrow{\mathbf{h}}_{\nu}^{\langle N_R,1 \rangle}} \\ \underrightarrow{\mathbf{h}}_{\nu}^{\langle 1,2 \rangle} & \cdots & \underrightarrow{\mathbf{h}}_{\nu}^{\langle N_R,2 \rangle} \\ & \vdots & \\ \underrightarrow{\mathbf{h}}_{\nu}^{\langle 1,N_T \rangle} & \cdots & \underrightarrow{\mathbf{h}}_{\nu}^{\langle N_R,N_T \rangle} \end{bmatrix} + \begin{bmatrix} \tilde{\mathbf{z}}^{\langle 1 \rangle} \\ \tilde{\mathbf{z}}^{\langle 2 \rangle} \\ \vdots \\ \tilde{\mathbf{z}}^{\langle N_R \rangle} \end{bmatrix} \tag{4.30}$$

where $\underrightarrow{\mathbf{h}}_{\mu}^{\langle j \rangle}$ and $\underrightarrow{\mathbf{h}}_{\nu}^{\langle j \rangle}$ is the set of modified CIR related to the j-th receiver, and finally:

$$\mathbf{y}_f^{\langle j \rangle,(i)} = \begin{bmatrix} \mathbf{A}_1 & \mathbf{A}_2 \end{bmatrix} \begin{bmatrix} \underrightarrow{\mathbf{h}}_{\mu}^{\langle j \rangle,(i)} \\ \underrightarrow{\mathbf{h}}_{\nu}^{\langle j \rangle,(i)} \end{bmatrix} + \tilde{\mathbf{z}}^{\langle j \rangle}. \tag{4.31}$$

Following the same approach as adopted in (4.15) the initial estimates of CFO can be obtained using the received vector from each antenna using the following linear model. The modified channel coefficients obtained from (4.31) using two successive training sequences (i.e. i=1, 2) can be used to calculate the RCS CFO estimates for the j-th receive antenna following (4.18):

$$\hat{\phi}^{\langle j \rangle} = \frac{1}{\kappa}\tan^{-1}\left(\frac{\Im\{\underrightarrow{\mathbf{h}}_{\mu}^{\langle j \rangle,(1)^H}\underrightarrow{\mathbf{h}}_{\mu}^{\langle j \rangle,(2)}\}}{\Re\{\underrightarrow{\mathbf{h}}_{\mu}^{\langle j \rangle,(1)^H}\underrightarrow{\mathbf{h}}_{\mu}^{\langle j \rangle,(2)}\}}\right) \quad -\frac{1}{2} \leq \phi \leq \frac{1}{2} \tag{4.32}$$

Once RCS estimates of CFO are available , the time domain signal of the received signal at j-th antenna can be expressed as

$$\begin{bmatrix}\mathbf{y}^{\langle j\rangle,(1)}\\ \mathbf{y}^{\langle j\rangle,(2)}\end{bmatrix} = \mathbb{A}_{\hat{\phi}^{\langle j\rangle}} \begin{bmatrix}\mathbf{h}_{\mu}^{\langle j\rangle}\\ \mathbf{h}_{\nu}^{\langle j\rangle}\end{bmatrix} + \begin{bmatrix}\mathbf{n}^{\langle j\rangle,(1)}\\ \mathbf{n}^{\langle j\rangle,(2)}\end{bmatrix} \tag{4.33}$$

where

$$\mathbb{A}_{\hat{\phi}^{\langle j\rangle}} = \begin{bmatrix}\hat{\mathbf{E}}^{\langle j\rangle,(1)}\mathbf{X}_c^{\langle j,1\rangle,(1)} & \dots & \hat{\mathbf{E}}^{\langle j\rangle,(1)}\mathbf{X}_c^{\langle j,N_T\rangle,(1)} & \hat{\mathbf{E}}^{\langle j\rangle,(1)^*}\mathbf{X}^{\langle j,1\rangle,(1)^*} & \dots & \hat{\mathbf{E}}^{\langle j\rangle,(1)^*}\mathbf{X}_c^{\langle j,N_T\rangle,(1)^*}\\ \hat{\mathbf{E}}^{\langle j\rangle,(2)}\mathbf{X}_c^{\langle j,1\rangle,(2)} & \dots & \hat{\mathbf{E}}^{\langle j\rangle,(2)}\mathbf{X}_c^{\langle j,N_T\rangle,(2)} & \hat{\mathbf{E}}^{\langle j\rangle,(2)^*}\mathbf{X}_c^{\langle j,1\rangle,(2)^*} & \dots & \hat{\mathbf{E}}^{\langle j\rangle,(2)^*}\mathbf{X}_c^{\langle j,N_T\rangle,(2)^*}\end{bmatrix}.$$

So the RCS CIR estimates pertaining to j-th receive antenna can be obtained through a simple LS solution as:

$$\begin{bmatrix}\hat{\mathbf{h}}_{\mu}^{\langle j\rangle}\\ \hat{\mathbf{h}}_{\nu}^{\langle j\rangle}\end{bmatrix} = \left(\mathbb{A}_{\hat{\phi}^{\langle j\rangle}}^H \mathbb{A}_{\hat{\phi}^{\langle j\rangle}}\right)^{-1} \mathbb{A}_{\hat{\phi}^{\langle j\rangle}}^H \bar{\mathbf{y}}^{\langle j\rangle}. \tag{4.34}$$

Using (4.11), the optimal (in LS sense) CFO estimate for the j-th receive antenna can be conveniently obtained as

$$\hat{\phi}_{\text{opt}}^{\langle j\rangle} = \arg\max_{\phi} \quad \bar{\mathbf{y}}^{\langle j\rangle^H} \mathbb{A}_{\phi^{\langle j\rangle}} (\mathbb{A}_{\phi^{\langle j\rangle}}^H \mathbb{A}_{\phi^{\langle j\rangle}})^{-1} \mathbb{A}_{\phi^{\langle j\rangle}}^H \bar{\mathbf{y}}^{\langle j\rangle}. \tag{4.35}$$

So in summary, the CFO can be estimated through (4.32) and (4.35) which can then be used to estimate the combined CIR using (4.34). Once these estimates are available then compensation of CFO, FS IQ imbalance and equalization of CIR can be performed using (4.30). The compact single stage expression for equalization is

$$\hat{\boldsymbol{s}} = \mathbb{\Lambda}_{\hat{\mu}}^{-1} \left[\mathbf{I}_{N\cdot N_R} - \mathbb{\Lambda}_{\hat{\nu}} \mathbb{\Lambda}_{\hat{\mu}}^{-*} \mathbb{\Lambda}_{\hat{\nu}}^{*} \mathbb{\Lambda}_{\hat{\mu}}^{-1}\right]^{-1} \left(\boldsymbol{y}_f - \mathbb{\Lambda}_{\hat{\nu}} \mathbb{\Lambda}_{\hat{\mu}}^{-*} \boldsymbol{y}_f^*\right). \tag{4.36}$$

The estimation complexity of the MIMO receiver increases with the number of unknowns to be estimated. The size of the equalizer matrix is proportional to the number of Tx and Rx antennae.

4.7 Simulation Results

For implementation a typical OFDM transmission system like WLAN (IEEE 802.11a) has been considered. The number of subcarriers in each OFDM symbol is N=64. The system bandwidth is assumed to be 20 MHz and the sampling period is defined as (T_s=0.05μs). The subcarrier spacing is assumed to be ΔF=312.5 kHz. The simulations are based on a Rayleigh fading process with a channel memory of L_h=6 taps and an exponential power delay profile $e^{-\underline{\gamma}l}$ with $\underline{\gamma}$=0.2 and l=$0, 1, \ldots, L_h-1$ is considered. To mitigate the effects of inter symbol interference (ISI), the guard interval is assumed to be longer than CIR, i.e. N_g=10. The transmitted data is assumed to be taken from a 16 QAM constellation and no channel coding is used in these simulations. Each OFDM block contains 10 OFDM symbols. The first two symbols (i=$1, 2$) of each block are known training sequences chosen from a BPSK constellation according to the criterion presented in [31]. The IQ imbalance process defined in (4.5) is assumed to be a random variable with uniformly distributed amplitude imbalance, $\eta \sim \mathcal{U}$[-0.1, 0.1], and phase imbalance, $\theta \sim \mathcal{U}$[-10°, 10°]. From data sheets of typical direct conversion modules it is known that the typical error in amplitude and phase imbalance is $\eta \sim 0.03$ / $\theta \sim 3°$. The normalized CFO is also assumed to be uniformly distributed, $\epsilon \sim \mathcal{U}$[-0.43, 0.43]. This normalized CFO corresponds to 130 kHz of spectral drift which corresponds to extreme CFO conditions. Therefore it can be said that the proposed schemes are being tested under severe IQ imbalance and CFO conditions. The LPF gains of the inphase and quadrature arms of the DC receiver used in this implementation are $\mathbf{k}^1$=$[0.01, 0.95, 0.1]^T$ and $\mathbf{k}^2$=$[0.01, 0.05, 0.01]^T$, where $k^q[n]$=$\{k^q(nT_s)\}|_{n=-1}^{1}$ in (4.7). These values present a plausible model for a frequency selective IQ imbalance which will be estimated in conjunction with the true CIR. Similar models have been used in [31], [32] and [28]. The IQ imbalance process is assumed to be varying much more slowly than the CIR. For section 4.5, the DCO coefficient (d_0) is assumed to be a complex constant and fixed as d_0=0.1+j0.1. Similar values have been considered in [35, 37].

To measure the error performance of the proposed techniques following definitions have been used MSE($\hat{\mathbf{h}}$)=$E\{\|\mathbf{h}-\hat{\mathbf{h}}\|^2\}$, MSE($\hat{\phi}$)=$E\{|\phi-\hat{\phi}|^2\}$ and MSE($\hat{d_0}$)=$E\{|d_0-\hat{d_0}|^2\}$.

The simulations are performed using 5,000 Monte-Carlo channel realizations for each SNR. Fig. 4.2 illustrates the MSE performance of the proposed CIR estimation scheme. It can be seen that the proposed estimator does not suffer

from any noise amplification and has a performance close to the CRLB [18]. The effects of CFO estimation error in RCS cause a slight degradation in channel estimation at high SNR.

The MSE performance of the CFO estimates is illustrated in Fig. 4.3. The estimate of the CFO obtained through RCS is very accurate in the low SNR region. The CFO estimation suffers from residual floor due to approximations made in (4.14). The CRLB analysis for CFO estimation (in the absence of IQ imbalance) available in [79] is presented as a reference.

It should be mentioned here that the scheme of [50] cannot be used for estimation of FS IQ imbalance whereas [32] can estimate FS IQ imbalance, but it will require many training sequences to obtain reliable estimates. In contrast to [43] and [32], the schemes proposed in this chapter (using LTS sequences (which are part of the IEEE 802.11 standard)) can estimate the FS IQ imbalance as effectively as the FI IQ imbalance, as long as a sufficient cyclic prefix is available. The BER performance for the uncoded 16 QAM modulation scheme using NLLS and RCS estimates is presented in Fig. 4.4. The BER performance of the proposed low complexity scheme (i.e. by estimating CFO through RCS and combined CIR through (4.10)) is within a 2dB range of the ideal case for the system under consideration. The MSE performance of combined CIR, DCO and CFO is presented in Fig. 4.5. Simulation results show that the estimates of DCO (obtained through RCS estimates of CFO) have near optimal performance for all SNRs of interest. The CFO estimation in the presence of DCO with RCS via (4.24) is slightly worse than the DCO free case. The optimal NLLS scheme provides near optimal performance. The CIR estimates (with RCS estimates and NLLS estimates) provide fair performance complexity trade-off. BER performance has not been simulated in the presence of DCO.

Like in the case of SISO systems the choice of training sequences plays an important part in the estimation accuracy in MIMO transmission. The optimal training sequences for CIR estimation in an MIMO-OFDM system have been proposed in [81, 82] but they do not yield optimal results in the presence of imperfections under consideration.

For simulation purposes a pair of pilot sequences have been found through an extensive search over the possible set of sequences and a pair was found which yields a better estimation performance on average. It would be of great interest to establish a criterion and find optimal training sequences but this would be a topic for further work.

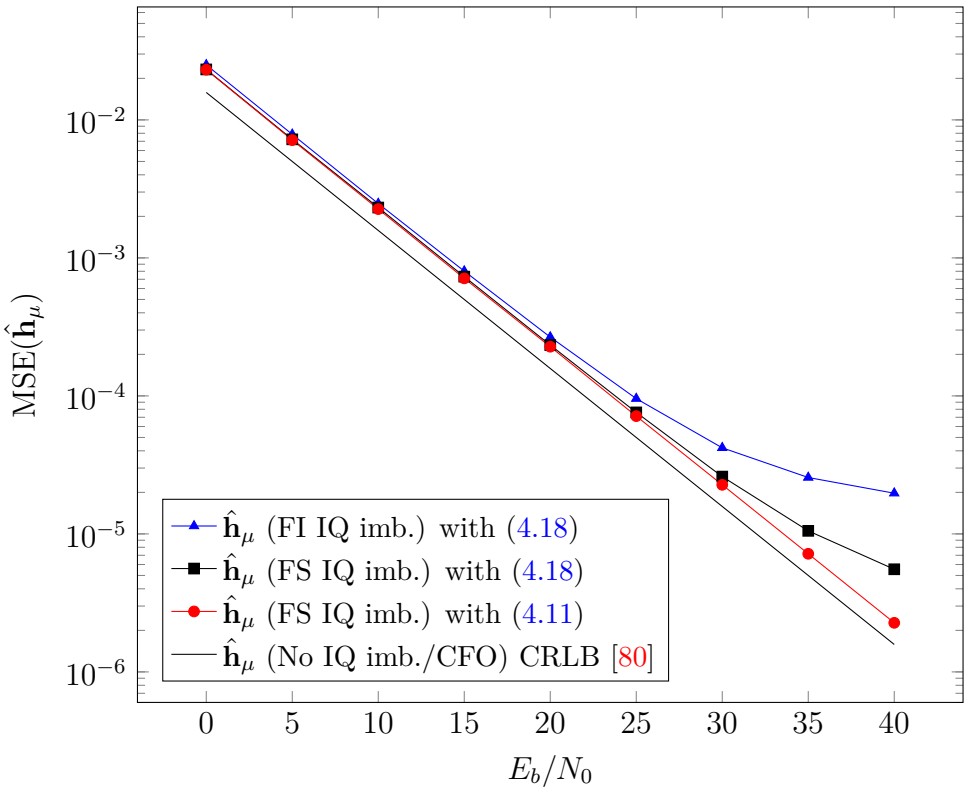

Figure 4.2: MSE of CIR estimation using (4.10), (4.18) and (4.11), in the presence of IQ imbalance $\eta \sim \mathcal{U}[\text{-}0.1, 0.1]$, $\theta \sim \mathcal{U}[\text{-}10^\circ, 10^\circ]$ and normalized CFO $\epsilon \sim \mathcal{U}[\text{-}0.43, 0.43]$, N=64, Rayleigh channel with L_h=6 taps and 5,000 Monte-Carlo realizations.

Fig. 4.6 illustrates the average estimation error of the CFO coefficient present at the receiver input. It can be noticed that like in the case of a SISO system, for CFO estimation performance both RCS and NLLS provide performance proportionate to the complexity. The average CIR estimation performance of the MIMO system while using the proposed CFO estimation methods is illustrated in Fig. 4.7. It can be seen that the estimation accuracy of the modified CIR depends completely on the CFO estimation accuracy.

Finally, the simulated BER performance of the 2×2 spatially multiplexed MIMO system with uncoded 16 QAM data in the presence of CFO and IQ imbalance is presented in Fig. 4.8. The simulations are performed with CIR estimates obtained through RCS and NLLS estimates of CFO. Simulations results reveal that BER performance of both schemes is comparable for low to moderate SNR. In the high SNR region near optimal BER can be achieved when CIR is estimated

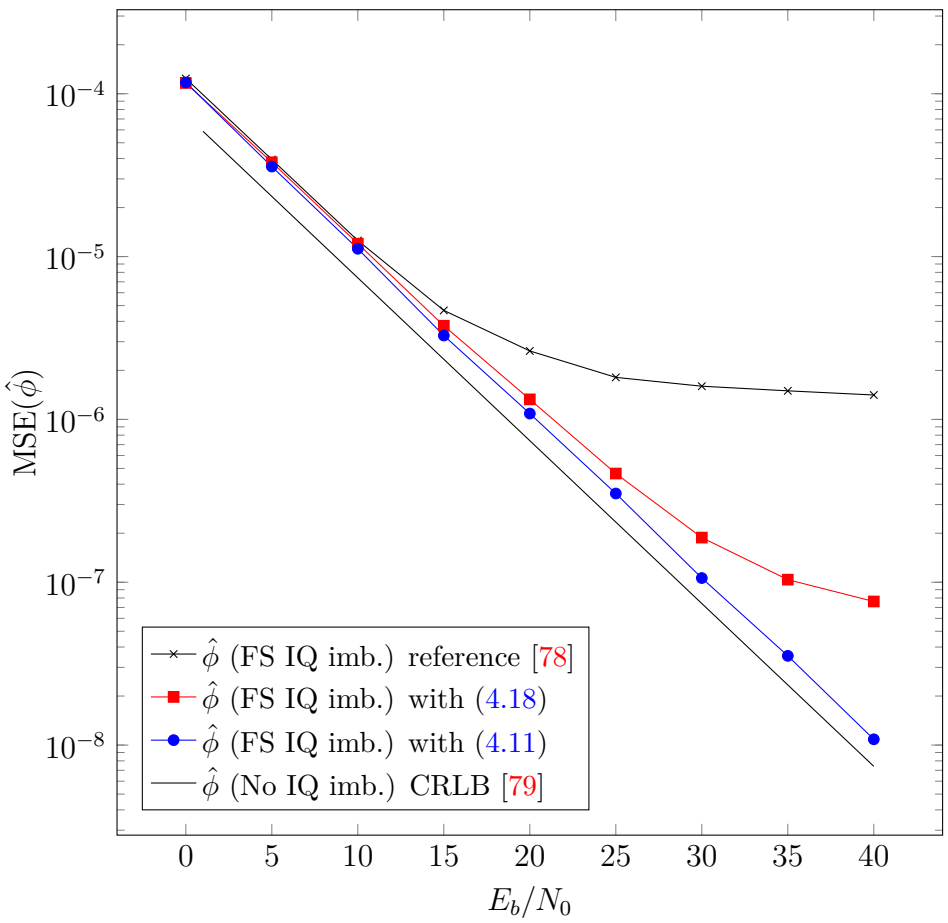

Figure 4.3: MSE performance of CFO estimation with (4.11) and (4.18), $\eta \sim \mathcal{U}[-0.1, 0.1]$, $\theta \sim \mathcal{U}[-10°, 10°]$ and normalized CFO $\epsilon \sim \mathcal{U}[-0.43, 0.43]$, N=64, Rayleigh channel with L_h=6 taps and 5,000 Monte-Carlo realizations.

using NLLS estimates.

4.8 Conclusions

This chapter presents a novel technique to jointly estimate the FS CIR and FI/FS Rx IQ imbalance in the presence of CFO and DCO for OFDM systems. A simple closed form expression was obtained for estimation of CFO without any a-priori information about CIR and FS IQ imbalance. The CIR and FS IQ imbalance is estimated as a set of two independent channels corresponding to the desired and interfering signals. The proposed schemes use ordinary training sequences

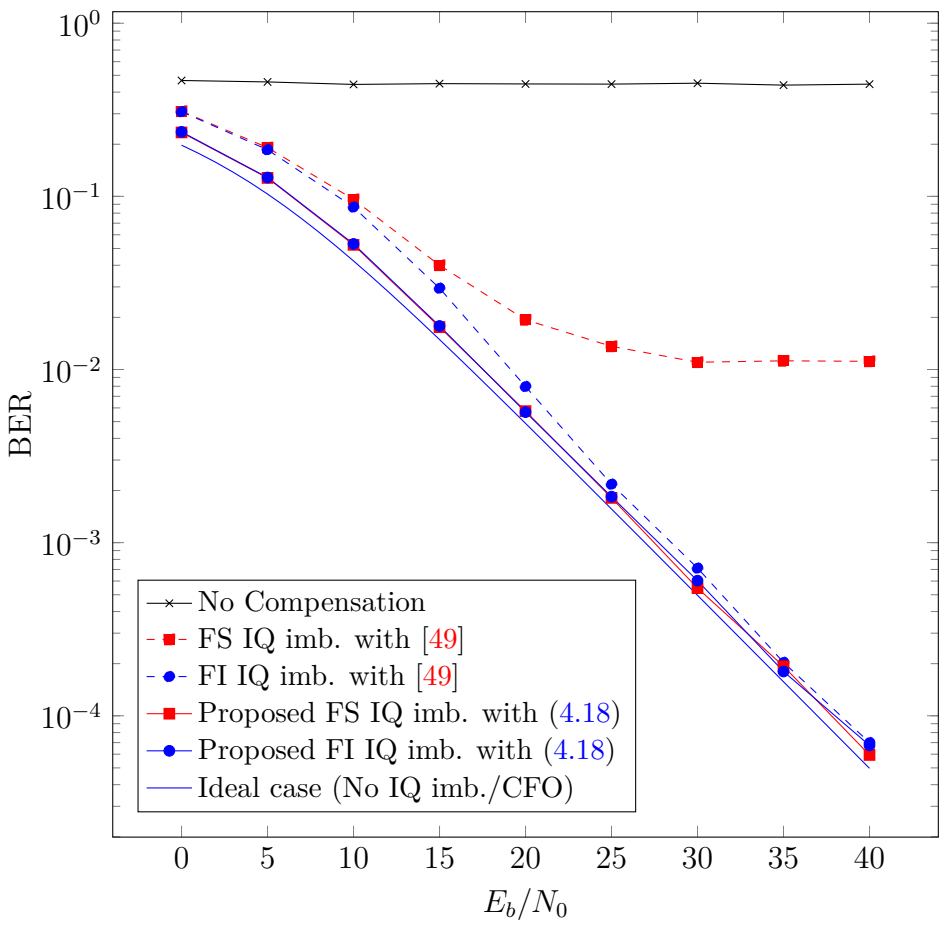

Figure 4.4: BER performance of proposed schemes with $\eta \sim \mathcal{U}[\text{-}0.1, 0.1]$, $\theta \sim \mathcal{U}[\text{-}10^\circ, 10^\circ]$ and normalized CFO $\epsilon \sim \mathcal{U}[\text{-}0.43, 0.43]$, N=64, Rayleigh channel with L_h=6 taps and 5,000 Monte-Carlo realizations.

already defined in the WLAN standards.

To equalize the CIR in the presence of these imperfections a low complexity single stage CFO, FS IQ imbalance compensation and CIR equalization scheme has been proposed which can effectively deal with FI/FS IQ imbalance in the presence of FS CIR. The proposed solutions have been shown to work equally well in MIMO-OFDM systems. The simulation results show that the proposed schemes provide an excellent performance/complexity trade-off.

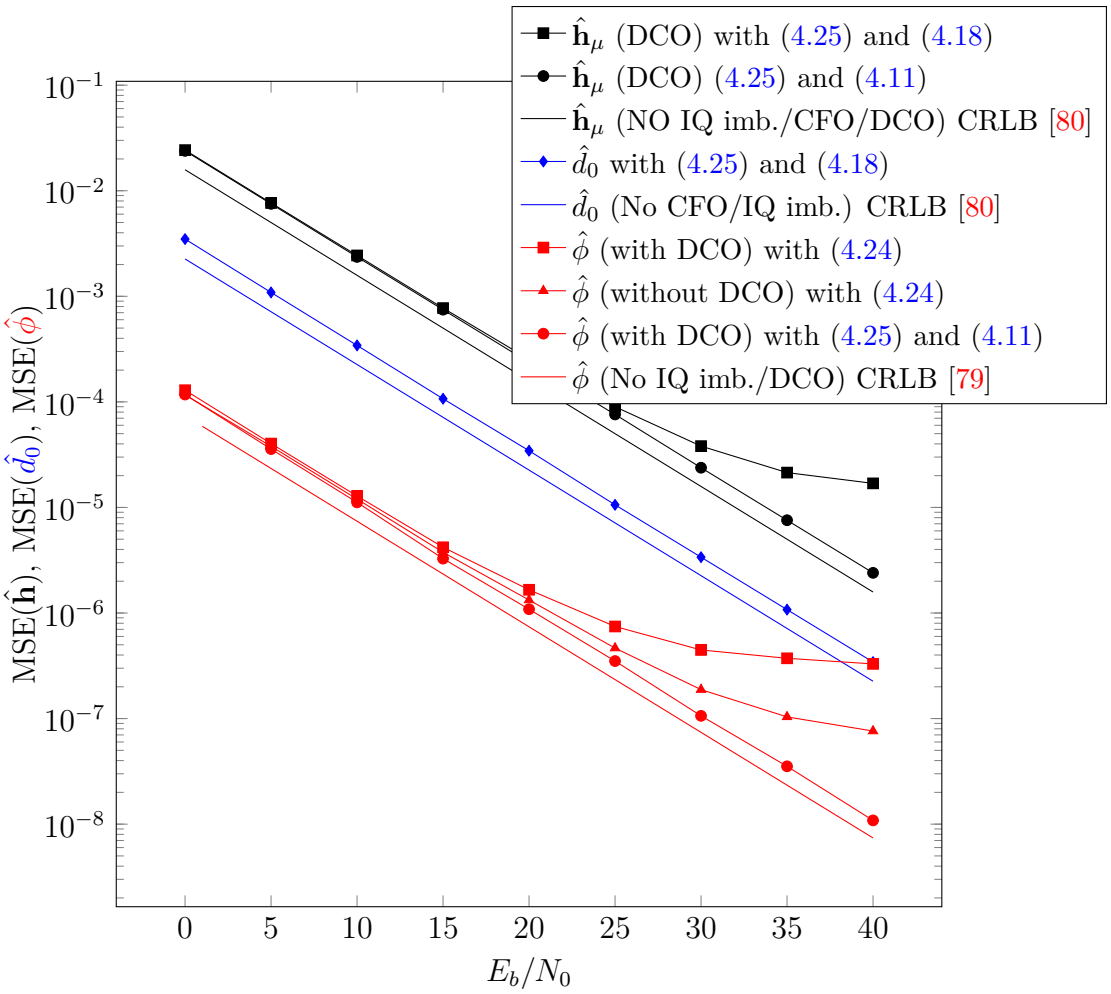

Figure 4.5: MSE performance of CIR, DCO and CFO estimation with (4.24), (4.25), (4.11) and (4.18), $\eta \sim \mathcal{U}[\text{-}0.1, 0.1]$, $\theta \sim \mathcal{U}[\text{-}10^\circ, 10^\circ]$, $d_0 = 0.1 + j0.1$ and normalized CFO $\epsilon \sim \mathcal{U}[\text{-}0.43, 0.43]$, N=64, Rayleigh channel with L_h=6 taps and 5,000 Monte-Carlo realizations.

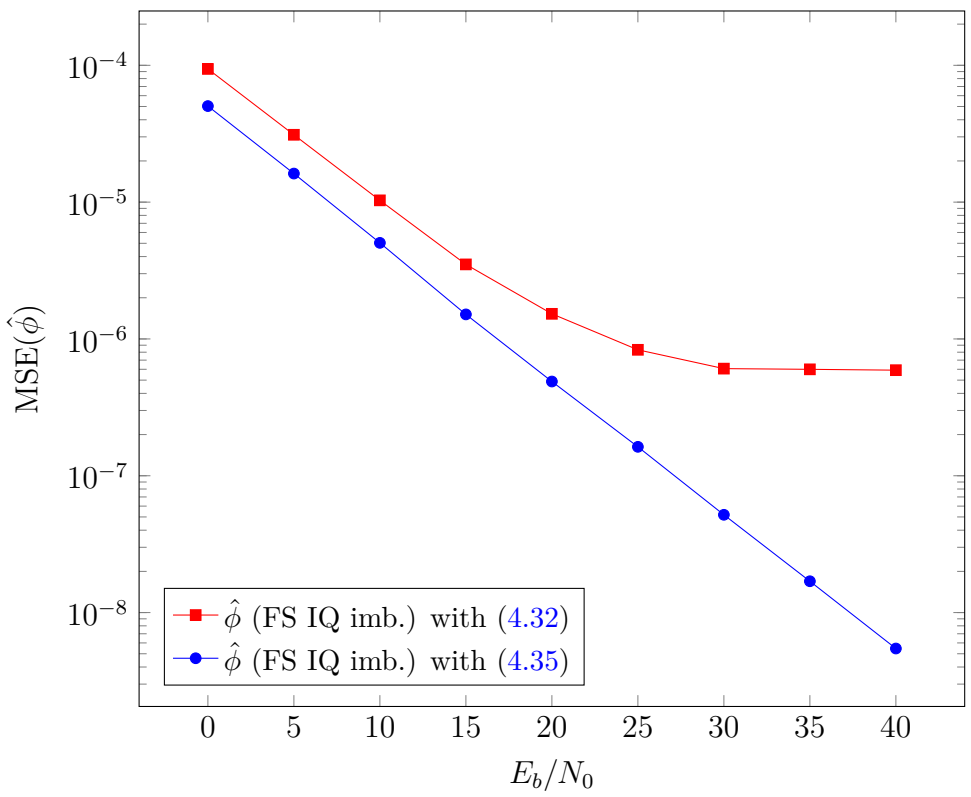

Figure 4.6: MSE of CFO estimation in MIMO 2×2 configuration using (4.31), (4.32) and (4.35), in the presence of IQ imbalance $\eta \sim \mathcal{U}[\text{-}0.1, 0.1]$, $\theta \sim \mathcal{U}[\text{-}10^\circ, 10^\circ]$ and normalized CFO $\epsilon \sim \mathcal{U}[\text{-}0.3, 0.3]$, N=64, Rayleigh channel with L_h=6 taps and 5,000 Monte-Carlo realizations.

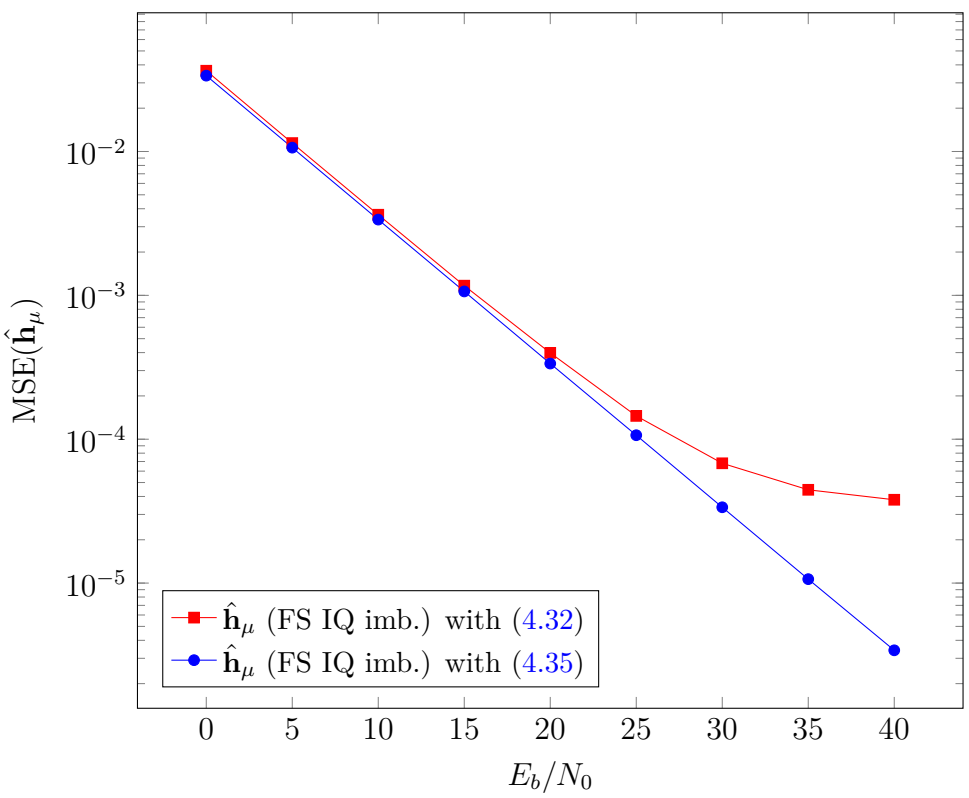

Figure 4.7: MSE of channel estimation in MIMO 2×2 configuration using (4.34), (4.32) and (4.35), in the presence of IQ imbalance $\eta \sim \mathcal{U}[\text{-}0.1, 0.1]$, $\theta \sim \mathcal{U}[\text{-}10^\circ, 10^\circ]$ and normalized CFO $\epsilon \sim \mathcal{U}[\text{-}0.3, 0.3]$, N=64, Rayleigh channel with L_h=6 taps and 5,000 Monte-Carlo realizations.

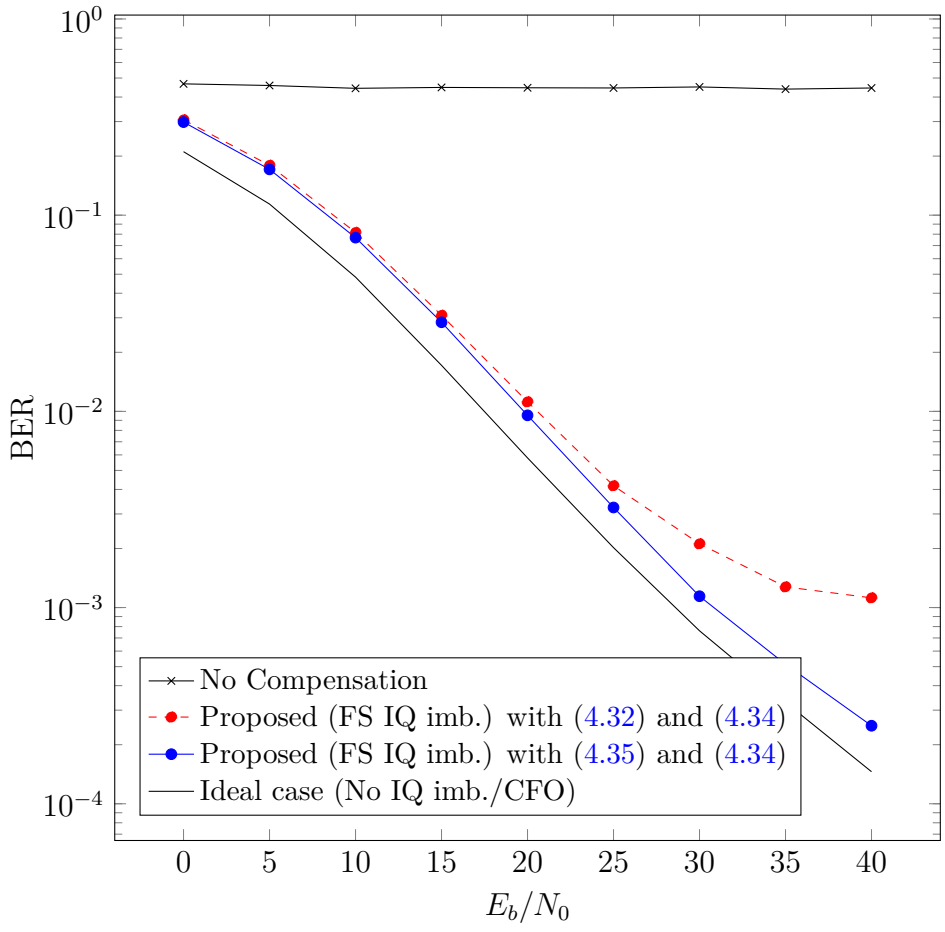

Figure 4.8: BER performance of proposed schemes in MIMO 2×2 configuration with $\eta \sim \mathcal{U}[\text{-}0.1, 0.1]$, $\theta \sim \mathcal{U}[\text{-}10^\circ, 10^\circ]$ and normalized CFO $\epsilon \sim \mathcal{U}[\text{-}0.3, 0.3]$, N=64, Rayleigh channel with L_h=6 taps and 5,000 Monte-Carlo realizations.

5 Joint CIR, CFO and FI Tx/Rx IQ Imbalance Estimation

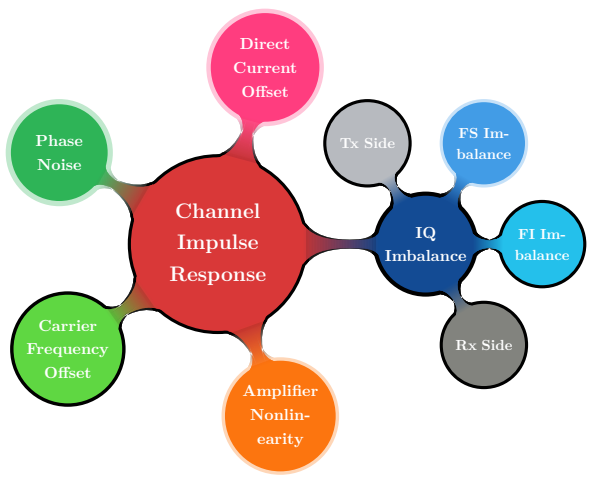

Abstract

The aim of this chapter is to design a simple receiver which can jointly estimate FS CIR, FI Tx/Rx IQ imbalance and CFO with minimal training and implementation complexity.

The estimation of CFO is performed using two scalable solutions already presented in the previous chapter. To estimate the FS CIR and FI Tx/Rx IQ imbalance two different estimation techniques have been proposed. The first technique is an iterative approach stemming from a doubly linear model of the transmission system in the presence of Tx/Rx IQ imbalance and FS CIR, while the second approach is a LS solution. Both these schemes provide a good performance/complexity trade-off. Although the iterative estimates of CIR are not optimal, they do provide a near ideal BER performance.

The proposed scheme blends seamlessly with IEEE 802.11 standard but can be adapted to work with any OFDM standard.

5.1 Introduction

The simple and low cost DC device is a preferred choice for RF front-end because of their desirable features like low cost/complexity and convenience of monolithic integration. This transceiver suffer from problems like IQ imbalance, CFO, DCO and PN. Therefore it is essential to design a receiver which can handle the effects of these practical limitations through low complexity signal processing techniques. The traditional approach is to transmit certain training sequences and then do joint estimation of both the channel and the non-ideal behaviour parameters. Many of the schemes require multiple LTS sequences to achieve acceptable CIR estimates.

Several techniques have been proposed in the literature to jointly estimate CFO, IQ imbalance and CIR. One of the simplest solutions proposed in literature [47] is to transmit a pilot sequence with only one non-zero symbol. The receiver can estimate the CFO by minimizing the effects of ICI to the adjacent subcarriers with a simple GS, and IQ imbalance can be estimated subsequently. [48] has proposed to estimate CFO and FI Rx IQ imbalance by transmitting a pilot sequence twice, IQ imbalance and CFO are then estimated by exploiting the fact that CIR and IQ imbalance are time invariant. Both [47] and [48] are specific to the case when IQ imbalance is present only in the receiver.

Numerous adaptive techniques are cited in literature and [27] proposed an LMS scheme which estimates FI/FS Rx IQ imbalance. An RLS based adaptive scheme has been proposed by [32] for joint estimation of FI Tx/Rx IQ imbalance and FS CIR in the presence of CFO. The authors have not proposed any specific solution for CFO compensation and only FI Tx/Rx IQ imbalance and FS CIR are estimated.

The estimation of FI Tx/Rx IQ imbalance and CIR for OFDM systems has been considered using pre- and post-FFT processing [44]. The authors have used the frequency domain model of channel and IQ imbalance to create a set of linear equations with the help of special training symbols. This scheme jointly estimates the CFR and FI Tx/Rx IQ imbalance using the fact that in an OFDM system each subcarrier is cross-coupled with its (frequency domain) mirror image. This is a low complexity scheme which avoids any matrix inversions. The main drawback of this scheme is that it requires several OFDM symbols to adaptively estimate both IQ imbalance and the CIR coefficients; this scheme does not consider the presence of CFO.

A set of low complexity schemes for joint CFO, FI Rx IQ imbalance and FS CIR have been proposed for MIMO and SISO cases respectively in [50,83]. These schemes require small pilot blocks to be transmitted repeatedly within a pilot symbol and can track any variation of CFO. However these schemes do not take Tx IQ imbalance into consideration thus may not be suitable for all applications. A joint iterative FS CIR, FI/FS Rx IQ imbalance estimation scheme has been proposed in [84], where grid search is performed to estimate CFO at the start of every iteration and desired and interfering CIRs are estimated taking the estimate of CFO into account.

In [85] the authors have developed an intricate linear model to estimate FS CIR, Tx/Rx IQ imbalance in the presence of CFO and phase offset using a least squares solution. However, this work does not propose any specific method to estimate CFO and phase offset.

Several blind Tx/Rx IQ imbalance estimation techniques have been proposed in the literature [57, 58] but these schemes require large data samples to acquire reliable estimates.

In this chapter a low complexity joint CIR, CFO and FI Tx/Rx IQ imbalance estimation is studied for an OFDM system. In contrast to other works proposed in the literature which require many training symbols, the proposed scheme can estimate the channel and the IQ imbalance using only the training sequences which are already part of the WLAN standards. Two different techniques have been proposed for joint estimation of FS CIR and FI Tx/Rx IQ imbalance. The first approach provides an iterative solution based on the doubly linear model of a system in the presence of FS CIR and FI Tx/Rx IQ imbalance, while the second scheme (slightly more complex) provides a CLFE for estimation of CIR. Simulation results show that even at high data-rate systems both schemes provide comparable BER performance.

The rest of the chapter is now organized as follows. Section 5.2 presents the model of a typical transmission system in the presence of non-ideal DC devices both in transmitter and receiver. A set of iterative and non-iterative solutions for joint CFO, FI Tx/Rx IQ imbalance and CIR estimation are presented in section 5.3. A simple joint CFO, Tx/Rx IQ imbalance compensation and channel equalizer in proposed in section 5.4. Section 5.5 presents the MSE of estimation and BER performance of the proposed schemes and section 5.6 concludes this chapter.

5.2 Signal Model

The typical diagram of a system in the presence of CFO and Tx/Rx IQ imbalance is illustrated in Fig. 5.1. In the case of lack of orthogonality in the in-phase and quadrature-phase arms of the IQ transceiver the system will suffer from the image problem. The transmit and receive filters $g_T^{I/Q}(t)$ and $g_R^{I/Q}(t)$ are assumed to be matched perfectly and therefore we consider only FI IQ imbalance. This can severely degrade the performance of the system and effectively limit the achievable SNR. A low cost local oscillator can also introduce a linear frequency offset to the received data sequence and so it will further degrade the performance of the receiver. These problems motivate us to design a simple yet robust receiver architecture which can handle the effects of this non-ideal behaviour and improve the operating SNR even in the presence of severe IQ imbalance, CFO and DCO. This chapter extends on the doubly linear model describing the input/output relation of the system in the presence of FI Tx/Rx IQ imbalance and CFO.

As explained in section 2.3.3 there are several ways of representing IQ imbalance in the literature and within the scope of this work the model presented in [26, 31, 34] is employed. The baseband equivalent of the transmitted signal at the RF front-end is defined as $u(t)$=LPF$\{u_{RF}(t)e^{-j\omega_c t}\}$ where ω_c is the carrier frequency and $u(t)$ is the equivalent complex baseband signal. By ignoring the presence of FS IQ imbalance in (2.41) the equivalent baseband transmit signal can be defined as

$$u(t) = \mu_T x(t) + \nu_T x^*(t) \tag{5.1}$$

where

$$\begin{aligned} \mu_T &:= \cos\theta_T + j\eta_T \sin\theta_T \\ \nu_T &:= \eta_T \cos\theta_T + j\sin\theta_T. \end{aligned} \tag{5.2}$$

where $x(t)$ is the modulated OFDM signal, η_T and θ_T respectively represent the amplitude and phase imbalances present on the transmitter side. The equivalent baseband received signal in the presence of FI Rx IQ imbalance, CFO , FS CIR and additive noise is defined as [28, 32]

$$\begin{aligned} y(t) = \mu_R e^{j2\pi\Delta f t}\Big(\mu_T x(t) + \nu_T x^*(t)\Big) \otimes h(t) \\ + \nu_R e^{-j2\pi\Delta f t}\bigg(\Big(\mu_T x(t) + \nu_T x^*(t)\Big) \otimes h(t)\bigg)^* + n(t) \end{aligned} \tag{5.3}$$

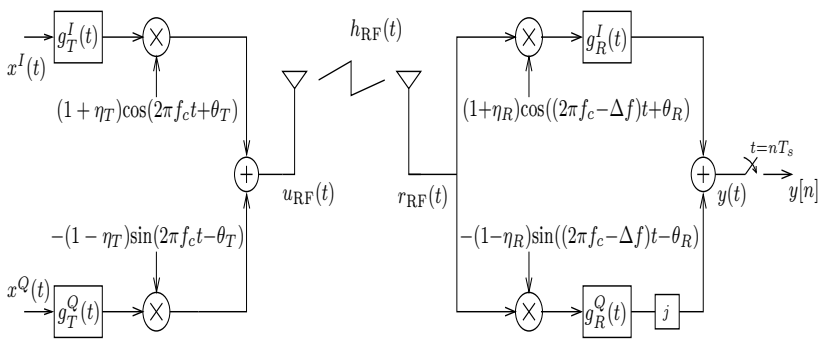

Figure 5.1: The equivalent model of a DCT in the presence of FI Tx/Rx IQ mismatch and CFO present at the receiver side.

where μ_R and ν_R are defined similarly as in (2.45), $h(t)$ is the complex baseband equivalent CIR and $n(t)$ is equivalent complex circularly symmetric additive white Gaussian noise. After baud-rate sampling and removing the cyclic prefix we can rewrite the above equation in the matrix notation

$$\begin{aligned}\mathbf{y}^{(i)} = &\underbrace{\mu_R\mu_T}_{\alpha}\mathbf{E}^{(i)}\mathbf{X}\mathbf{h} + \underbrace{\mu_R\nu_T}_{\beta}\mathbf{E}^{(i)}\mathbf{X}^*\mathbf{h} \\ &+ \underbrace{\nu_R\mu_T^*}_{\gamma}\mathbf{E}^{(i)^*}\mathbf{X}^*\mathbf{h}^* + \underbrace{\nu_R\nu_T^*}_{\delta}\mathbf{E}^{(i)^*}\mathbf{X}\mathbf{h}^* + \mathbf{n}^{(i)}\end{aligned} \tag{5.4}$$

where '(i)' is the symbol index; $\mathbf{X}$=circ($\mathbf{F}^H\mathbf{s}$) is the $N\times L_h$ circulant matrix constructed from the transmitted pilot vector; $\mathbf{h}$ is the $L_h\times 1$ equivalent discrete-time CIR; $\mathbf{E}^{(i)}$=diag($\{e^{j\frac{2\pi}{N}\epsilon[(i-1)(N+N_g)+N_g+n]}\}_{n=0}^{N-1}$), is the CFO process affecting the $i-$th OFDM symbol; N and N_g are respectively the size of the OFDM symbol and the cyclic prefix; ϵ is the CFO coefficient normalized to the subcarrier spacing, i.e. $\epsilon=T\Delta f$ ($T=NT_s$); $\mathbf{n}^{(i)}$ is $N\times 1$ vector of complex additive noise $\mathbf{n}\sim\mathcal{N}(0,\sigma_n^2\mathbf{I}_N)$ and α, β, γ and δ are the complex variables which fully represent the FI Tx/Rx IQ imbalance process. In this chapter we aim to estimate these parameters instead of the corresponding amplitude and phase imbalance (i.e. $\theta_{\mathrm{T/R}}$ and $\eta_{\mathrm{T/R}}$). In practice the normalized CFO can take any value of offset, which can then be decomposed into integer and fractional parts, namely $\epsilon=\tau+\phi$, where τ and ϕ are respectively integer and fractional, i.e. $-1\leq\phi\leq 1$. However in practice the maximum detectable range of the CFO using successive LTS sequences is defined as $|\phi|<N/2(N+N_g)$ [78]. In the literature, several schemes are available which can estimate the integer and fractional part of the CFO process. However

the scope of this work is limited to the fractional part of the CFO only. The equivalent frequency domain model of (5.4) can be defined as

$$\begin{aligned}\mathbf{y}_f^{(i)} = \mathbf{F}\mathbf{y}^{(i)} = \alpha\mathbf{P}^{(i)}\mathbf{\Lambda}_h\mathbf{s} + \beta\mathbf{P}^{(i)}\mathbf{\Lambda}_h\mathbf{Q}\mathbf{s}^* + \gamma{\mathbf{P}^{(i)}}^H\mathbf{Q}\mathbf{\Lambda}_h^*\mathbf{s}^* \\ + \delta{\mathbf{P}^{(i)}}^H\mathbf{Q}\mathbf{\Lambda}_h^*\mathbf{Q}\mathbf{s} + \mathbf{z}^{(i)}\end{aligned} \tag{5.5}$$

where $\mathbf{S}$=diag($\mathbf{s}$) is the known pilot sequence; $\mathbf{Q}$ is the permutation matrix defined as $\mathbf{Q} = \mathbf{F}\mathbf{F}^T$; $\mathbf{z}^{(i)}$=$\mathbf{F}\mathbf{n}^{(i)}$; $\mathbf{P}^{(i)}$ is the circulant matrix of the CFO process which is defined as $\mathbf{P}^{(i)}$=$\mathbf{F}\mathbf{E}^{(i)}\mathbf{F}^H$ [18]; $\mathbf{\Lambda}_h$ is the diagonal CFR matrix (i.e. $\mathbf{\Lambda}_h$=diag($\mathbf{W}\mathbf{h}$)).

From the analysis of the interfering terms in (5.5) it is known that the magnitude of last data dependent interfering term is negligible compared to the other components. Therefore this term is discarded in further discussion. Rewriting (5.4) in terms of the real and imaginary components the following linear relation can be obtained.

$$\begin{bmatrix}\mathbf{y}^{I_{(i)}} \\ \mathbf{y}^{Q_{(i)}}\end{bmatrix} = \begin{bmatrix}\mathbf{A}^{I_{(i)}} & \mathbf{B}^{I_{(i)}} & \mathbf{C}^{I_{(i)}} & \mathbf{A}^{Q_{(i)}} & \text{-}\mathbf{B}^{Q_{(i)}} & \text{-}\mathbf{C}^{Q_{(i)}} \\ \mathbf{A}^{Q_{(i)}} & \mathbf{B}^{Q_{(i)}} & \mathbf{C}^{Q_{(i)}} & \text{-}\mathbf{A}^{I_{(i)}} & \mathbf{B}^{I_{(i)}} & \mathbf{C}^{I_{(i)}}\end{bmatrix}.$$
$$\left(\begin{bmatrix}\alpha^I & -\alpha^Q \\ \beta^I & \beta^Q \\ \gamma^I & \gamma^Q \\ -\alpha^Q & -\alpha^I \\ \beta^Q & -\beta^I \\ \gamma^Q & -\gamma^I\end{bmatrix} \odot \mathbf{I}_{L_h}\right)\begin{bmatrix}\mathbf{h}^{\mathrm{I}} \\ \mathbf{h}^Q\end{bmatrix} + \begin{bmatrix}\mathbf{n}^{I_{(i)}} \\ \mathbf{n}^{Q_{(i)}}\end{bmatrix} \tag{5.6}$$

where $\mathbf{A}^{(i)}$=$\mathbf{E}^{(i)}\mathbf{X}$, $\mathbf{B}^{(i)}$=$\mathbf{E}^{(i)}\mathbf{X}^*$ and $\mathbf{C}^{(i)}$=$(\mathbf{E}^{(i)}\mathbf{X})^*$; superscripts '$I$' and '$Q$' represent respectively the real and imaginary components of a particular complex variable; and (5.6) can be compactly written as

$$\underline{\mathbf{y}}^{(i)} = \mathbf{X}_1^{(i)}\Big(\mathbf{\Theta}_1 \odot \mathbf{I}_{L_h}\Big)\underline{\mathbf{h}} + \underline{\mathbf{n}}^{(i)} \tag{5.7}$$

where $\mathbf{X}_1^{(i)}$ is the matrix pertaining to the transmitted pilot sequence, $\mathbf{\Theta}_1$ is the matrix pertaining to the effects of the overall IQ imbalance process and $\underline{\mathbf{h}}$ is the real-valued vector of CIR. Now rewriting (5.4) in terms of real and imaginary

components another equivalent representation can be formulated as

$$\begin{bmatrix} \mathbf{y}^{I_{(i)}} \\ \mathbf{y}^{Q_{(i)}} \end{bmatrix} = \begin{bmatrix} \mathbf{A}^{I_{(i)}} & \mathbf{B}^{I_{(i)}} & \mathbf{C}^{I_{(i)}} & \text{-}\mathbf{A}^{Q_{(i)}} & \text{-}\mathbf{B}^{Q_{(i)}} & \text{-}\mathbf{C}^{Q_{(i)}} \\ \mathbf{A}^{Q_{(i)}} & \mathbf{B}^{Q_{(i)}} & \mathbf{C}^{Q_{(i)}} & \mathbf{A}^{I_{(i)}} & \mathbf{B}^{I_{(i)}} & \mathbf{C}^{I_{(i)}} \end{bmatrix} \cdot \begin{bmatrix} \mathbf{h}^I & -\mathbf{h}^Q & \mathbf{0} & \mathbf{0} & \mathbf{0} & \mathbf{0} \\ \mathbf{0} & \mathbf{0} & \mathbf{h}^I & -\mathbf{h}^Q & \mathbf{0} & \mathbf{0} \\ \mathbf{0} & \mathbf{0} & \mathbf{0} & \mathbf{0} & \mathbf{h}^I & \mathbf{h}^Q \\ \mathbf{h}^Q & \mathbf{h}^I & \mathbf{0} & \mathbf{0} & \mathbf{0} & \mathbf{0} \\ \mathbf{0} & \mathbf{0} & \mathbf{h}^Q & \mathbf{h}^I & \mathbf{0} & \mathbf{0} \\ \mathbf{0} & \mathbf{0} & \mathbf{0} & \mathbf{0} & \mathbf{h}^Q & -\mathbf{h}^I \end{bmatrix} \begin{bmatrix} \alpha^I \\ \alpha^Q \\ \beta^I \\ \beta^Q \\ \gamma^I \\ \gamma^Q \end{bmatrix} + \begin{bmatrix} \mathbf{n}^{I_{(i)}} \\ \mathbf{n}^{Q_{(i)}} \end{bmatrix}. \tag{5.8}$$

Here (5.8) can be compactly written as

$$\underline{\mathbf{y}}^{(i)} = \mathbf{X}_2^{(i)} \mathbf{A}_{\boldsymbol{h}} \boldsymbol{\theta} + \underline{\mathbf{n}}^{(i)} \tag{5.9}$$

where $\mathbf{X}_2^{(i)}$ is an alternative representation of the transmitted pilot sequence and $\mathbf{A}_{\boldsymbol{h}}$ is the corresponding matrix pertaining to the CIR and $\boldsymbol{\theta}$=$[\alpha^{\mathrm{I}}\ \alpha^{\mathrm{Q}}\ \beta^{\mathrm{I}}\ \beta^{\mathrm{Q}}\ \gamma^{\mathrm{I}}\ \gamma^{\mathrm{Q}}]^T$.

In this section we have derived a set of different (but equivalent) linear equations which describe the OFDM transmission system in the presence of FI Tx/Rx IQ imbalance and CFO. In the next section we propose to use the frequency domain model of (5.5) to estimate the CFO and the *doubly linear* model of (5.7) and (5.9) to estimate FS CIR and FI Tx/Rx IQ imbalance parameters.

5.3 Parameter Estimation

The idea is to obtain a CFO estimate through scalable techniques already proposed in chapter 4. In the next sections we extend the models to accommodate Tx IQ imbalance and then a simple iterative scheme is proposed in section 5.3.3 and a closed for expression is derived in section 5.3.4. Ignoring the least significant data dependent component associated with δ we can rewrite the received signal as

$$\begin{aligned} \mathbf{y}_f^{(i)} \approx\ & p_0^{(i)} \mathbf{S}\mathbf{W}\mathbf{h}_\alpha + \mathbf{P}_{\mathrm{ICI}}^{(i)} \mathbf{S}\mathbf{W}\mathbf{h}_\alpha \\ & + p_0^{(i)} \mathbf{Q}\mathbf{S}^H\mathbf{W}^*\mathbf{h}_\beta + \mathbf{P}_{\mathrm{ICI}}^{(i)} \mathbf{Q}\mathbf{S}^H\mathbf{W}^*\mathbf{h}_\beta \\ & + p_0^{(i)^*} \mathbf{Q}\mathbf{S}^H\mathbf{W}^*\mathbf{h}_\gamma + \mathbf{P}_{\mathrm{ICI}}^{(i)^H} \mathbf{Q}\mathbf{S}^H\mathbf{W}^*\mathbf{h}_\gamma + \mathbf{z}^{(i)} \end{aligned} \tag{5.10}$$

where $\mathbf{P}^{(i)}{=}p_0^{(i)}\mathbf{I}_N + \mathbf{P}_{\mathrm{ICI}}^{(i)}$ and $p_0^{(i)}{=}e^{j\frac{2\pi}{N}\epsilon[(i-1)(N+N_g)+N_g+\frac{N}{2}]}$ is the mean value of the CFO process referred to as CPR, while $\mathbf{P}_{\mathrm{ICI}}^{(i)}$ is the ICI component caused by CFO which results in spectral leakage to adjacent subcarriers. From statistical analysis of Tx/Rx IQ imbalance we know that the component α contains upto 99% of overall energy of the useful transmitted signal and therefore ignoring the interfering components would not lead to significant degradation in channel and CFO estimation. Taking the data dependent interference and additive noise into account we can rewrite (5.10) as

$$\mathbf{y}_f^{(i)} = \mathbf{S}\mathbf{W}\underrightarrow{\mathbf{h}}_{\alpha}^{(i)}{+}\mathbf{Q}\mathbf{S}^H\mathbf{W}^*\underrightarrow{\mathbf{h}}_{\xi}^{(i)}{+}\tilde{\mathbf{z}}^{(i)} \tag{5.11}$$

where $\underrightarrow{\mathbf{h}}_{\alpha}^{(i)}{=}p_0^{(i)}\mathbf{h}_{\alpha}$ and $\underrightarrow{\mathbf{h}}_{\xi}^{(i)}{=}p_0^{(i)}\mathbf{h}_{\beta}{+}{p_0^{(i)}}^*\mathbf{h}_{\gamma}$ and $\tilde{\mathbf{z}}^{(i)}$ is the sum of the remaining interfering terms in (5.10). In the following section we propose two schemes which can estimate CFO in the presence of Tx/Rx IQ imbalance. The first scheme is a low complexity scheme while the second scheme is slightly more complex. These schemes provide proportionate improvement in parameter estimation performance.

5.3.1 Reduced Complexity Scheme

Using the approximate model defined in (5.11) (also previously mentioned in chapter 4) we can see that the estimation accuracy of the CIR is directly related to the CFO coefficients. The above equation can be equivalently rewritten in matrix notation as

$$\mathbf{y}_f^{(i)} = \underbrace{\begin{bmatrix}\mathbf{S}\mathbf{W} & \mathbf{Q}\mathbf{S}^H\mathbf{W}^*\end{bmatrix}}_{\mathbf{U}}\begin{bmatrix}\underrightarrow{\mathbf{h}}_{\alpha}^{(i)}\\ \underrightarrow{\mathbf{h}}_{\xi}^{(i)}\end{bmatrix}{+}\tilde{\mathbf{z}}^{(i)}.$$

A simple least-squares estimator can determine the modified CIRs as

$$\begin{bmatrix}\underrightarrow{\hat{\mathbf{h}}}_{\alpha}^{(i)}\\ \underrightarrow{\hat{\mathbf{h}}}_{\xi}^{(i)}\end{bmatrix} = \left(\mathbf{U}^H\mathbf{U}\right)^{-1}\mathbf{U}^H\mathbf{y}_f^{(i)}. \tag{5.12}$$

Note that this estimator does not require any matrix inversion during run-time, as the pilot sequence is known a-priori at the receiver. The LS estimates of $\underrightarrow{\mathbf{h}}_{\alpha}^{(i)}$ and $\underrightarrow{\mathbf{h}}_{\xi}^{(i)}$ are obtained using the two consecutive LTS sequences which are defined in the IEEE 802.11 standards. Assuming that the channel does not change within

a transmission frame and all OFDM symbols are affected by the same CFO coefficient, it can be easily shown that we can estimate the CFO as

$$\hat{\phi} = \frac{1}{\kappa}\tan^{-1}\left(\frac{\Im\{\hat{\underrightarrow{\mathbf{h}}}_{\alpha}^{(1)^H}\hat{\underrightarrow{\mathbf{h}}}_{\alpha}^{(2)}\}}{\Re\{\hat{\underrightarrow{\mathbf{h}}}_{\alpha}^{(1)^H}\hat{\underrightarrow{\mathbf{h}}}_{\alpha}^{(2)}\}}\right) \quad -\frac{1}{2} \leq \phi \leq \frac{1}{2} \tag{5.13}$$

where $\kappa{=}2\pi(N{+}N_g)/N$. The performance of this scheme suffers from residual interference in the high SNR region.

Once the estimate of CFO is known then the CIR, FI Tx/Rx IQ imbalance coefficients can be estimated through any of the schemes presented in section 5.3.3 and 5.3.4.

5.3.2 Non-linear Least Squares Scheme

The RCS scheme is very robust in estimation of CFO coefficient. This estimate can be used to obtain normalized estimates of CIR and FI Tx/Rx IQ imbalance coefficients. The estimation accuracy can be improved further by maximization of the following cost function

$$\hat{\phi}_{\text{opt}} = \arg\max_{\phi} \quad \bar{\mathbf{y}}^H\mathbf{\Delta}_{\phi}(\mathbf{\Delta}_{\phi}^H\mathbf{\Delta}_{\phi})^{-1}\mathbf{\Delta}_{\phi}^H\bar{\mathbf{y}} \tag{5.14}$$

where

$$\mathbf{\Delta}_{\phi} = \begin{bmatrix}\mathbf{E}^{(1)}\mathbf{X} & \mathbf{E}^{(1)}\mathbf{X}^* & (\mathbf{E}^{(1)}\mathbf{X})^* \\ \mathbf{E}^{(2)}\mathbf{X} & \mathbf{E}^{(2)}\mathbf{X}^* & (\mathbf{E}^{(2)}\mathbf{X})^*\end{bmatrix} \tag{5.15}$$

and maximization is performed via simple one dimensional GS. Using the estimates of ϕ from (5.13) as an initial search point in (5.14) the search convergence time can be minimized. The NLLS scheme yields improved CFO estimates at the expense of additional complexity.

5.3.3 Iterative CIR and IQ Imbalance Estimation

Once the estimates of $\mathbf{E}^{(i)}$ in (5.4) are available via (5.13) or (5.14) these estimates can be used in (5.6) and (5.8) to estimate $\mathbf{h}$ and $\boldsymbol{\theta}$ in an iterative manner. Using (5.7) the CIR can be estimated (assuming no IQ imbalance is present in the system):

$$\hat{\underline{\mathbf{h}}} = \left(\mathbf{X}_{\boldsymbol{\theta}}^T\mathbf{X}_{\boldsymbol{\theta}}\right)^{-1}\mathbf{X}_{\boldsymbol{\theta}}^T\underline{\mathbf{y}}^{(i)} \tag{5.16}$$

where $\mathbf{X}_{\boldsymbol{\theta}}$=$\mathbf{X}_1(\boldsymbol{\Theta}_1 \odot \mathbf{I}_{L_h})$. Now that the initial estimates of the FS CIR are available the estimates of the FI Tx/Rx IQ imbalance can be obtained through (5.9) as

$$\hat{\boldsymbol{\theta}} = \left(\mathbf{X}_{\boldsymbol{h}}^T \mathbf{X}_{\boldsymbol{h}}\right)^{-1} \mathbf{X}_{\boldsymbol{h}}^T \underline{\mathbf{y}}^{(i)} \tag{5.17}$$

where $\mathbf{X}_{\boldsymbol{h}}$=$\mathbf{X}_2\mathbf{A}_{\boldsymbol{h}}$. Using (5.16) and (5.17) iteratively, the required estimates can be achieved within a few steps. The overall scheme is organized in algorithm 2. The estimation performance results are illustrated in section 5.5, the estimates obtained from proposed scheme provide near ideal BER performance at a fraction of computational complexity.

5.3.4 Non-iterative CIR and IQ imbalance Estimation

Using the time-domain equivalent model of (5.5) a scaled version of CIR estimates can be conveniently obtained through a LS solution of

$$\begin{bmatrix} \mathbf{y}^{(1)} \\ \mathbf{y}^{(2)} \end{bmatrix} = \begin{bmatrix} \hat{\mathbf{E}}^{(1)}\mathbf{X} & \hat{\mathbf{E}}^{(1)}\mathbf{X}^* & (\hat{\mathbf{E}}^{(1)}\mathbf{X})^* \\ \hat{\mathbf{E}}^{(2)}\mathbf{X} & \hat{\mathbf{E}}^{(2)}\mathbf{X}^* & (\hat{\mathbf{E}}^{(2)}\mathbf{X})^* \end{bmatrix} \cdot \begin{bmatrix} \mathbf{h}_\alpha \\ \mathbf{h}_\beta \\ \mathbf{h}_\gamma \end{bmatrix} + \begin{bmatrix} \mathbf{n}^{(1)} \\ \mathbf{n}^{(2)} \end{bmatrix}. \tag{5.21}$$

The magnitude of vector $\hat{\mathbf{h}}_\alpha$ is dominant because this vector is associated with the desired component of the received signal. The analysis of coefficient α shows that $\alpha \approx 1$ (even for moderate values of $\eta_{T/R}$,$\theta_{T/R}$), and thus $\hat{\mathbf{h}}_\alpha$ can be approximated as $\hat{\mathbf{h}}$. The estimates of the IQ imbalance coefficients can be obtained through (5.9).

As it will be evident from simulations the BER performance with the estimates obtained through iterative estimates from Section 5.3.3 provide near optimal BER performance. It is for this reason that obtaining more accurate estimates of FS CIR is not essential.

5.4 CIR and Tx/Rx IQ Imbalance Equalization

The estimates of CFO obtained through (5.13) and (5.14), Tx/Rx IQ imbalance through (5.18) and CIR through (5.19) are used in the system model defined in

Algorithm 2 Joint Tx/Rx IQ Imbalance, CFO and Channel Estimation.
An iterative algorithm for estimating the IQ imbalance, CFO and channel using LTS pilot symbols as defined in WLAN standards.

1: **Input:** $\underline{\mathbf{y}}^{(i)}$ with i=1, 2.
2: **Output:** $\hat{\mathbf{h}}$, $\hat{\epsilon}$, and $\hat{\boldsymbol{\theta}}$
3: **Calculate:** $\hat{p}_0^{(i)}\hat{\mathbf{h}}_\alpha^{(i)}$ and $\hat{p}_0^{(i+1)}\hat{\mathbf{h}}_\alpha^{(i+1)}$ using the system model presented in (5.12) and then estimate ϵ using (5.13).
4: **intialization:** $\boldsymbol{\theta}^{(0)} = [1\ 0\ 0\ 0\ 0\ 0]^T$,
which corresponds to the no Tx/Rx IQ imbalance case.
5: **calculate:** $\hat{\underline{\mathbf{h}}}^{(0)} = \left(\mathbf{X}_{\boldsymbol{\theta}^{(0)}}^T \mathbf{X}_{\boldsymbol{\theta}^{(0)}}\right)^{-1} \mathbf{X}_{\boldsymbol{\theta}^{(0)}}^T \underline{\mathbf{y}}$ assuming no Tx/Rx IQ imbalance and calculate $\mathbf{X}_{\boldsymbol{\theta}^{(0)}}$ using the model in (5.9)
6: **If** BER / estimation error criteria is not met
7: **repeat**
8: Calculate

$$\hat{\boldsymbol{\theta}}^{(k)} = \left(\mathbf{X}_{\hat{\boldsymbol{h}}^{(k-1)}}^T \mathbf{X}_{\hat{\boldsymbol{h}}^{(k-1)}}\right)^{-1} \mathbf{X}_{\hat{\boldsymbol{h}}^{(k-1)}}^T \underline{\mathbf{y}} \tag{5.18}$$

9: Calculate $\mathbf{X}_\theta$ using the estimates of $\boldsymbol{\theta}^{(k)}$ in model of (5.6)
10: LS estimates of CIR

$$\hat{\underline{\mathbf{h}}}^{(k)} = \left(\mathbf{X}_{\hat{\boldsymbol{\theta}}^{(k)}}^T \mathbf{X}_{\hat{\boldsymbol{\theta}}^{(k)}}\right)^{-1} \mathbf{X}_{\hat{\boldsymbol{\theta}}^{(k)}}^T \underline{\mathbf{y}} \tag{5.19}$$

11: Calculate $\mathbf{X}_{\hat{\boldsymbol{\theta}}^{(k)}}$ using the model in (5.8) with estimates $\hat{\underline{\mathbf{h}}}^{(k)}$
12: k=k+1
13: **until** No significant improvement in cost function

$$\left\| \underline{\mathbf{y}} - \mathbf{X}_1 \left(\hat{\boldsymbol{\Theta}}_1^{(k)} \odot \mathbf{I}_{L_h} \right) \hat{\underline{\mathbf{h}}}^{(k)} \right\|^2 < e \tag{5.20}$$

or maximum numbers of iterations is reached.

(5.5). We can reformulate the system as

$$\begin{bmatrix} \mathbf{y}_f^{I_{(i)}} \\ \mathbf{y}_f^{Q_{(i)}} \end{bmatrix} = \begin{bmatrix} \bar{\mathbf{A}}^{I_{(i)}} & \bar{\mathbf{B}}^{I_{(i)}} & \bar{\mathbf{C}}^{I_{(i)}} & \text{-}\bar{\mathbf{A}}^{Q_{(i)}} & \text{-}\bar{\mathbf{B}}^{Q_{(i)}} & \text{-}\bar{\mathbf{C}}^{Q_{(i)}} \\ \bar{\mathbf{A}}^{Q_{(i)}} & \bar{\mathbf{B}}^{Q_{(i)}} & \bar{\mathbf{C}}^{Q_{(i)}} & \bar{\mathbf{A}}^{I_{(i)}} & \bar{\mathbf{B}}^{I_{(i)}} & \bar{\mathbf{C}}^{I_{(i)}} \end{bmatrix} \cdot \left(\begin{bmatrix} \alpha^I & -\alpha^Q \\ \beta^I & \beta^Q \\ \gamma^I & \gamma^Q \\ \alpha^Q & \alpha^I \\ \beta^Q & -\beta^I \\ \gamma^Q & -\gamma^I \end{bmatrix} \odot \mathbf{I}_N \right) \begin{bmatrix} \mathbf{s}^{I_{(i)}} \\ \mathbf{s}^{Q_{(i)}} \end{bmatrix} + \begin{bmatrix} \mathbf{z}^{I_{(i)}} \\ \mathbf{z}^{Q_{(i)}} \end{bmatrix} \tag{5.22}$$

where $\bar{\mathbf{A}}^{(i)}$=$\mathbf{P}^{(i)}\mathbf{\Lambda}_h$, $\bar{\mathbf{B}}^{(i)}$=$\mathbf{P}^{(i)}\mathbf{\Lambda}_h\mathbf{Q}$ and $\bar{\mathbf{C}}^{(i)}$=$\mathbf{P}^{(i)^H}\mathbf{Q}\mathbf{\Lambda}_h^*$. In compact notation this can be expressed as

$$\underline{\mathbf{y}}_f^{(i)} = \mathbb{\Lambda}_{\boldsymbol{h}}^{(i)} \Big(\mathbf{\Theta}_2 \odot \mathbf{I}_N \Big) \underline{\mathbf{s}}^{(i)} + \underline{\mathbf{z}}^{(i)}. \tag{5.23}$$

If we can define the overall effect of the CIR, CFO and the FI Tx/Rx IQ imbalance as $\hat{\mathbf{H}}^{(i)}$=$\mathbb{\Lambda}_{\hat{h}}^{(i)} \Big(\hat{\mathbf{\Theta}}_2 \odot \mathbf{I}_N \Big)$ using the estimates obtained through (5.13), (5.18) and (5.19) then these effects can be compensated using a simple MMSE equalizer as follows

$$\hat{\underline{\mathbf{s}}}^{(i)} = \Big(\hat{\mathbf{H}}^{(i)^H} \hat{\mathbf{H}}^{(i)} + \sigma_z^2 \mathbf{I}_{2N} \Big)^{-1} \hat{\mathbf{H}}^{(i)^H} \underline{\mathbf{y}}_f^{(i)}. \tag{5.24}$$

Although the matrix inversion required in (5.24) has no obvious reduced complexity solution but this method allows a single stage compensation of FS CIR, CFO and FI Tx/Rx IQ imbalance. The estimation error and BER performance of the proposed schemes is presented in the next section.

5.5 Simulation Results

This chapter is focused on a typical SISO OFDM transmission system (such as WLAN/WiMAX). The number of subcarriers in each OFDM symbol is N=64. The system bandwidth is assumed to be 20 MHz and the sampling rate is defined as (T_s=0.05μs). The subcarrier spacing is assumed to be ΔF=312.5 kHz. We consider an L_h=6 tap Rayleigh fading process with exponential power delay profile $e^{-\underline{\gamma}l}$ with $\underline{\gamma}$=0.2 and l=0, 1, ..., L_h−1. To mitigate the effects of ISI, the

guard interval is assumed to be longer than the CIR, i.e. N_g=10. The transmitted data is assumed to be taken from a 16 QAM constellation and no channel coding is used in these simulations. Each OFDM block contains 10 OFDM symbols. The first two symbols of each block are assumed to be known training sequences chosen from a BPSK constellation according to the criterion presented in [31]. The IQ imbalance process defined in (5.3) is assumed to be a random variable with a uniformly distributed amplitude imbalance, $\eta_{T/R}\sim\mathcal{U}$[-0.05, 0.05], and phase imbalance, $\theta_{T/R}\sim\mathcal{U}[-5^\circ, 5^\circ]$. The Tx/Rx IQ imbalance model used in this chapter is the same as that considered in chapter 3 and chapter 4 and also used in [18, 31, 44, 86]. The CFO coefficient ϵ is assumed to be uniformly distributed, $\epsilon\sim\mathcal{U}$[-0.3125, 0.3125], which corresponds to a spectral range of $\pm$100 kHz. An independent CIR and IQ imbalance realization is generated for every simulated OFDM block. The simulations are performed using 5,000 Monte-Carlo channel realizations for each SNR.

To measure the error performance of the proposed techniques following definitions have been used MSE($\hat{\mathbf{h}}$)=$E\{\|\mathbf{h}-\hat{\mathbf{h}}\|^2\}$ and MSE($\hat{\phi}$)=$E\{|\phi-\hat{\phi}|^2\}$.

Fig. 5.2 illustrates the MSE performance of the CFO process estimation. If the presence of FI Tx/Rx IQ imbalance is ignored in the transmission system as in [78], the CFO estimation performance suffers an error floor even at moderate SNR. Estimation of the CFO using the proposed RCS scheme (5.13) slightly improves the estimation error. The estimation accuracy of the CFO can be improved significantly with the simple GS algorithm (5.14). The estimate of CFO obtained through (5.14) is not optimal due to the approximations made in (5.12).

The MSE performance of one of the IQ imbalance coefficient β (see (5.4)) is illustrated in Fig. 5.3. The CRLB for this estimation is presented as a reference [80]. As mentioned earlier some of the coefficients in $\boldsymbol{\theta}$ have a very small magnitude and their estimation is ignored in the proposed model.

The CIR estimation performance of iterative and CLFE techniques have been illustrated in Fig. 5.4 and Fig. 5.5 respectively. The iterative scheme requires just one pilot symbol to perform the required estimation while the non-iterative scheme requires two pilots and this is computationally intensive. The iterative scheme provide near optimal BER performance after just one iteration. The CIR estimation accuracy of the iterative scheme is "floored" after 25 dB and this is due to the approximations made in (5.4).

The BER performance for the uncoded 16 QAM modulation scheme using the proposed scheme is presented in Fig. 5.6. It can be seen that in the case

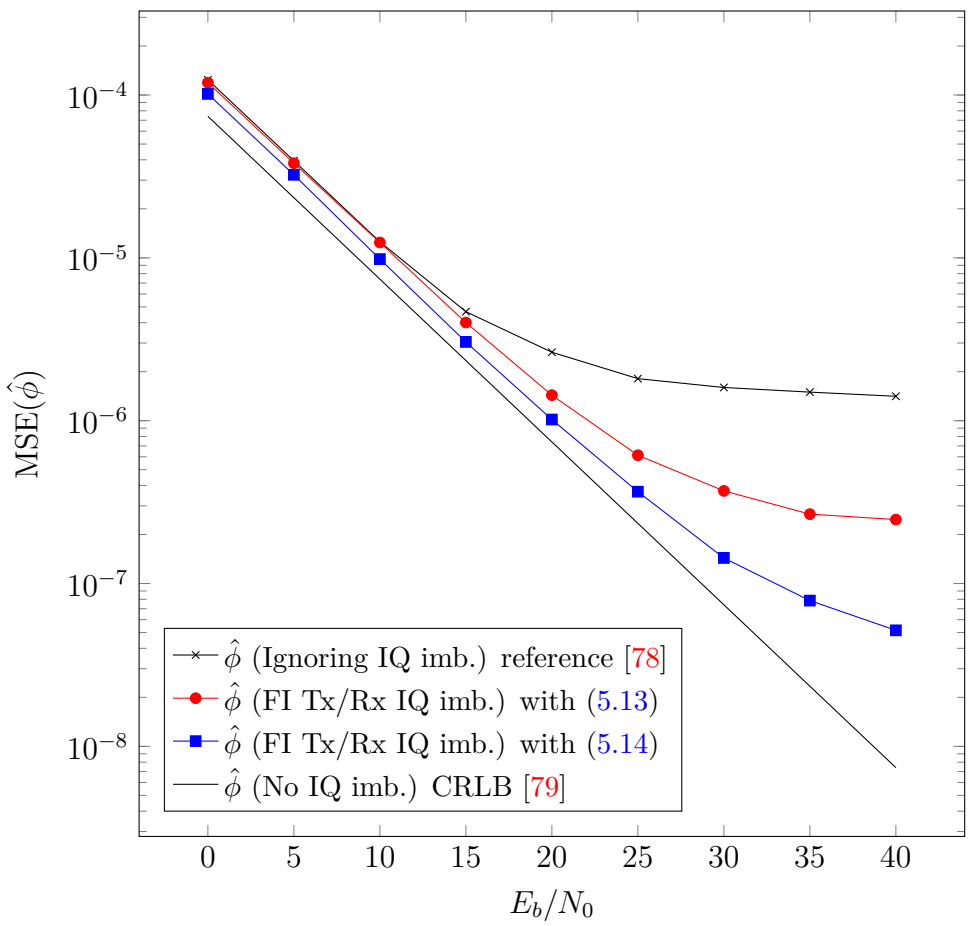

Figure 5.2: MSE of CFO estimation using (5.13) and (5.14), in the presence of IQ imbalance $\eta_{\mathrm{T/R}} \sim \mathcal{U}[\text{-}0.05, 0.05]$, $\theta_{\mathrm{T/R}} \sim \mathcal{U}[\text{-}5^{\circ}, 5^{\circ}]$ and normalized CFO $\epsilon \sim \mathcal{U}[\text{-}0.3, 0.3]$,N=64, Rayleigh channel with L_h=6 taps and 5,000 Monte-Carlo realizations.

of ignoring CFO and IQ imbalance in the process of CIR estimation and equalization the system is completely useless. If CFO is estimated and IQ imbalance is not considered in the channel estimation and equalization process the BER performance of the system is still not acceptable. To assess the performance of the system while considering only Rx IQ imbalance in addition to CFO process provides slight improvement to the overall performance.

The BER performance of the proposed RCS and NLLS schemes for CFO estimation and iterative CIR and Tx/Rx IQ imbalance estimation provide near ideal performance for the system under consideration. Although the CFO estimates obtained through RCS scheme are not as accurate as the estimates obtained

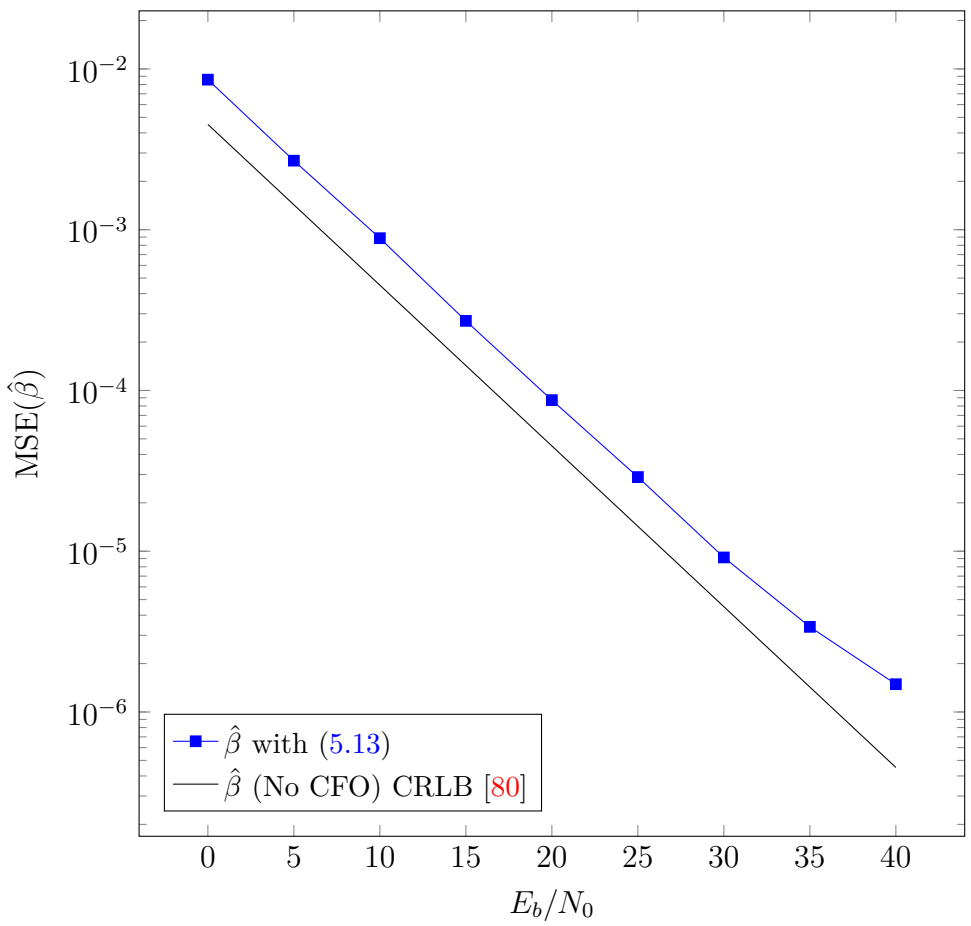

Figure 5.3: MSE of IQ imbalance coefficient β using (5.18) and (5.19) in the presence of Tx/Rx IQ imbalance, CFO estimated via (5.13), $\eta_{\mathrm{T/R}} \sim \mathcal{U}[-0.05, 0.05]$, $\theta_{\mathrm{T/R}} \sim \mathcal{U}[-5°, 5°]$ and normalized CFO $\epsilon \sim \mathcal{U}[-0.3, 0.3]$, N=64, Rayleigh channel with L_h=6 taps and 5,000 Monte-Carlo realizations.

through NLLS however the subsequent CIR, IQ imbalance and BER estimation performance of the system is not far away from the ideal case.

It is also worth mentioning that the performance of the proposed scheme is equally effective for higher modulation schemes such as 64 QAM but these results are not presented within this work.

5.6 Conclusions

In this chapter we have studied the joint estimation of CIR, CFO and FI Tx/Rx IQ imbalance for OFDM systems. Using a previously proposed low complexity

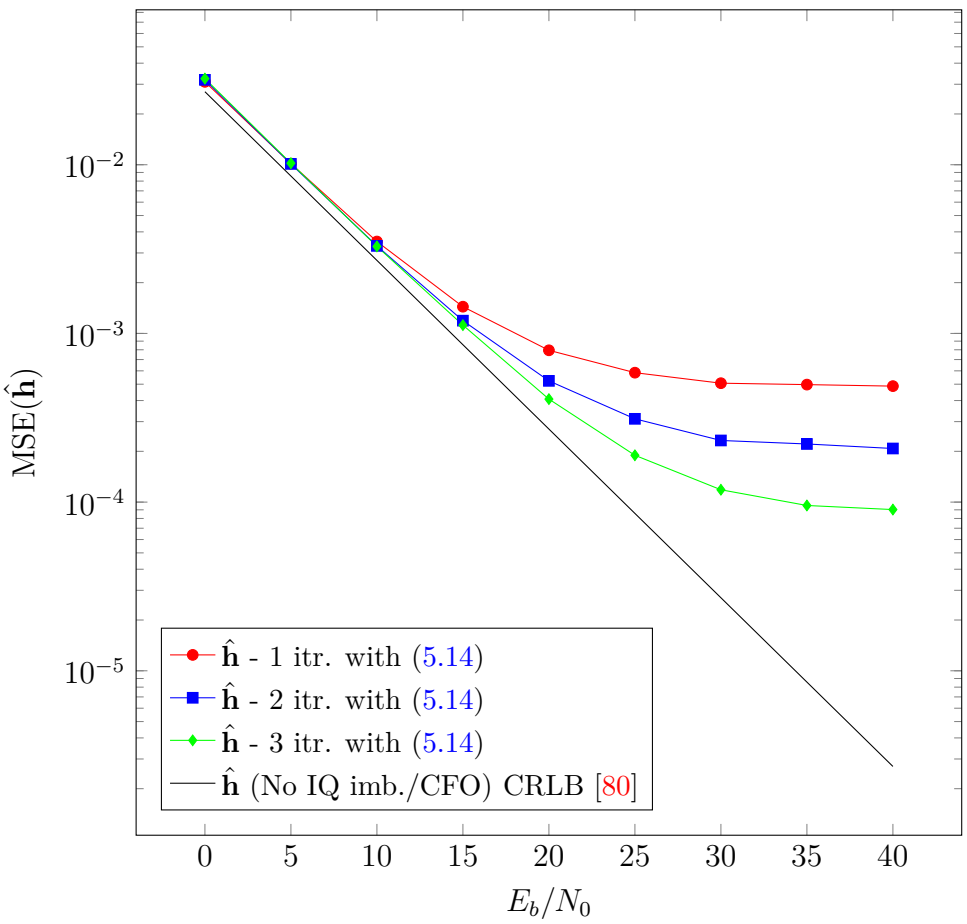

Figure 5.4: MSE performance of the CIR estimation with algorithm 2, $\eta_{\mathrm{T/R}} \sim \mathcal{U}[-0.05, 0.05]$, $\theta_{\mathrm{T/R}} \sim \mathcal{U}[-5^\circ, 5^\circ]$ and normalized CFO $\epsilon \sim \mathcal{U}[-0.3, 0.3]$, N=64, Rayleigh channel with L_h=6 taps and 5,000 Monte-Carlo realizations.

scheme which can estimate CFO very effectively in the presence of IQ imbalance two different techniques have been considered for the estimation of CIR and FI Tx/Rx IQ imbalance. All of the above system is based on pilot sequences defined within the WLAN standards. Simulation results show that the CFO, CIR and IQ imbalance estimation performance is acceptable even for higher throughput systems.

We have also proposed a low complexity single stage joint Tx/Rx IQ imbalance, CFO compensation and channel equalization scheme which can effectively deal with IQ imbalance and a FS CIR. The proposed system is equally effective for systems with only Tx and/or Rx IQ imbalance. The simulation results show that the proposed schemes provide an excellent performance/complexity trade-off.

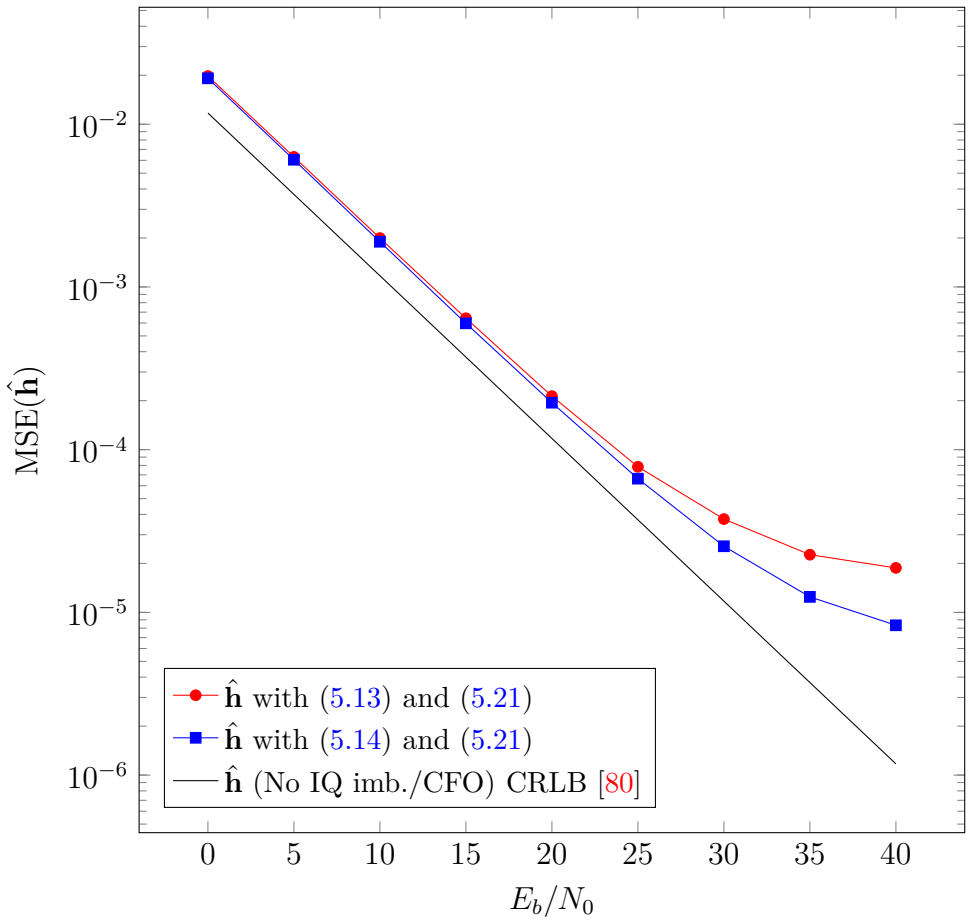

Figure 5.5: MSE performance of the normalized CIR estimation with LS solution of (5.21), $\eta_{\mathrm{T/R}} \sim \mathcal{U}[\text{-}0.05, 0.05]$, $\theta_{\mathrm{T/R}} \sim \mathcal{U}[\text{-}5^\circ, 5^\circ]$ and normalized CFO $\epsilon \sim \mathcal{U}[\text{-}0.3, 0.3]$, N=64, Rayleigh channel with L_h=6 taps and 5,000 Monte-Carlo realizations.

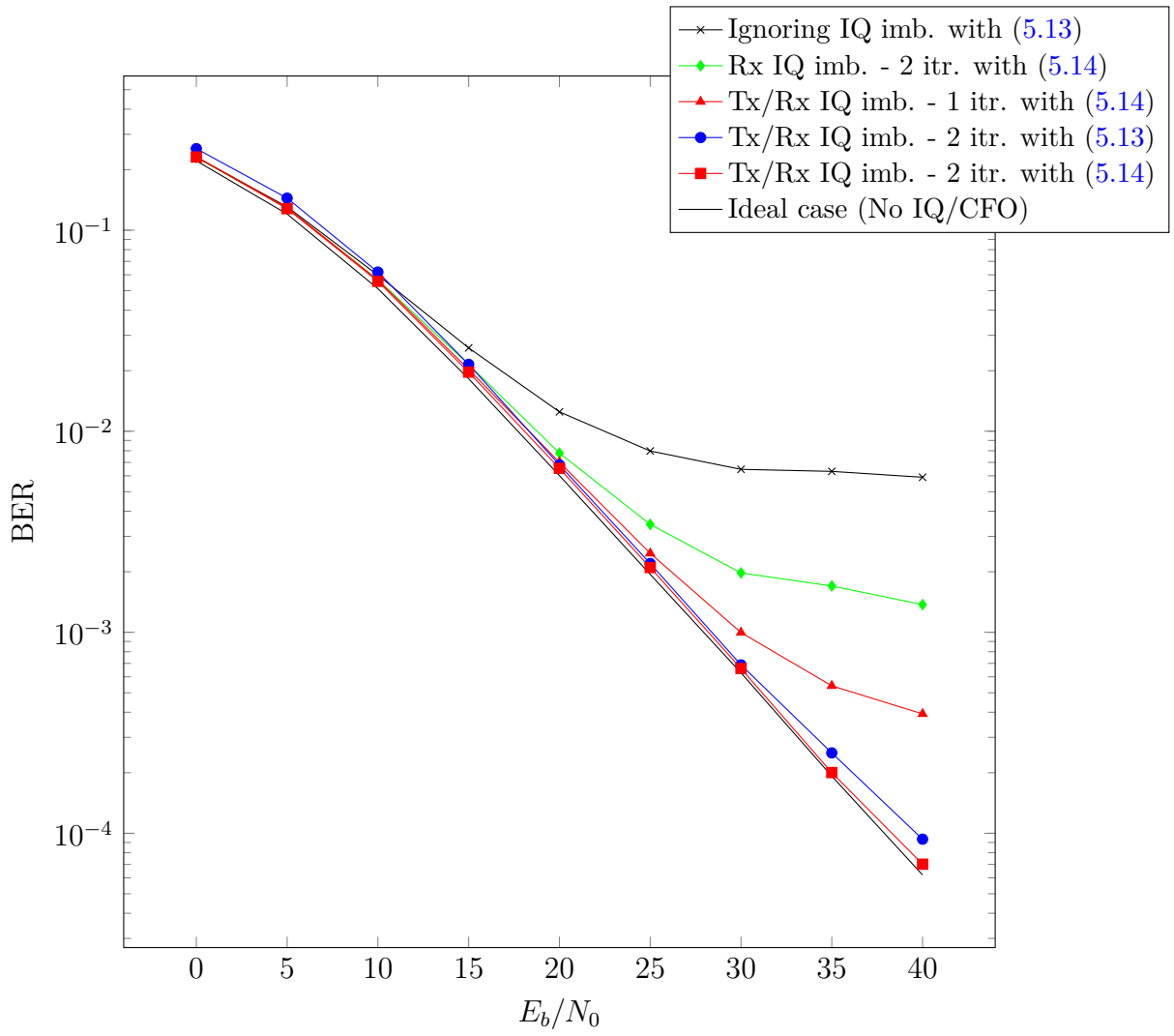

Figure 5.6: BER performance of proposed scheme (5.24) using channel estimation based on (5.19) and IQ imbalance estimates (5.18); CFO estimation schemes of (5.13) and (5.14), N=64, $\eta_{\mathrm{T/R}} \sim \mathcal{U}[-0.05, 0.05]$, $\theta_{\mathrm{T/R}} \sim \mathcal{U}[-5^{\circ}, 5^{\circ}]$ and normalized CFO $\epsilon \sim \mathcal{U}$[-0.3, 0.3], Rayleigh channel with L_h=6 taps and 5,000 Monte-Carlo realizations.

6 Joint CIR, FI Rx IQ Imbalance and Amplifier Non-linearity Estimation

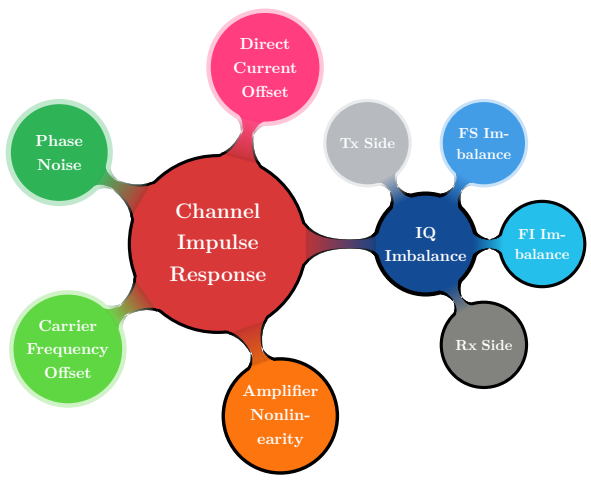

Abstract

The objective of this chapter is to study joint estimation of FS CIR, FI Rx IQ imbalance in the presence of amplifier non-linearity. Instead of predistorting the transmitted signal to placate the effects of non-linearity, the proposed scheme makes no effort to combat non-linearity at the transmitter while the receiver estimates all the unknown parameters using pilot sequences.

To estimate these unknowns, special training sequences have been found. A low complexity scheme has been proposed to estimate FS CIR, FI Rx IQ imbalance. The parameters of non-linearity are estimated through GS.

A two stage data detection technique is also proposed to alleviate the effects of amplifier non-linearity from the received data.

6.1 Introduction

OFDM is the underlying principle in most communication techniques standardized for different applications. The most common examples are IEEE wireless standards 802.16e (WiMAX), 802.11a/b/g (WLAN) and power line communication standards. The most expensive components in any modem are the analog components such as LO and the DC modules which are cost-effective (but can cause distortion) and occupy small board space as compared to multi-stage heterodyne receivers. But the estimation of channel and other parameters in the presence of a HPA is often not reliable even at higher SNRs. Therefore it is very important that we take these non-ideal effects into consideration while estimating CIR and IQ imbalance parameters and also while estimating the data.

In this work an optimal training sequence is found which minimizes the effects of an HPA on the CIR estimation. Then we work out a joint CIR and FI Rx IQ imbalance estimation scheme to estimate these parameters in a non-iterative manner. In the presence of an accurate estimate of the CIR and IQ imbalance the effects of non-linearity (NL) can still limit the BER performance even at high SNR levels. To remove this limitation we propose some techniques which can alleviate this problem in a scalable manner.

The effect of non-linearity can be minimized in a number of ways -e.g., by using a pre-distorter (PD) before modulating the signal [87] and other schemes that have been proposed to reduce the peak-to-average-power-ratio (PAPR) of the transmitted signal [88]. Predistortion functions require complex mathematical modelling of the PD function, which requires a feedback loop from the RF output after the HPA and needs several iterations to converge. Similarly, precoding which allocates reserved subcarriers in the OFDM symbol, can reduce the effect of NL at the cost of bandwidth efficiency of the system. The effect of amplifier NL and IQ imbalance is considered in [89] and the authors have derived analytical expressions for the BER performance in the presence of IQ imbalance and amplifier NL. Iterative ML detection of data in the presence of NL is discussed in [68]. Some very insightful work on the mitigation of clipping effects can also be found in [69].

The objective of this study is to evaluate the performance of an OFDM system in the presence of transmit amplifier NL and FI Rx IQ imbalance. The schemes used to estimate FS CIR, FI IQ imbalance and NL are non-iterative and do not incur any additional complexity. However, data detection requires a two-stage detection to gradually eliminate the effects of the NL.

Unlike most of the previous work [68,69] dealing with amplifier NL, this work considers the CIR to be unknown and estimates it every OFDM block. This requires an optimal training sequence which can yield good estimates of all unknown parameters in the presence of severe non-linear distortion. The proposed scheme does not require any sophisticated pre-distorter or precoding scheme to obtain acceptable system performance. However, the overall performance of the system can certainly be improved by considering the above-mentioned techniques. The most significant effect of amplifier NL is the spectral leakage to adjacent channels. This can degrade the performance of adjacent carriers in addition to affecting the data on the carrier itself. Most of the literature dealing with amplifier NL does not consider the spectral leakage. A transmit bandpass filter is also considered in this work to limit the effect on adjacent carriers. To consider the spectral leakage effects the transmitted signal is over-sampled.

We assume that the band-pass filter following the HPA can safely eliminate this out of band distortion. Here a typical downlink scenario is considered where the base-station has a high quality LO and the receiver LO is the main source of IQ imbalance. The estimation of the CIR, FI Rx IQ imbalance and non-linearity process is done post FFT.

This chapter is organized as follows. Section 6.2 describes the baseband model of the amplifier NL and IQ imbalance. These models are then incorporated into an OFDM system model and the estimation of CIR in the presence of IQ imbalance is described. In Section 6.3 the mitigation of distortion (caused by the non-linear amplifier) using iterative feedback is discussed. In Section 6.4 the performance using Monte-Carlo simulation is analyzed.

Notation: In addition to previously assigned notations some additional terms are also defined. $\mathbf{F_U}$ is a DFT matrix of size $U(N \times N)$ where U is the oversampling factor; $\mathbf{F_U}$ is partitioned into sub-blocks, i.e. , $\mathbf{F_U} = [\mathbf{W}|\mathbf{V}]$ where $\mathbf{W}$ is now the $UN \times L_h$ portion of $\mathbf{F_U}$.

6.2 Transmission Model

A typical OFDM transmission system in the presence of a transmit amplifier NL and FS CIR is considered. It is assumed that the system under consideration suffers from only FI Rx IQ imbalance. We consider a block transmission system where the first symbol of every block contains a completely known training sequence for estimation purposes and the FS CIR is considered to be time-invariant for the whole block. We assume furthermore that the receiver has no knowledge

of the NL parameters of the HPA and we will use a special training sequence to estimate these coefficients. Since the HPA characteristics are assumed to be very slowly time varying, they need not to be estimated as frequently as the other parameters. As explained in Section 2.3.5, in the literature two types of high power amplifier are widely considered - namely the travelling wave tube amplifier (TWTA) [39] and the solid state power amplifier (SSPA) [38]. Here only the SSPA amplifier model will be considered because this model accurately describes the behaviour of the HPA used in mobile devices.

By expressing the HPA input signal in polar coordinates as $x[n] := |x[n]|\exp(j\phi[n])$, the magnitude and phase transfer functions of a SSPA can be respectively modelled as

$$\begin{aligned} f(|x[n]|) &= \frac{|x[n]|}{\left[1+\left(\frac{|x[n]|}{A_{\max}}\right)^{2p}\right]^{\frac{1}{2p}}}, \\ \Phi(x[n]) &\simeq 0. \end{aligned} \tag{6.1}$$

Now (6.1) defines the AM/AM and AM/PM conversion characteristics for a typical SSPA; p is the non-linearity factor and as $p \to \infty$, this model approaches soft limiter characteristics as defined in (2.50); $A_{\max}$ is the maximum unclipped signal amplitude (as defined in (6.18)). The AM/PM effect is negligible and is not considered in this work. The overall output of an SSPA is described as $g(x[n]) = f(|x[n]|)\exp(j(\Phi(x[n]) + \phi[n]))$. So the received signal in the absence of IQ imbalance can be defined as

$$\mathbf{r} = \mathbf{H}_c\mathbf{A}\mathbf{F}_{\mathrm{U}}^{H}\mathbf{s} + \mathbf{n} \tag{6.2}$$

where $\mathbf{s}$ is the $UN \times 1$ transmitted symbol as defined in (6.3), and U is the oversampling factor; $\mathbf{H}_c$ is the circulant channel matrix of size $U(N \times N)$ corresponding to a slowly time-varying channel; $\mathbf{A}$ is the HPA non-linearity transfer function which depends on the transmitted symbol $\mathbf{s}$ as defined in (6.1); $\mathbf{n}$ is the circularly symmetric complex additive white Gaussian noise vector of size $UN \times 1$ i.e., $\mathbf{n} \sim \mathcal{CN}(\mathbf{0}, \mathbf{\Xi}_n)$, where $\mathbf{\Xi}_n = \sigma_n^2\mathbf{I}$ and

$$\mathbf{s} = [s_0, \cdots, s_{N/2-1}, \underbrace{0, \cdots, 0}_{(U-1)N \text{ zeros}}, s_{N/2}, \cdots, s_{N-1}]^T. \tag{6.3}$$

Now the received signal in presence of IQ imbalance is defined as

$$\mathbf{y} = \mu \mathbf{H}_c \mathbf{A} \mathbf{F}_{\mathrm{U}}^H \mathbf{s} + \nu (\mathbf{H}_c \mathbf{A} \mathbf{F}_{\mathrm{U}}^H \mathbf{s})^* + \mathbf{n}, \tag{6.4}$$

with μ and ν defined as

$$\begin{aligned} \mu &= \cos\theta + j\eta\sin\theta \\ \nu &= \eta\cos\theta - j\sin\theta, \end{aligned} \tag{6.5}$$

where θ and η are phase and amplitude imbalance coefficients respectively. This block is then transmitted over a (slowly) time-variant channel. Fig. 6.1 illustrates

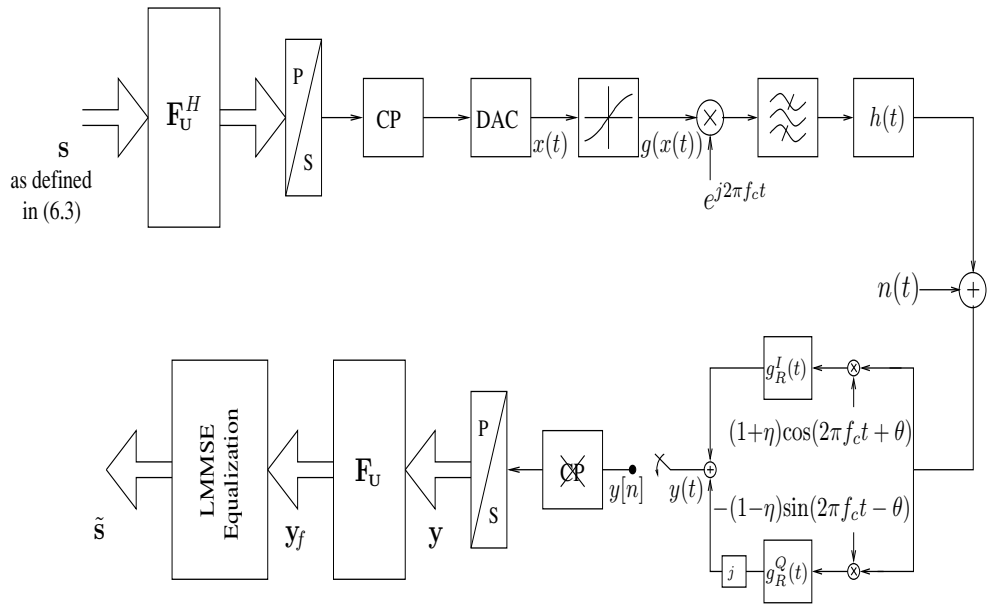

Figure 6.1: General OFDM transmission system in the presence of amplifier non-linearity and IQ imbalance.

the transmission model in the presence of non-ideal behaviour. The implementation of the bandpass filter is ignored as it does not effect the subcarriers of interest, see Fig. 6.4. The received signal after demodulation in the presence of IQ imbalance can be written as

$$\mathbf{y}_f = \mu \underbrace{\mathbf{D}\mathbf{W}}_{\mathbf{D_1}} \mathbf{h} + \nu \underbrace{\mathbf{F}_{\mathrm{U}} \mathbf{F}_{\mathrm{U}}^T \mathbf{D}^H \mathbf{W}^*}_{\mathbf{D_2}} \mathbf{h}^* + \mathbf{z}, \tag{6.6}$$

where $\mathbf{D} := \text{diag}(\mathbf{F}_{\text{U}}\mathbf{A}\mathbf{F}_{\text{U}}^{H}\mathbf{s})$ and $\mathbf{z}$ is the equivalent additive white Gaussian noise.

6.2.1 Channel Estimation

To mitigate the effects of FI Rx IQ imbalance, the CIR needs to be estimated in the presence of this non-ideal behaviour. CIR estimation in the presence of IQ imbalance and other effects is a challenging problem and has been considered for an OFDM system in [18, 25, 90]. We use a maximum likelihood (ML) estimator to determine the FI Rx IQ imbalance and CIR by using a full-pilot sequence. We use a carefully chosen BPSK sequence with normalized energy in every bin.

In the presence of additive Gaussian noise the log-likelihood function can be expressed as

$$\begin{aligned}\mathcal{L}(\mu,\nu,\mathbf{h}) \;=\; & (\mathbf{y}_f - \mu\mathbf{D}\mathbf{W}\mathbf{h} - \nu\mathbf{F}_{\text{U}}\mathbf{F}_{\text{U}}^{T}\mathbf{D}^{H}\mathbf{W}^{*}\mathbf{h}^{*})^{H} \\ & \boldsymbol{\Xi}_{z}^{-1}(\mathbf{y}_f - \mu\mathbf{D}\mathbf{W}\mathbf{h} - \nu\mathbf{F}_{\text{U}}\mathbf{F}_{\text{U}}^{T}\mathbf{D}^{H}\mathbf{W}^{*}\mathbf{h}^{*}) \\ & + \text{constant}. \end{aligned} \tag{6.7}$$

In the presence of non-linearity, the use of any arbitrary pilot sequence may render channel estimation process completely useless. However, through an appropriate choice of pilot symbol it is possible to minimize the effects of non-linearity and therefore the overall interference can be conveniently assumed to be additive white Gaussian. With this assumption the ML estimate of the FS CIR is thus

$$\hat{\mathbf{h}} = (|\mu|^2\mathbf{D}_1^{H}\mathbf{D}_1 - |\nu|^2\mathbf{D}_2^{T}\mathbf{D}_2^{*})^{-1}[\mu^{*}\mathbf{D}_1^{H}\mathbf{y}_f - \nu\mathbf{D}_2^{T}\mathbf{y}_f^{*}], \tag{6.8}$$

where $\mathbf{D}_1$ and $\mathbf{D}_2$ are defined in (6.6). The inverse matrix in (6.8) can be approximated by the identity matrix since $|\mu|^2 \approx 1$, $|\nu|^2 \approx 0$ and $\mathbf{D} \approx \mathbf{I}$ (by appropriately choosing a training sequence).

The optimal training sequences to estimate the FS CIR and FI Rx IQ imbalance values are obtained via:

$$\mathbf{s}_i = \arg\ \min_{\dot{\mathbf{s}}}/\max \|\mathbf{F}_{\text{U}}^{H}\dot{\mathbf{s}} - \mathbf{A}\mathbf{F}_{\text{U}}^{H}\dot{\mathbf{s}}\|^2, \quad i = 1, 2 \tag{6.9}$$

here $\mathbf{s}=[\dot{s}[0], \ldots, \dot{s}[\frac{N}{2}-1], 0, \ldots, 0, \dot{s}[\frac{N}{2}], \ldots, \dot{s}[N-1]]^{T}$ is an $UN\times 1$ sequence with $\dot{s}_k \in \{\pm 1\}$, where $0 \le k \le N-1$. The sequence $\mathbf{s}_1$ (used to estimate CIR and FI Rx IQ imbalance) is obtained by minimizing this criterion and similarly $\mathbf{s}_2$ (used

to estimate non-linearity parameters) is obtained by maximization. These solutions are obtained through exhaustive search and used in the system as defined in (6.9).

6.2.2 Imbalance Estimation

Substituting (6.8) back into (6.6) and introducing the new expression $\alpha_0 = \nu/\mu^*$, we find

$$\begin{aligned}\hat{\alpha}_0 = \arg \min_{\alpha_0} &(\mathcal{Q}_1\mathbf{y}_f - |\alpha_0|^2\mathcal{Q}_2\mathbf{y}_f + \alpha_0\mathcal{Q}_3\mathbf{y}_f^*)^H \\ &\cdot (\mathcal{Q}_1\mathbf{y}_f - |\alpha_0|^2\mathcal{Q}_2\mathbf{y}_f + \alpha_0\mathcal{Q}_3\mathbf{y}_f^*)\end{aligned} \tag{6.10}$$

where

$$\begin{aligned}\mathcal{Q}_1 &= \mathbf{D}\mathbf{W}\mathbf{W}^H\mathbf{D}^H \\ \mathcal{Q}_2 &= \mathbf{F}_\mathrm{U}\mathbf{F}_\mathrm{U}^T\mathbf{D}^H\mathbf{W}^*\mathbf{W}^T\mathbf{D}\mathbf{F}_\mathrm{U}^*\mathbf{F}_\mathrm{U}^H \\ \mathcal{Q}_3 &= \mathbf{F}_\mathrm{U}{\mathbf{F}_\mathrm{U}}^T\mathbf{D}^*\mathbf{W}^*\mathbf{W}^T\mathbf{D}^T \\ &\qquad - \mathbf{D}\mathbf{W}\mathbf{W}^H\mathbf{D}^H\mathbf{F}_\mathrm{U}\mathbf{F}_\mathrm{U}^T.\end{aligned} \tag{6.11}$$

So from (6.10) we have

$$\hat{\alpha}_0 = \frac{-\mathbf{y}_f^T\mathcal{Q}_3^H\mathcal{Q}_1\mathbf{y}_f}{\mathbf{y}_f^T\mathcal{Q}_3^H\mathcal{Q}_3\mathbf{y}_f^* - \mathbf{y}_f^H\mathcal{Q}_1^H\mathcal{Q}_2\mathbf{y}_f - \mathbf{y}_f^H\mathcal{Q}_2^H\mathcal{Q}_1\mathbf{y}_f}. \tag{6.12}$$

From (6.12) α_0 can be expressed as

$$\begin{aligned}\hat{\alpha}_0 = \frac{\nu}{\mu^*} &= \frac{\eta\cos\theta - j\sin\theta}{\cos\theta - j\eta\sin\theta} \\ &\approx \eta(1+\tan^2\theta) + j(\eta^2-1)\tan\theta,\end{aligned} \tag{6.13}$$

and these approximations hold for small values of imbalance (i.e., $\eta^2\sin\theta\to 0$). From the approximation in (6.13) the estimates of η and θ can be obtained through

$$\hat{\eta} \approx \frac{\Re\{\hat{\alpha}_0\}}{1+\Im\{\hat{\alpha}_0\}^2}, \quad \sin(\hat{\theta}) \approx \frac{-\Im\{\hat{\alpha}_0\}}{\sqrt{1+\Im\{\hat{\alpha}_0\}^2}}. \tag{6.14}$$

From (6.14) the estimates of μ and ν can be obtained via (6.5). The estimate of the CIR can then be obtained by replacing $\hat{\mu}$ and $\hat{\nu}$ back into (6.8).

6.2.3 IQ Imbalance Mitigation and Channel Equalization

Now that the estimate of CIR and FI Rx IQ imbalance coefficients have been found it is possible to compensate them and equalize the CIR at different stages. The IQ imbalance can be more conveniently compensated in the time domain as

$$\mathbf{y}^{\mathrm{i/q}} = \frac{1}{|\hat{\mu}|^2 - |\hat{\nu}|^2}(\hat{\mu}^*\mathbf{y} - \hat{\nu}\mathbf{y}^*), \tag{6.15}$$

where $\mathbf{y}^{\mathrm{i/q}}$ is the received signal after compensation of estimated IQ imbalance parameters. Now the CIR can be easily equalized in the frequency domain using a simple MMSE equalizer

$$\tilde{\mathbf{s}} = \left[\mathbf{\Lambda}_{\hat{h}}\mathbf{\Lambda}_{\hat{h}}^H + \mathbf{I}_{UN}\sigma_n^2\right]^{-1}\mathbf{\Lambda}_{\hat{h}}^H\mathbf{F}_{\mathrm{U}}\mathbf{y}^{\mathrm{i/q}}, \tag{6.16}$$

where $\mathbf{\Lambda}_{\hat{h}} = \mathrm{diag}([\hat{H}[0], \ldots, \hat{H}[UN-1]]^T)$ is the diagonal matrix obtained from the estimated CFR vector.

6.2.4 Estimation of the Non-linearity Coefficients

The amplifier non-linearity is related to the non-linearity parameter p and the clipping level. The effect of these parameters can be assessed in (6.1). These parameters are much more slowly time-varying than the other unknowns such as the CIR, IQ imbalance and CFO. NL coefficients are affected by temperature and ageing. These parameters can be estimated using a simple grid search scheme. The grid search can also be approximated using a polynomial function and its minima can be found analytically as presented in [91]. The cost function is defined as

$$\hat{p}, \hat{A}_{\max} = \underset{\mathrm{p}, A_{\max}}{\arg\min} \|\check{\mathbf{s}} - \mathbf{F}_{\mathrm{U}}g(\mathbf{F}_{\mathrm{U}}^H\mathbf{s}_2)\|^2, \tag{6.17}$$

where $\check{\mathbf{s}}$ is the $N \times 1$ vector of soft decisions (see Fig. 6.1) obtained after channel equalization and IQ imbalance compensation obtained through (6.15) and (6.16).

6.3 Nonlinearity Mitigation and Data Detection

The previous sections discuss the FS CIR estimation in the presence of FI Rx IQ imbalance using a full pilot symbol. The effect of amplifier NL is minimized by selecting an optimal training sequence. The NL coefficients are estimated using a simple GS. In the data symbols the influence of amplifier NL can not be controlled, therefore this NL must be compensated while estimating the data samples. This work proposes a simple decision feedback strategy to compensate these effects by estimating the distortion based on the NL model.

The effect of the NL is directly related to the clipping level which defines the maximum amplitude of a signal that can pass through without distortion:

$$\text{Clip Level} = 20\log_{10}\left(\frac{A_{\max}}{\sigma_s}\right) \text{ dB}, \tag{6.18}$$

where $A_{\max}$ is the maximum unclipped signal amplitude and σ_s^2 is the power of the modulated symbols.

A suitably selected training sequence allows estimation of CIR and FI IQ imbalance parameters in the presence of the HPA non-linearity. The distortion present in the data symbols can still be significant. One of the simplest ways to eliminate this problem is to perform a hard decision on the received sequence and then using the hard estimates compensate the distortion from the actual soft-value iteratively. The algorithm is explained as follows:

1. Obtain hard decision $\hat{\mathbf{s}}$ using estimates from (6.16).

2. Determine the non-linearity distortion as

$$\mathbf{e}_f^{(\mathbf{x},\hat{g})} = \mathbf{F}_{\mathrm{U}}\left(\mathbf{e}^{(\mathbf{x},\hat{g})}\right) = \mathbf{F}_{\mathrm{U}}\left(\hat{g}(\mathbf{x}) - \mathbf{x}\right), \tag{6.19}$$

   where $\mathbf{x} = \mathbf{F}_{\mathrm{U}}^H \hat{\mathbf{s}}$.

3. Taking this distortion into account the second stage estimates can be obtained as

$$\hat{\mathbf{s}} = \left(\mathbf{\Lambda}_{\hat{h}}\mathbf{\Lambda}_{\hat{h}}^H + \mathbf{I}_{UN}\sigma_n^2\right)^{-1}\mathbf{\Lambda}_{\hat{h}}^H\mathbf{F}_{\mathrm{U}}\mathbf{y}^{\mathrm{i/q}} - \mathbf{e}_f^{(\mathbf{x},\hat{g})}. \tag{6.20}$$

Steps (2) - (3) can be repeated a few times to obtain a better BER performance. This approach is useful only when a few symbol errors are present. Oth-

erwise, errors propagation has a very negative effect. The graphical illustration of the proposed scheme is presented in Fig. 6.2.

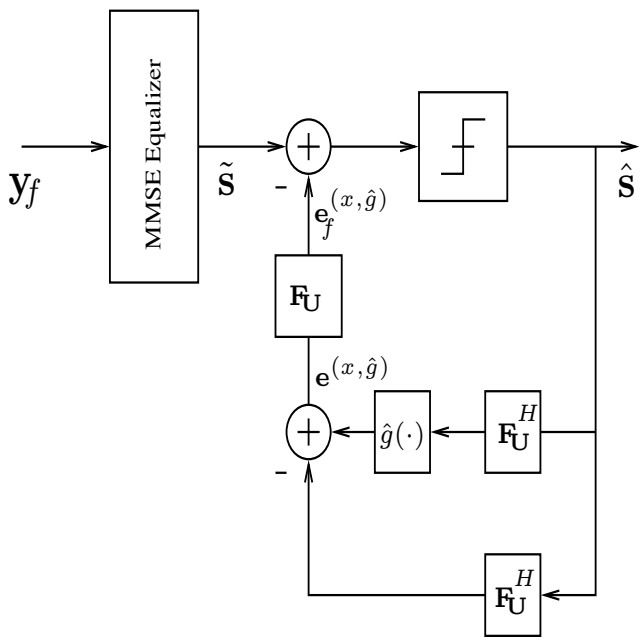

Figure 6.2: The iterative data-detection and non-linearity mitigation process.

6.4 Simulation Results

In the last sections we have presented the framework for estimation and compensation of CIR and IQ imbalance in the presence of NL and later single stage compensation of non-linear distortion using decision feedback. In this section we present Monte-Carlo simulation results to demonstrate the effectiveness of the proposed scheme.

We consider an $L_h = 4$ tap Rayleigh fading process with exponential power delay profile $e^{-\underline{\gamma}l}$ with $\underline{\gamma} = 0.2$ and $l = 0, 1, \ldots L_h - 1$. The oversampling factor is $U = 2$. The IQ imbalance process defined in (6.5) is assumed to be a random variable with uniformly distributed amplitude imbalance, $\eta \sim \mathcal{U}[\text{-}0.05, 0.05]$, and phase imbalance, $\theta \sim \mathcal{U}[\text{-}5^\circ, 5^\circ]$. Without loss of generality each block consists of 10 N-length OFDM symbols and we used 5000 blocks in the Monte-Carlo realizations. The first symbol of each block is a full pilot symbol. The channel and IQ imbalance is assumed to be constant for a complete block and the HPA NL is assumed to change after 100 blocks and thus an additional pilot sequence is sent to estimate the non-linearity parameters. In these simulation NL parameters are modelled as uniformly-distributed with $p \sim \mathcal{U}[1.5, 2.5]$ and CL$\sim \mathcal{U}[4, 6]$ dB. For each SNR, 50,000 uncoded symbols with 64-QAM modulation have been considered. For implementation of all block transmission systems a structure similar to the IEEE 802.11a system has been considered. For fair comparison the same symbol size of $N = 64$ and CP size of 16 have been chosen for all transmission systems. The bandwidth of the OFDM system is 20 MHz and the subcarrier spacing is 312 kHz. The out-of-band leakage has been filtered out using a bandpass filter which has a cut-off of 3.2 MHz above the bandwidth of the system (see Fig. 6.4).

The BER performance of the different schemes is presented in Fig. 6.3. It can be observed that the performance of a system impaired by IQ imbalance and HPA non-linearity can be improved using the proposed method. The MSE of CIR estimates suffers a floor due to non-linearity. The performance of the proposed scheme is even better when the CIR is fully known and in this case the proposed method can approach the performance of a linear system. The choice of a suitable training sequence can certainly minimize the effect of the NL on the estimation of CIR and imbalance coefficients, which in turn have a severe effect on the overall performance of the system.

The estimation of the SSPA model coefficients is carried out using an optimal sequence which ensures that the effects of the NL are pronounced. The MSE of the parameter estimation is illustrated in Fig. 6.5. The estimation of these

parameters is fairly accurate at high SNR's, but at low SNR the performance of the cost function is effected by additive noise. A plot of the cost function defined in (6.17) is provided in Fig. 6.6 with $p = 2$ and CL=7dB. It must be mentioned that the GS algorithm does not yield high accuracy estimates of the non-linearity coefficients due to the nature of the cost function as illustrated in Fig. 6.6.

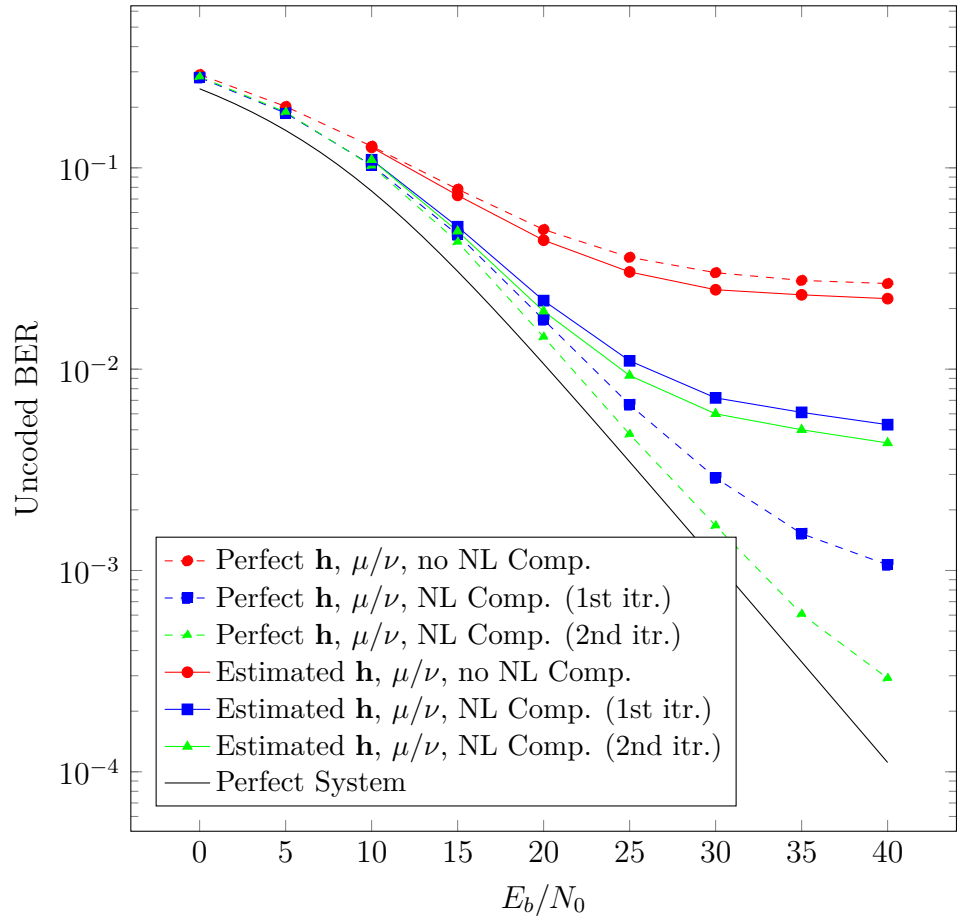

Figure 6.3: BER performance after channel estimation in the presence of IQ imbalance $\eta \sim \mathcal{U}[-0.05, 0.05]$, $\theta \sim \mathcal{U}[-5^\circ, 5^\circ]$, clipping level 5 dB, Rayleigh channel $L_h = 4$ taps, 64-QAM constellation and 50,000 symbols with two iterations of NL compensation.

6.5 Conclusions

The objective of this chapter is to study the estimation of FS CIR in the presence of FI Rx IQ imbalance and amplifier non-linearity. A simple non-iterative

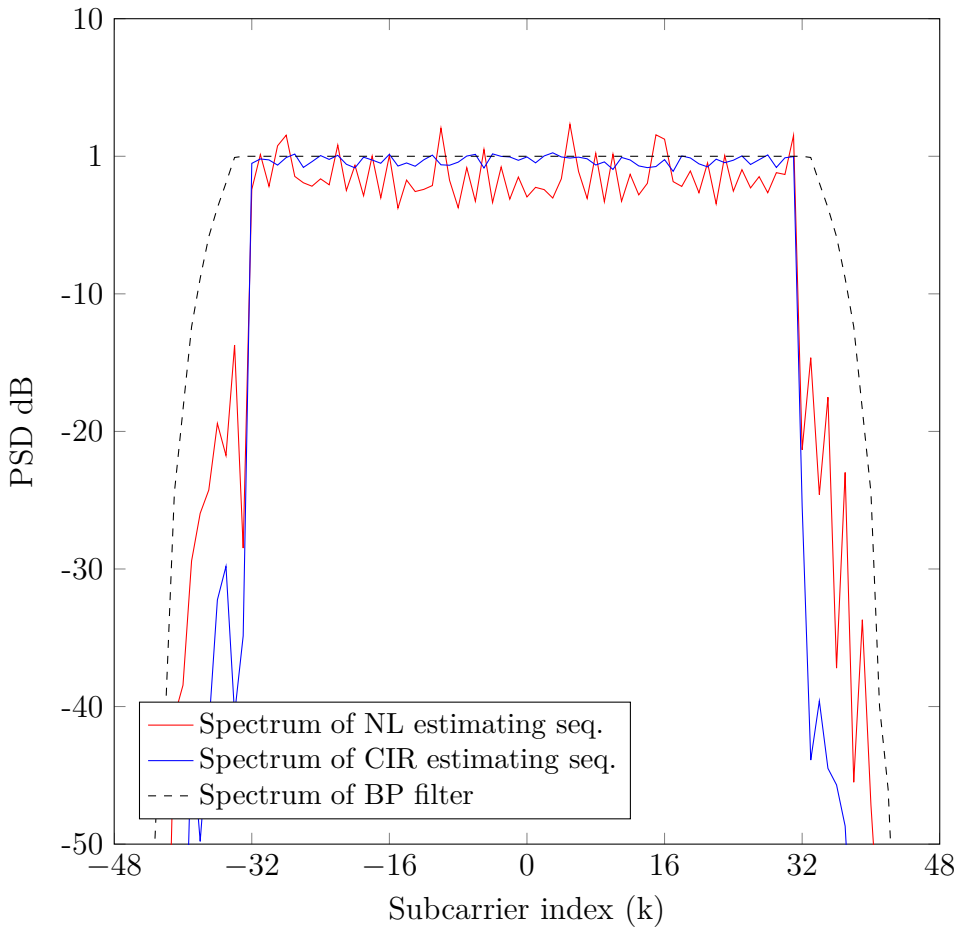

Figure 6.4: Frequency response of Tx bandpass filter. Spectral leakage characteristics of amplifier non-linearity (CL=5dB, $p = 2$) in AWGN channel.

CIR and FI Rx IQ imbalance estimation has been proposed in the presence of the HPA non-linearity with the help of an optimal (known) training sequence. The estimate of transmit amplifier non-linearity has been obtained in addition to the receiver parameters. The simulation results show that this estimation is reasonably accurate in the moderate and high SNR region. Simulations demonstrate that using a suitable training sequence can enhance the performance of the system in the presence of IQ imbalance and moderate clipping effects.

Predistortion is a good solution but the computational overhead required to pre-process the transmitted signal is taxing. As demonstrated in this work, if accurate CIR estimates are available the HPA non-linearity can be conveniently

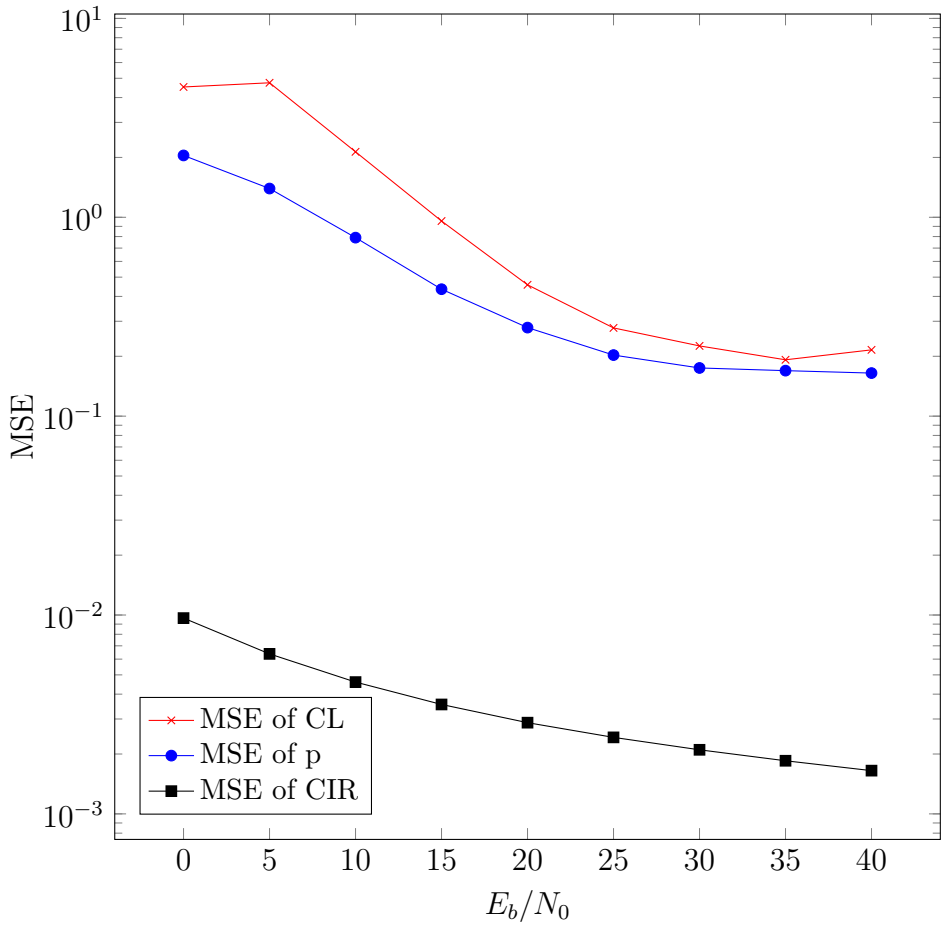

Figure 6.5: MSE performance of CIR and non-linearity parameters (p and CL) estimates.

compensated at the cost of only a few additional FFT operations.

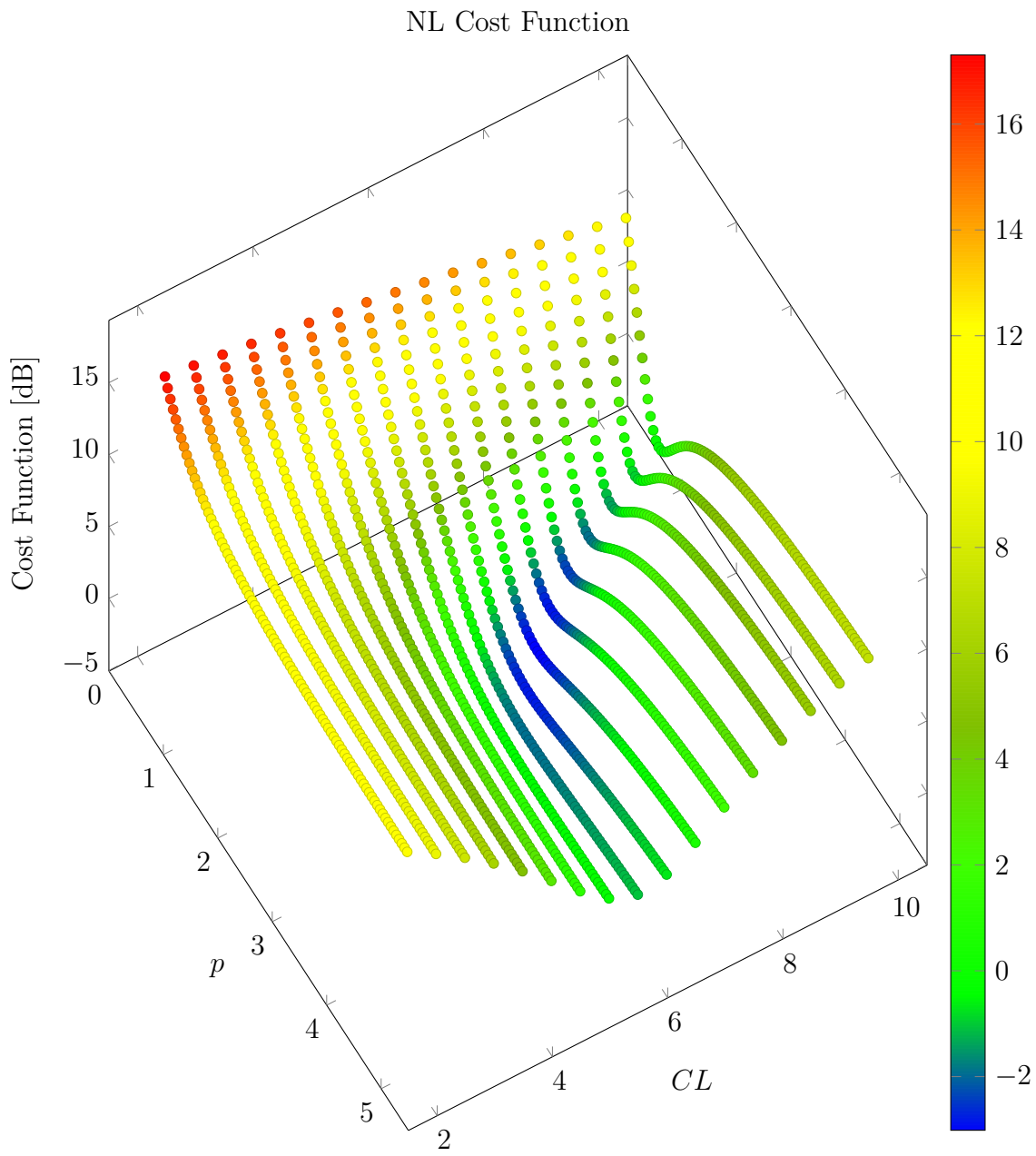

Figure 6.6: Joint estimation of non-linearity parameter p and clipping level (see(6.18)) with (CL=7dB, $p = 2$) for SNR= 25dB.

7

Phase Noise and CIR Estimation in SCUW Systems

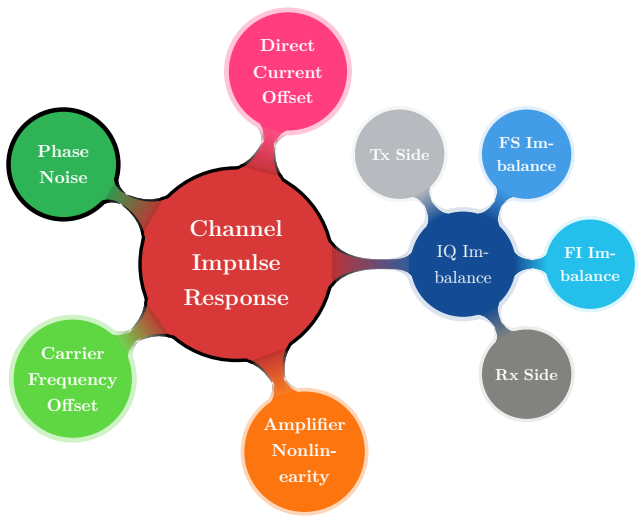

Abstract

The objective of this chapter is to estimate CIR in the presence of a strong PN process. The system under consideration is an SCCP based system. The SCCP scheme has been modified further to transmit a known cyclic prefix (a unique word) such that more knowledge about the PN process can be obtained.

To eliminate the effects of PN from the system several interpolation techniques have been proposed to reconstruct the actual PN process from available pilot samples.

Simulation results show that the performance of an SCCP system with a known cyclic prefix is superior to SCCP systems with conventional compensation schemes in the moderate and higher SNR region for all values of PN.

7.1 Introduction

SCCP has attracted significant attention in recent years. SCCP exploits frequency domain equalization (FDE) to simplify the equalizer complexity[1] (i.e., SCFDE). It finds application in LTE and was proposed as a physical layer interface for fourth generation wireless communication standards [10]. Recent works [11, 12, 92] have revitalized interest in this transmission scheme. SCCP relaxes the limitations of an OFDM system (e.g. peak-to-average power ratio, amplifier non-linearity, etc.) while maintaining low equalizer complexity and a remarkable structure similarity with an OFDM system. The authors in [11,12,26] demonstrate that SCCP offers comparable (and in some scenarios better) BER performance than OFDM transmission systems. It was shown in [93] that maximum multipath diversity and coding gain can be obtained with SCCP.

Now a slight modification in the (unknown) cyclic prefix (CP) concept for a SCCP system is to use a known CP, henceforth called *unique word* (UW). Unlike the CP which is discarded in OFDM and SCCP receivers, the UW can be used to track system parameters. The advantages over OFDM and SCCP systems motivates us to explore the single carrier unique word (SCUW) system further.

The impact of imperfections such as CFO, timing offset, PN and IQ imbalance on OFDM have been studied extensively in recent years. Several schemes have been proposed to mitigate these effects in OFDM for the single and multi-user scenario with space-time coding and spatial multiplexing - see [18, 90] and references therein. However, to the best of our knowledge very little work has been done to mitigate these imperfections in SCCP systems.

The use of a UW (i.e., known CP) ensures cyclic convolution with the wireless CIR and it can also be exploited to estimate timing-offset and CFO. The authors in [94] have used it to compensate residual CFO, while [95] has used a UW to obtain better frame synchronization. The effects of PN on OFDM and SCCP systems have also been compared in [14].

The UW sequences can also be exploited to estimate the CIR , IQ imbalance and the PN process. The use of a UW to ensure circular convolution has been presented in the literature, with the assumption of a slowly time-varying CIR. Under this assumption the UW training provides throughput comparable to OFDM systems along with better timing offset, PN and IQ imbalance cancellation.

[1] In the literature the term SCCP is used sometimes interchangeably with SCFDE (single carrier frequency domain equalization) and SCFDMA (single carrier frequency domain multiple access).

In this chapter the performance of a SCUW system is studied in the presence of PN using the known CP to enhance estimation of the PN process. The proposed scheme is non-iterative and does not incur any additional complexity. In this chapter the estimation of the PN process is done in the time domain and under certain conditions our system outperforms other schemes proposed for OFDM and SCCP systems.

Here the SCUW system is analyzed in a typical downlink scenario where the base station has a high quality LO and the receiver LO is the main source of PN. The chapter is organized as follows. In section 7.2 the system model and the estimation of the CIR in the presence of the PN process is described. Section 7.3 is concerned with the PN estimation, tracking and compensation using pilot bins and the UW. In section 7.4 the performance of SCCP with SCUW systems is compared using Monte-Carlo simulation.

Notation: In addition to previously defined notations $\mathbf{F_1}$ is a unitary DFT matrix of size $N_G \times N_G$.

7.2 Transmission Model

SCCP systems have similar system blocks to OFDM systems - as illustrated in Fig. 7.1. The vector $\mathbf{d}^{(i)}$ (which includes the information bearing data and additional pilots) is combined with a UW. So after appending this UW to the transmitted data block and pilots we have $\mathbf{s}^{(i)} = [s^{(i)}[0], s^{(i)}[1], \cdots, s^{(i)}[N-1], u_1, \cdots, u_G]^T$. The superscript '$i$' refers to the i-th transmitted symbol. This block is then transmitted over a (slowly) time-variant channel. Fig. 7.1 illustrates the SCUW transmission model with equalization and the structure of the transmitted symbols is shown in Fig. 7.2. In contrast to OFDM and SCCP systems the convolution in SCUW can be considered cyclic only if the DFT matrix is of size $N_G \times N_G$, where N_G represents the length of a complete block at the receiver (i.e. data, UW and pilots) as in Fig. 7.2. The UW from the previous symbol ensures cyclic convolution. One of the serious drawback of the proposed scheme is that it yields a non-standard block of transmit symbol $\mathbf{s}^{(i)}$ and is not be compatible with industrial implementation of SCCP systems such as LTE.

In the discrete-time baseband domain the argument of the PN process $e^{j\phi[n]}$ is modelled as a Gauss-Markov process: i.e., $\phi[n] = \phi[n-1] + w[n]$, where $w[n] \sim \mathcal{N}(0, \sigma_w^2)$. The parameter σ_w^2 for the PN process is associated with β_0 (the 3-dB bandwidth of the local oscillator) to give $\sigma_w^2 \approx 2\pi\beta_0 T_s$, where T_s is the symbol duration of length N_G in Fig. 7.2, as defined in [25] and references

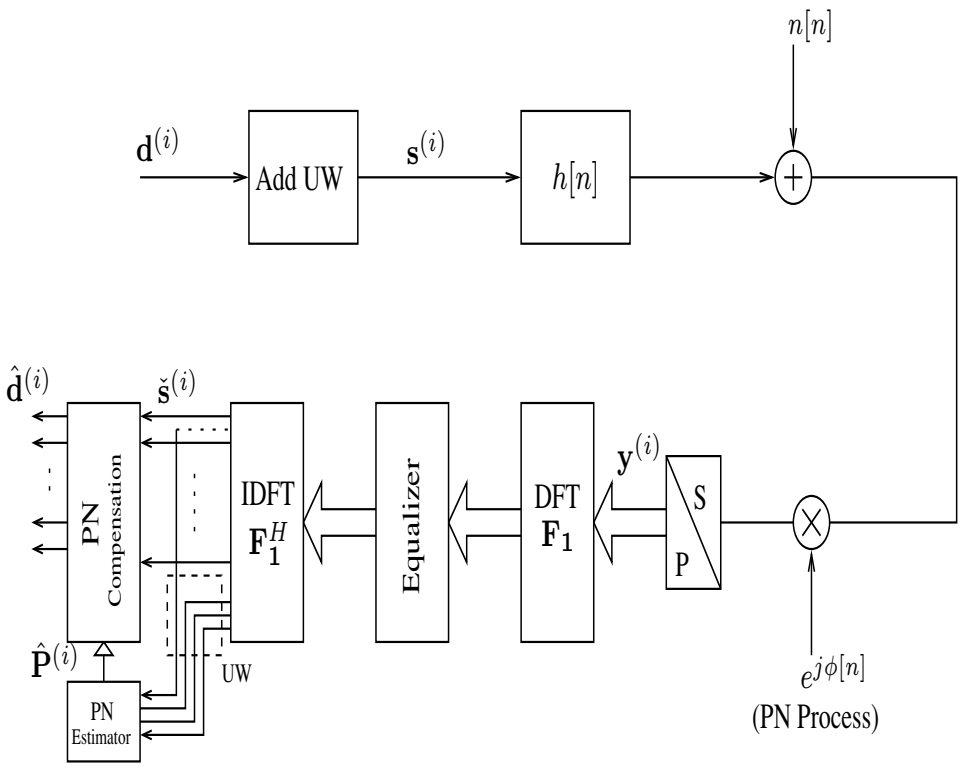

Figure 7.1: Block diagram of a SCUW transmission model.

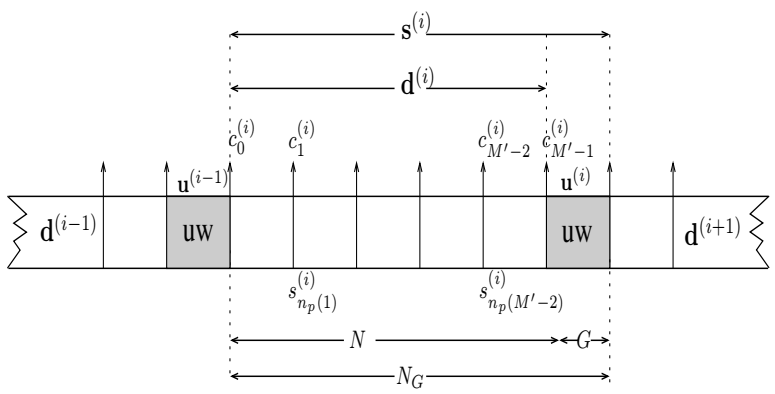

Figure 7.2: Block structure for SCUW, where $c_0^{(i)}, c_1^{(i)}, \ldots, c_{M'-1}^{(i)}$ (not actually transmitted) refer to the $\phi^{(i)}[n]$ values from the PN that are to be estimated and $k_p(1)$ to $k_p(M'-2)$ refer to the positions of the $M'-2$ pilots.

therein. So the received signal vector $\mathbf{y}^{(i)}$ in presence of PN , CIR distortion and AWGN (see Fig. 7.1) can be expressed in vector form as follows:

$$\mathbf{y}^{(i)} = \mathbf{E}^{(i)}\mathbf{H}_c\mathbf{s}^{(i)} + \mathbf{n}^{(i)} \tag{7.1}$$

where $\mathbf{E}^{(i)} = \text{diag}([e^{j\phi^{(i)}[0]}, e^{j\phi^{(i)}[1]}, \ldots, e^{j\phi^{(i)}[N_G-1]}]^T)$ is the diagonal PN matrix; $\mathbf{H}_c$ is the circulant CIR matrix of size $N_G \times N_G$; $\mathbf{s}^{(i)}$ is the $N_G \times 1$ transmitted symbol; and $\mathbf{n}$ a circularly symmetric complex Gaussian noise vector of size $N_G \times 1$, i.e., $\mathbf{n} \sim \mathcal{CN}(\mathbf{0}, \mathbf{I}\sigma_n^2)$. When $i = 0$ we have a full pilot symbol with conventional CP, while the rest of the data symbols are considered to use a UW.

7.2.1 Channel Estimation

To mitigate PN we need to estimate the CIR, $h[n]$, in the presence of PN. CIR estimation in the presence of PN and other effects is a challenging problem and has been considered for OFDM transmission systems in [18,25,90]. An ML estimator is used to determine the PN and CIR using a full-pilot sequence. The conditional probability density function for $\mathbf{y}^{(0)}$ is:

$$p(\mathbf{y}^{(0)}|\mathbf{E}^{(0)}, \mathbf{h}) = \frac{1}{\pi^N}\exp\left\{-\|\mathbf{y}^{(0)} - \mathbf{E}^{(0)}\mathbf{H}_c\mathbf{x}\|^2\right\} \tag{7.2}$$

where $\mathbf{x}$ is a full pilot symbol of size $N \times 1$, $\mathbf{y}^{(0)}$ (i.e. $i = 0$ in (7.1)) is the corresponding received vector, $\mathbf{E}^{(0)}$ and $\mathbf{H}_c$ are respectively the PN and circulant CIR matrices (of size $N \times N$) and $\mathbf{h}$ (first column of $\mathbf{H}_c$) is the unknown CIR vector. Defining $\mathbf{X} = \text{diag}(\mathbf{x})$ and rewriting (7.2) in terms of its log-likelihood function we have

$$\begin{aligned}
\mathcal{L}(\mathbf{y}^{(0)}|\mathbf{E}^{(0)}, \mathbf{h}) &= \log(\pi^N) - \|\mathbf{y}^{(0)} - \mathbf{E}^{(0)}\mathbf{H}_c\mathbf{x}\|^2 \\
&\Rightarrow \hat{\mathbf{h}} = \arg\min_{\mathbf{h}} \|\mathbf{y}^{(0)} - \mathbf{P}^{(0)}\mathbf{X}\mathbf{W}\mathbf{h}\|^2 \qquad (7.3)\\
&\Rightarrow \hat{\mathbf{h}} = \mathcal{E}_s^{-1}\mathbf{W}^H\mathbf{X}^H{\mathbf{P}^{(0)}}^H\mathbf{y}^{(0)} \qquad (7.4)
\end{aligned}$$

where $\mathbf{P}^{(0)}$ is the circulant PN matrix corresponding to a full-pilot symbol (defined as $\mathbf{P}^{(0)} = \mathbf{F}\mathbf{E}^{(0)}\mathbf{F}^H$) and $\mathcal{E}_s$ is the energy of a pilot bin. Substituting $\hat{\mathbf{h}}$ back into (7.3), the estimate for $\mathbf{P}^{(0)}$ now becomes

$$\hat{\mathbf{P}}^{(0)} = \arg\min_{\mathbf{P}^{(0)}} \|\mathbf{y}^{(0)} - \mathbf{P}^{(0)}\mathbf{X}\mathbf{W}\mathbf{W}^H{\mathbf{P}^{(0)}}^H\mathbf{y}^{(0)}\|^2. \tag{7.5}$$

Using the fact that $\mathbf{W}\mathbf{W}^H = \mathbf{I}_N - \mathbf{V}\mathbf{V}^H$ and $\mathbf{y}^{(0)^H}\mathbf{P}^{(0)} = \mathbf{q}\mathbf{Y}^H$ then estimating $\mathbf{q}$ (instead of $\mathbf{P}^{(0)}$) we have

$$\hat{\mathbf{q}} = \arg\min_{\mathbf{q}} \mathbf{q}\mathbf{Y}^H\mathbf{X}\mathbf{V}\mathbf{V}^H\mathbf{X}^H\mathbf{Y}\mathbf{q}^H = \arg\min_{\mathbf{q}} \mathbf{q}\mathbf{M}\mathbf{q}^H \tag{7.6}$$

where $\mathbf{q}$ is a row vector (the first row of $\mathbf{P}^{(0)}$) and the n-th element of $\mathbf{q}$ is defined as $q[n] = 1/N\sum_{k=0}^{N-1} e^{j\phi[k]}e^{-j2\pi nk/N}, n = 0, 1, \cdots, N-1$ [18]. Also $\mathbf{Y}$ is the circulant matrix whose first column is $\mathbf{y}^{(0)}$. Then we assume small $|\phi[k]|$ so $e^{j\phi[k]} \approx 1 + j\phi[k]$ and the dc component is $q[0] = 1/N\sum_{k=0}^{N-1} e^{j\phi[k]} \approx 1 + j/N\sum_{k=0}^{N-1}\phi[k]$. So adding the constraint (real($q[0]$) = 1) to (7.6) (to avoid the trivial solution) we get

$$\hat{\mathbf{q}} = \arg\min_{\mathbf{q}} \mathbf{q}\mathbf{M}\mathbf{q}^H - \lambda(\mathbf{e}\mathbf{q}^{I^T} - 1). \tag{7.7}$$

The solution to this constrained optimization problem is given in [25] as:

$$\begin{aligned}\hat{\mathbf{q}}^{I^T} &= \mathbf{\Gamma}^{-1}\mathbf{\Upsilon}^T\hat{\mathbf{q}}^{Q^T} + \lambda\mathbf{\Gamma}^{-1}\mathbf{e}^T \\ \hat{\mathbf{q}}^{Q^T} &= \lambda\mathbf{\Delta}\mathbf{e}^T\end{aligned} \tag{7.8}$$

where $\hat{\mathbf{q}}^I$ and $\hat{\mathbf{q}}^Q$ are the real and imaginary components respectively of $\hat{\mathbf{q}}$, $\mathbf{e}$ is a $(1 \times N)$ row vector with its first entry one and the rest are zero. In addition

$$\lambda = \frac{1}{\mathbf{e}[\mathbf{\Gamma}^{-1}\mathbf{\Upsilon}^T\mathbf{\Delta} + \mathbf{\Gamma}^{-1}]\mathbf{e}^T} \tag{7.9}$$

where $\mathbf{M} = \mathbf{\Gamma} + j\mathbf{\Upsilon}$ and $\mathbf{\Delta} = [\mathbf{I}_N + (\mathbf{\Gamma}^{-1}\mathbf{\Upsilon})^2]^{-1}\mathbf{\Gamma}^{-1}\mathbf{\Upsilon}\mathbf{\Gamma}^{-1}$.

The estimate of $\hat{\mathbf{q}}$ from (7.8) can be used to reconstruct the circulant matrix $\hat{\mathbf{P}}^{(0)}$ and then used to estimate the CIR in (7.4). Using the fact that the PN is a low-pass process [17] only a few components $\hat{q}[n]$ with $\hat{q}[N-D], \ldots, \hat{q}[N-1], \hat{q}[0], \ldots, \hat{q}[D]$ are used to construct $\hat{\mathbf{P}}^{(0)}$. In this implementation $D = 2$.

7.2.2 Channel Equalization

At the receiver, zero forcing (ZF), decision feedback (DF) or MMSE equalizers can be employed for frequency domain equalization. Let us first consider a ZF equalizer for simplicity and illustration of the basic principle. So, the receiver

after frequency domain equalization yields (see also Fig. 7.1 and [14])

$$\check{\mathbf{s}}^{(i)} = \mathbf{F}_{\mathbf{1}}^{H} \mathbf{\Lambda}_{\hat{h}}^{-1} \mathbf{F}_{\mathbf{1}} \mathbf{y}^{(i)} \tag{7.10}$$

where $\check{\mathbf{s}}^{(i)}$ is the received vector after CIR equalization and $\mathbf{\Lambda}_{\hat{h}}$ is the diagonal matrix of the estimated CFR. Now since $\mathbf{H}_c = \mathbf{F}_{\mathbf{1}}^{H} \mathbf{\Lambda}_h \mathbf{F}_{\mathbf{1}}$ and $\mathbf{P}^{(i)} = \mathbf{F}_{\mathbf{1}} \mathbf{E}^{(i)} \mathbf{F}_{\mathbf{1}}^{H}$, then from (7.1) and (7.10) we can write

$$\check{\mathbf{s}}^{(i)} = \mathbf{F}_{\mathbf{1}}^{H} \mathbf{\Lambda}_{\hat{h}}^{-1} \mathbf{P}^{(i)} \mathbf{\Lambda}_h \mathbf{F}_{\mathbf{1}} \mathbf{s}^{(i)} + \mathbf{z}^{(i)}. \tag{7.11}$$

The matrix $\mathbf{P}^{(i)}$ can be further defined as

$$\mathbf{P}_{n,k}^{(i)} = \begin{cases} \frac{1}{N_G} \sum_{r=0}^{N_G-1} e^{j\phi^{(i)}[r]}, & \text{for} \quad n = k \\ \frac{1}{N_G} \sum_{r=0}^{N_G-1} e^{j(\phi^{(i)}[r] - \frac{2\pi}{N}[n-k]r)}, & \text{for} \quad n \neq k \end{cases}$$

$$\Rightarrow \mathbf{P}^{(i)} = p_0^{(i)} \mathbf{I}_{N_G} + \mathbf{P}_{\text{ICI}}^{(i)} \tag{7.12}$$

where $p_0^{(i)} \mathbf{I}_{N_G}$ is the main diagonal component referred to as the CPR and $\mathbf{P}_{\text{ICI}}^{(i)}$ is the off-diagonal component referred to as the ICI. Then from (7.11) and (7.12) we have

$$\check{\mathbf{s}}^{(i)} = \mathbf{F}_{\mathbf{1}}^{H} \left[\mathbf{\Lambda}_{\hat{h}}^{-1} \{ p_0^{(i)} \mathbf{I}_{N_G} + \mathbf{P}_{\text{ICI}}^{(i)} \} \mathbf{\Lambda}_h \right] \mathbf{F}_{\mathbf{1}} \mathbf{s}^{(i)} + \mathbf{z}^{(i)}. \tag{7.13}$$

The magnitude of the off-diagonal components of $\mathbf{P}_{\text{ICI}}^{(i)}$ is directly related to σ_w^2 in the PN model. From simulations it is evident that the term $\mathbf{\Lambda}_{\hat{h}}^{-1} \mathbf{P}_{\text{ICI}}^{(i)} \mathbf{\Lambda}_h$ is approximately circulant when $\mathbf{P}_{\text{ICI}}^{(i)}$ is a sparse circulant matrix. Although it is not possible to obtain the off-diagonal components of the matrix $\mathbf{\Lambda}_{\hat{h}}^{-1} \mathbf{P}_{\text{ICI}}^{(i)} \mathbf{\Lambda}_h$, the impact of these terms on the PN process estimation depends on SNR and channel estimation accuracy. For moderate SNR and accurate channel estimation, these non-diagonal terms can be considered as an additional noise. So by defining a new noise term $\tilde{\mathbf{z}}$, the term $\mathbf{F}_{\mathbf{1}}^{H} \mathbf{\Lambda}_{\hat{h}}^{-1} \mathbf{P}_{\text{ICI}}^{(i)} \mathbf{\Lambda}_h \mathbf{F}_{\mathbf{1}}$ can be expressed approximately as a diagonal matrix $\tilde{\mathbf{P}}_{\text{ICI}}^{(i)}$ to get:

$$\check{\mathbf{s}}^{(i)} \approx (p_0^{(i)} \mathbf{I}_{N_G} + \tilde{\mathbf{P}}_{\text{ICI}}^{(i)}) \mathbf{s}^{(i)} + \tilde{\mathbf{z}}^{(i)} \tag{7.14}$$

and the objective is now to estimate the diagonal matrix $p_0^{(i)} \mathbf{I}_{N_G} + \tilde{\mathbf{P}}_{\text{ICI}}^{(i)}$. At the receiver the PN process can be estimated from the pilot elements and the UW sequence present in $\check{\mathbf{s}}^{(i)}$.

7.3 PN Mitigation and Data Detection

In the previous section we estimated the FS CIR in the presence of PN using the full pilot symbol and then obtained the relationship between the estimate $\check{\mathbf{s}}^{(i)}$ and the transmitted $\mathbf{s}^{(i)}$. In this section we present the PN estimation and compensation mechanism for $\check{\mathbf{s}}^{(i)}$. The estimates of the PN process are obtained through $\check{\mathbf{s}}^{(i)}$ by using the pilot bins inserted in the data symbols and the UW training sequence - see Fig. 7.2. The argument of the estimated PN is defined as $\hat{\mathbf{c}}^{(i)} = [\hat{c}_0^i, \cdots, \hat{c}_{M'-1}^{(i)}]^T = [\hat{\phi}^{(i)}(0), \hat{\phi}^{(i)}(k_p(1)), \ldots, \hat{\phi}^{(i)}(k_p(M'-2)), \hat{\phi}^{(i)}(N-1)]^T$. The initial and final values of the PN process within a symbol are essential for enhancing the estimation performance. It can be shown that PN estimates at the edges of the symbol are obtained through adjacent UW's as

$$\begin{aligned} \hat{c}_0^{(i)} &= \arg\left\{\sum_{k=1}^{G} a_k \check{u}_k^{(i-1)} u_k^{(i-1)*}\right\} \\ \hat{c}_{M'-1}^{(i)} &= \arg\left\{\sum_{k=1}^{G} b_k \check{u}_k^{i} u_k^{i*}\right\} \end{aligned} \tag{7.15}$$

where $\check{u}_k^{(i)}$ is the k-th element of the received UW sample from $\check{\mathbf{s}}^{(i)}$ in (7.14), $u_k^{(i)}$ is from the transmitted word and a_k and b_k are weighting coefficients defined in Table 7.1. These coefficients ensure that recent phase samples are weighted differently. The remaining PN estimates $\hat{c}_1^{(i)}, \ldots, \hat{c}_{M'-2}^{(i)}$ are obtained from the pilot bins as

$$\hat{c}_m^{(i)} = \arg\{\check{s}_{k_p(m)}^i s_{k_p(m)}^{i*}\}, \quad m = 1, 2, \ldots, M'-2 \tag{7.16}$$

where $\check{\mathbf{s}}^{(i)}$ is the received vector from (7.14) and $\{k_p(m)\}_{m=1}^{M'-2}$ represent the indices of the pilot positions within $\check{\mathbf{s}}^{(i)}$ (see Fig. 7.2).

7.3.1 Simple CPR Compensation

In many PN compensation techniques, only the CPR term $p_0^{(i)}$ is compensated in (7.14) while considering the ICI components $\tilde{\mathbf{P}}_{\text{ICI}}^{(i)}$ as additive noise. It can be seen that an estimate of $p_0^{(i)}$ in (7.14) may be obtained by

$$\hat{p}_0^{(i)} = \frac{1}{M'} \sum_{m=0}^{M'-1} \hat{c}_m^{(i)}. \tag{7.17}$$

This scheme does not require storage of past or future symbols. The PN compensation matrix based on the CPR estimate in (7.17) is defined as

$$\boldsymbol{\vartheta}^{(i)} = \exp(-j\hat{p}_0^{(i)})\mathbf{I}_N. \tag{7.18}$$

7.3.2 CPR Based Interpolation

The CPE estimate obtained in (7.17) can be used to provide linear interpolation to estimate the unknown values with the following $N + N_g$ values

$$\hat{\phi}[k] = \frac{1}{N+G}\begin{bmatrix}3N/2+G-k & k-N/2\end{bmatrix}\begin{bmatrix}\hat{p}_0^{(i)} \\ \hat{p}_0^{(i+1)}\end{bmatrix} \tag{7.19}$$
$$N/2 \leq k \leq 3N/2+G-1.$$

These N+G values map directly onto the N+G estimates for the PN across two symbols: $\hat{\boldsymbol{\phi}} = [\hat{\phi}^{(i)}[\frac{N}{2}], \hat{\phi}^{(i)}[\frac{N}{2}+1], \cdots, \hat{\phi}^{(i)}[N+G-1], \hat{\phi}^{(i+1)}[0], \hat{\phi}^{(i+1)}[1], \cdots, \hat{\phi}^{(i+1)}[\frac{N}{2}-1]]$, (see Fig. 7.5). The PN estimates for i-th symbol depend on the CPR estimates for the $(i-1)$ and $(i+1)$ symbols. So the compensation matrix based on CPR interpolation is defined as

$$\boldsymbol{\vartheta}^{(i)} = \text{diag}(\exp(-j[\hat{\phi}^{(i)}[0], \hat{\phi}^{(i)}[1], \ldots, \hat{\phi}^{(i)}[N-1]])). \tag{7.20}$$

7.3.3 Linear Interpolation

In contrast to the above mentioned schemes a symbol-wise linear interpolation to estimate both $p_0^{(i)}$ and $\tilde{\mathbf{P}}_{\text{ICI}}^{(i)}$ is considered in (7.14). The PN process can be approximated by a linear interpolator $\boldsymbol{\Theta}$ defined in (7.23). Through linear interpolation, the PN samples are estimated as

$$\boldsymbol{\psi}^{(i)} = \boldsymbol{\Theta}\hat{\mathbf{c}}^{(i)} \tag{7.21}$$

where $\boldsymbol{\psi}^{(i)} = [\hat{\phi}^{(i)}[0], \ldots, \hat{\phi}^{(i)}[N-1]]^T$ is the vector of the interpolated PN estimates and $\hat{\mathbf{c}}^{(i)}$ is obtained from (7.15) and (7.16). The compensation matrix obtained through linear interpolation is defined as

$$\boldsymbol{\vartheta}^{(i)} = \text{diag}(\exp(-j\boldsymbol{\psi}^{(i)})). \tag{7.22}$$

This scheme does not require storage of past or future symbols, thus reducing complexity in contrast to CPR interpolation schemes.

$$\mathbf{\Theta}_{k,m} = \begin{cases} m-(k-1)\frac{M'-1}{N-1}, & \text{if} \quad \frac{(m-1)(N-1)}{M'-1} \leq k-1 < \frac{m(N-1)}{M'-1} \\ \frac{(k-1)(M'-1)}{N-1} - (m-2), & \text{if} \quad \frac{(m-2)(N-1)}{M'-1} \leq k-1 < \frac{(m-1)(N-1)}{M'-1} \\ 0 \quad \text{, otherwise} \end{cases} \tag{7.23}$$

(M' is the number of interpolation points and $0 \leq m \leq M'-1$. N is the number of interpolated points and $0 \leq k \leq N-1$.)

7.3.4 Data Detection

To estimate data MMSE equalization is considered as it provides better BER performance in the low SNR region. The MMSE channel equalization is performed as follows:

$$\check{\mathbf{s}}^{(i)} = \mathbf{F}_{\mathbf{1}}^{H} \left([\mathbf{\Lambda}_{\hat{h}} \mathbf{\Lambda}_{\hat{h}}^{H} + \mathbf{I}_{N_G} \sigma_z^2]^{-1} \mathbf{\Lambda}_{\hat{h}}^{H} \right) \mathbf{F}_{\mathbf{1}} \mathbf{y}^{(i)}. \tag{7.24}$$

The $N \times 1$ data sequence $\mathbf{d}$ can be estimated in the following manner

$$\hat{\mathbf{d}}^{(i)} = \boldsymbol{\vartheta}^{(i)} \mathbf{\Pi}^{-1} \check{\mathbf{s}}^{(i)} \tag{7.25}$$

where $\boldsymbol{\vartheta}^{(i)}$ is the PN compensation matrix using either (7.18), (7.20) or (7.22) and $\mathbf{\Pi}^{-1}$ is the appropriate UW removal matrix of size $N \times N_G$.

7.4 Simulation Results

This section presents the BER performance of both the SCUW and the SCCP schemes in the presence of a moderate PN process. The simulations are based on Rayleigh fading process with a channel memory of L_h=4 taps and an exponential power delay profile $e^{-\underline{\gamma} l}$ with $\underline{\gamma}$=0.2 and l=$0, 1, \ldots, L_h-1$ is considered. The 3-dB bandwidth of the PN process is taken as $\beta_0 = 1000$ Hz. Without loss of generality each block consists of 10 N_G-length symbols and 2000 blocks are used in the Monte-Carlo realizations. The first symbol of each block is a full pilot symbol. The channel is assumed to be constant for a complete block. The pilot bins in the data sequence and the UW sequence are chosen from a BPSK constellation.

For implementation of all block transmission systems a structure similar to the IEEE 802.11a system is considered for all methods. For fair comparison the same symbol size of $N = 64$ and UW size of $N_g = 16$ has been chosen for all transmission systems. The four pilot bins are inserted at equi-spaced positions.

For the linear interpolation of PN process as discussed in 7.3.3 the interpolation samples (M') is assumed to be M'=6.

The BER performance of the different schemes is presented in Fig. 7.3. It can be observed that the performance of the SCUW schemes is similar to SCCP at low SNR because as the noise power increases, the estimate $\hat{\mathbf{c}}$ of the PN samples is not reliable. At low SNR, the SCUW (CPR interp. and CPE-only) schemes are preferable. The performance of SCUW with CPR interpolation improves at higher SNR. The performance of SCUW (CPR interp.) is better than SCCP (CPR interp.) at SNRs greater than 15 dB.

The performance of these schemes has also been simulated in Fig. 7.4 against different values of β_0, the 3-dB bandwidth of the PN process. The SCUW system always performs marginally better than SCCP, while the CPR-only scheme has a similar performance. It is of interest to note that the performance of SCUW (CPR only) of (7.18) is similar to SCCP (CPR interp.) of (7.20) in all scenarios.

Finally, Fig. 7.5 illustrates how (7.20) (with SCUW and SCCP), (7.18) (with estimate $\hat{p}_0^{(i)}$), (7.22) and (7.23) (using $\mathbf{\Theta}$) perform in tracking $\phi^{(i)}[n]$ from the PN, $e^{j\phi^{(i)}[n]}$. As expected, SCUW with and without the CPR interpolation scheme gives a reasonable performance in tracking the true $\phi^{(i)}[n]$.

7.5 Conclusions

This chapter focused on estimation of the channel and PN process in SCUW. Simple CPR and ICI mitigation schemes have been devised for SCCP systems using an interpolated PN process with the help of a known training sequence. It is demonstrated that the performance of SCUW is better than conventional SCCP at typical values of PN bandwidth. The known training sequence can also be used to jointly estimate other system parameters such as IQ imbalance, CFO, CIR and timing offsets. Finally, the design of optimal training sequences which can simultaneously estimate all these parameters is an open question.

Table 7.1: Scaling coefficients a_k used in (7.15) where $b_k = a_{G-(k-1)}$

k	1...4	5...7	8...10	11...13	14...16
a_k	0	0.017	0.05	0.1	0.17

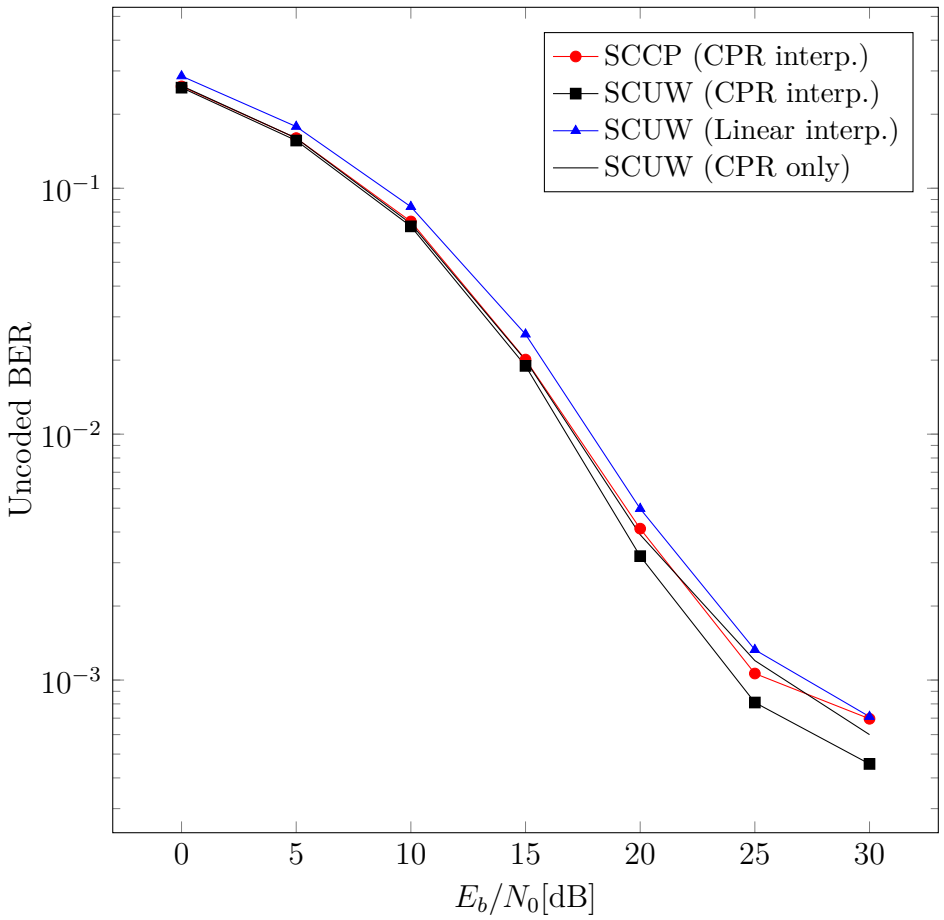

Figure 7.3: Performance of PN compensation schemes, $\beta_0 = 1000$Hz, Rayleigh channel $L_h = 4$ taps, 16-QAM constellation and 20,000 symbols. SCCP and SCUW (CPR interp.) refer to (7.20) while SCUW (linear interp.) refers to (7.22) and SCUW (CPR only) refers to (7.18).

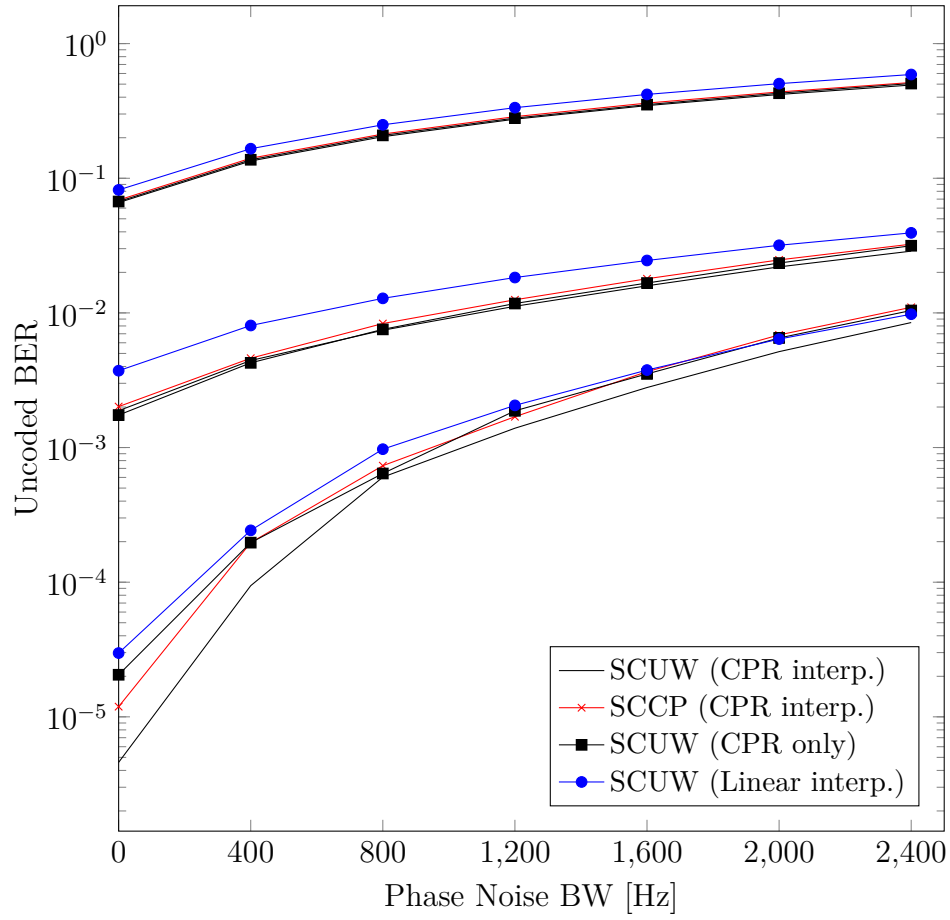

Figure 7.4: BER performance of the received data sequence after PN compensation and channel equalization, Rayleigh channel $L_h = 4$ taps, $\beta_0 = 0, \ldots, 2400$Hz and SNR=$10, 20, 30$dB.

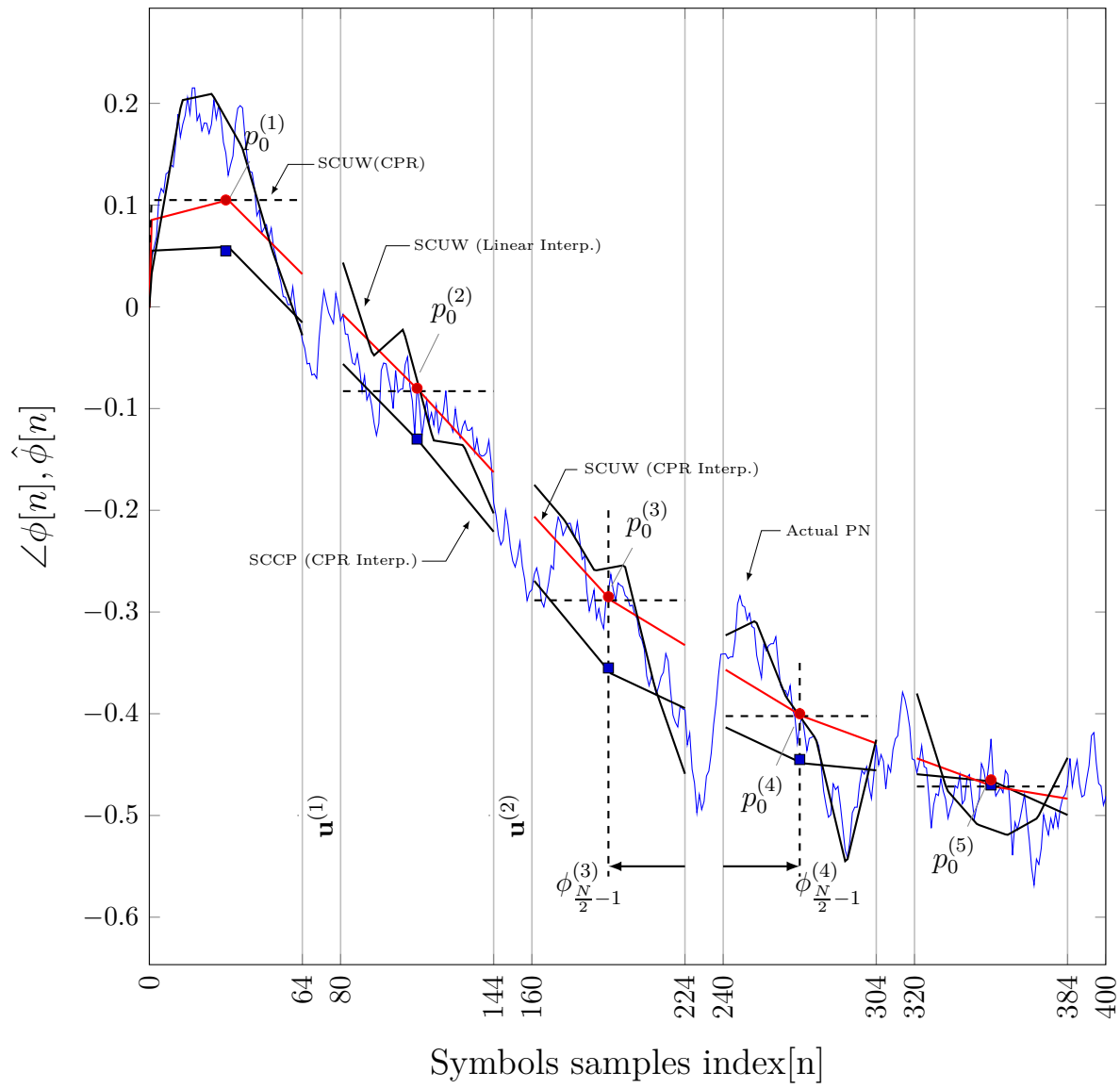

Figure 7.5: PN estimation (using either interpolation or just CPR estimates) over 5 symbols, $\beta_0 = 1000$ Hz and SNR=35dB.

8 Conclusion & Future Work

8.1 Conclusions

In this work we have studied mitigation of the transmitter and the receiver imperfections present in the direct conversion devices. The objective is to estimate the FS CIR in conjunction with these non-idealities.

Chapter 3 considers a simple low complexity joint estimation of FS CIR and FI Tx/Rx IQ imbalance using a linear model of the system in the presence of these impairments. Chapter 4 is based on joint estimation of FS CIR, FI/FS Rx IQ imbalance in the presence of CFO and DCO. Chapter 5 extends the work of chapter 3 to include CFO estimation in the system model. Chapter 6 considers joint estimation of FS CIR and FI Rx IQ imbalance in the presence of amplifier non-linearity. Finally, chapter 7 considers estimation of FS CIR in the presence of strong PN process by trying to exploit a known unique word which is appended at the start of every data symbol as a cyclic prefix. All of the proposed solutions conform to the specifications laid down by IEEE 802.11 standard but these schemes can also be applied to any given multi-carrier transmission system.

Several optimal and sub-optimal schemes have been proposed for joint estimation of FS CIR in conjunction with FI/FS Tx/Rx IQ imbalance, CFO, DCO, amplifier non-linearity and PN. The proposed schemes have been shown to yield near optimal BER performance even in the presence of severely impaired RF front-ends.

It can be said that the proposed solutions encompass many of the typical problems experienced by a multi-carrier system in the presence of direct conversion devices. But a robust solution which can approach near ideal performance in the presence of PN is still illusive.

The semi-blind estimation of the FS CIR in MIMO-OFDM systems in the presence of PN process was also studied but these results are not discussed in this thesis because the computational complexity and resulting performance do not strike a balance which may be of any practical use. Estimation of CFO and FI IQ imbalance was also considered in TV channels although the performance of the studied scheme was unacceptable but this problem can be approached with different techniques.

8.2 Future Work

The problems of joint estimation techniques can be extended further to consider more parameters such as timing/phase offset. A few more considerations are as follows.

Hardware implementation

Within the scope of this thesis all the work has been considered through Matlab simulations. Due to time constraints, hardware implementation of the proposed scheme could not be carried out. The performance of these schemes in practical systems should be assessed in future.

Joint FI/FS Tx/Rx IQ Imbalance, FS CIR, CFO and DCO Estimation

After having found low complexity solutions which can jointly estimation FI/FS Rx IQ imbalance in the presence of other impairments (in chapter 4), it is possible to extend these techniques to include the FI/FS Tx IQ imbalance in the model and find the CLFE solution to estimate all the unknowns with minimal complexity and training.

PN Mitigation

As shown in chapter 3,4 and 5 the estimation of CIR, IQ mismatch, DCO and CFO can be carrierd out very effectively. In the presence of PN process the number of unknown coefficients is too large to be estimated. The state-of-art solutions available in the literature perform adequate compensation of CPR. The BER performance of PN process can be improved further if higher-order components of PN process can be estimated.

5G standard

More recently the research on standardization of fifth generation (5G) modulation schemes is under way. The filter bank multi-carrier (FBMC) technique is amongst many possible multi-carrier transmission schemes which have been considered. It would be of great interest to study the effects of transceiver non-idealities on MFB transmission schemes.

Time-varying channels

Although mobility is an important parameter of mobile wireless communication systems, this problem has not been considered within the scope of this work. It would be interesting to explore the estimation of TV channels in the presence of transceiver impairments. The problems of mobility and impairments have been studied for OFDM in [96] and for an SCCP system in [86], but better solutions can be found through frequency domain interpolation or basis expansion model.

Massive MIMO Systems

Massive MIMO systems have attracted significant attention in recent years. These systems can operate at higher through-put rates but the effects of front-end imperfections has not been studied so far in literature and it would be useful to assess the performance bounds of large scale systems in the presence of front-end imperfections.

A DCR with CFO and IQ imbalance

The following derivation provides the input/output relation between the transmitted and received signal when receiver is under the influence of FS/FI IQ imbalance and CFO is also present in the system as illustrated in the Fig. 4.1. The overall received signal after the DC receiver can be defined as

$$y(t) = \mu r(t) e^{j\Delta\omega t} + \nu r^*(t) e^{-j\Delta\omega t}. \tag{A.1}$$

Looking at the Fig. 4.1 , the real and imaginary components of the received signal can be defined as

$$y^I(t) = (1+\eta)\Big([(r^I(t)\cos\omega_c t - r^Q(t)\sin\omega_c t)]\cos(\omega_c t - \Delta\omega t + \theta)\Big) \otimes g^I(t) \tag{A.2}$$

$$y^Q(t) = -(1-\eta)\Big([(r^I\cos\omega_c t - r^Q(t)\sin\omega_c t)]\sin(\omega_c t - \Delta\omega t - \theta)\Big) \otimes g^Q(t). \tag{A.3}$$

Through straight-forward calculation (A.2) and (A.3) can be simplified to

$$\begin{aligned} y^I(t) &= (1+\eta)\cos(\Delta\omega t - \theta) r^I(t) \otimes g^I(t) - (1+\eta)\sin(\Delta\omega t - \theta) r^Q(t) \otimes g^I(t) \\ y^Q(t) &= (1-\eta)\sin(\Delta\omega t + \theta) r^I(t) \otimes g^Q(t) + (1-\eta)\cos(\Delta\omega t + \theta) r^Q(t) \otimes g^Q(t). \end{aligned} \tag{A.4}$$

Rewriting (A.4) in terms of $r(t)$ and $r^*(t)$ we find

$$\begin{aligned} y^I(t) = (1+\eta)\Big[&(\cos\Delta\omega t\cos\theta + \sin\Delta\omega t\sin\theta)\Big(\frac{r(t)+r^*(t)}{2}\Big) \otimes g^I(t) \\ &+ j(\sin\Delta\omega t\cos\theta - \cos\Delta\omega\sin\theta)\Big(\frac{r(t)-r^*(t)}{2}\Big) \otimes g^I(t)\Big] \qquad \text{(A.5)} \\ y^Q(t) = (1-\eta)\Big[&(\sin\Delta\omega t\cos\theta + \cos\Delta\omega t\sin\theta)\Big(\frac{r(t)+r^*(t)}{2}\Big) \otimes g^Q(t) \\ &- j(\cos\Delta\omega t\cos\theta - \sin\Delta\omega t\sin\theta)\Big(\frac{r(t)-r^*(t)}{2}\Big) \otimes g^I(t)\Big]. \qquad \text{(A.6)} \end{aligned}$$

Since $y(t) = y^I(t) + jy^Q(t)$, then

$$\begin{aligned} y(t) = (1+\eta)&\Big[(\cos\Delta\omega t\cos\theta + \sin\Delta\omega t\sin\theta) + j(\sin\Delta\omega t\cos\theta - \cos\Delta\omega t\sin\theta)\Big] r(t) \otimes g^I(t) \\ &+ j(1-\eta)\Big[(\sin\Delta\omega t\cos\theta + \cos\Delta\omega t\sin\theta) - j(\cos\Delta\omega t\cos\theta - \sin\Delta\omega t\sin\theta)\Big] r(t) \otimes g^Q(t) \\ &+ (1+\eta)\Big[(\cos\Delta\omega t\cos\theta + \sin\Delta\omega t\sin\theta) - j(\sin\Delta\omega t\cos\theta - \cos\Delta\omega t\sin\theta)\Big] r^*(t) \otimes g^I(t) \\ &+ j(1-\eta)\Big[(\sin\Delta\omega t\cos\theta + \cos\Delta\omega t\sin\theta) + j(\cos\Delta\omega t\cos\theta - \sin\Delta\omega t\sin\theta)\Big] r^*(t) \otimes g^Q(t). \end{aligned} \qquad \text{(A.7)}$$

After further simplification and grouping the terms together we can write

$$\begin{aligned} y = \cos\Delta\omega t\Big(&\cos\theta \cdot g^I(t) - j\sin\theta g^I(t) + \eta\cos\theta g^I(t) - j\eta\sin\theta g^I(t) \\ &+ j\sin\theta g^Q(t) + \cos\theta g^Q(t) - j\eta\sin\theta \cdot g^Q(t) - \eta\cos\theta g^Q(t)\Big) \otimes r(t) \\ + j\sin\Delta\omega t\ \Big(&- j\sin\theta g^I(t) + j\cos\theta g^I(t) - j\eta\sin\theta g^I(t) + \eta\cos\theta g^I(t) \\ &+ \cos\theta g^Q(t) + j\sin\theta g^Q(t) - j\eta\cos\theta g^Q(t) - j\eta\sin\theta g^Q(t)\Big) \otimes r(t) \\ + \cos\Delta\omega t\ \Big(&\cos\theta \cdot g^I(t) + j\sin\theta g^I(t) + \eta\cos\theta g^I(t) + j\eta\sin\theta g^I(t) \\ &+ j\sin\theta g^Q(t) - \cos\theta g^Q(t) - j\eta\sin\theta \cdot g^Q(t) + \eta\cos\theta g^Q(t)\Big) \otimes r * (t) \\ - j\sin\Delta\omega t\ \Big(&j\sin\theta g^I(t) + \cos\theta g^I(t) + j\eta\sin\theta g^I(t) + \eta\cos\theta g^I(t) \\ &- \cos\theta g^Q(t) + j\sin\theta g^Q(t) + \eta\cos\theta g^Q(t) - j\eta\sin\theta g^Q(t)\Big) \otimes r^*(t). \end{aligned} \qquad \text{(A.8)}$$

Finally we can write

$$\begin{aligned} y =& e^{j\Delta\omega t}\Big[(\cos\theta - j\eta\sin\theta)\Big(\frac{g^I(t)+g^Q(t)}{2}\Big) + (\eta\cos\theta - j\sin\theta)\Big(\frac{g^I(t)-g^Q(t)}{2}\Big]\otimes r(t) \\ &+ e^{-j\Delta\omega t}\Big[(\cos\theta + j\eta\sin\theta)\Big(\frac{g^I(t)-g^Q(t)}{2}\Big) + (\eta\cos\theta + j\sin\theta)\Big(\frac{g^I(t)-g^Q(t)}{2}\Big)\Big]\otimes r^*(t). \end{aligned} \tag{A.9}$$

Through (2.45) and (2.47), the model defined in (A.9) can be expanded to encompass the FS/FI Tx IQ imbalance also, but this scenario is not treated in this work.

References

[1] M. Windisch and G. Fettweis, "Standard-independent I/Q imbalance compensation in OFDM direct-conversion receivers," in *Proc. 9th Intl. OFDM Workshop (InOWo)*, pp. 57–61, Citeseer, 2004. xvii, 18

[2] B. Razavi, *Fundamentals of Microelectronics*. Wiley, 2008. xvii, 16, 18, 31

[3] R. Hartley, "Relations of carrier and side-bands in radio transmission," *Proceedings of the Institute of Radio Engineers*, vol. 11, no. 1, pp. 34–56, 1923. 1, 18, 34

[4] T. Rappaport, *Wireless communications: principles and practice*. Prentice Hall communications engineering and emerging technologies series, Prentice Hall PTR, 1996. 9, 10

[5] P. Hoeher, "A statistical discrete-time model for the WSSUS multipath channel," *Vehicular Technology, IEEE Transactions on*, vol. 41, no. 4, pp. 461–468, 1992. 10

[6] J. A. C. Bingham, "Multicarrier modulation for data transmission: an idea whose time has come," *Communications Magazine, IEEE*, vol. 28, no. 5, pp. 5–14, 1990. 12

[7] A. Bahai and B. Saltzberg, *Multi-carrier Digital Communications: Theory and Applications of OFDM*. Information Technology Series, Kluwer Academic/Plenum, 1999. 12

[8] L. Hanzo and T. Keller, *OFDM and MC-CDMA: A Primer*. Wiley, 2006. 12

[9] G. Strang, *Linear Algebra and Its Applications*. Thomson, Brooks/Cole, 2006. 14

[10] D. Falconer, S. Ariyavisitakul, A. Benyamin-Seeyar, and B. Eidson, "Frequency Domain Equalization for Single-Carrier Broadband Wireless Systems," *Communications Magazine, IEEE*, vol. 40, pp. 58 –66, Apr. 2002. 15, 112

[11] Z. Wang, X. Ma, and G. Giannakis, "OFDM or single-carrier block transmissions?," *Communications, IEEE Transactions on*, vol. 52, pp. 380 – 394, Mar. 2004. 15, 112

[12] F. Pancaldi, G. Vitetta, R. Kalbasi, N. Al-Dhahir, M. Uysal, and H. Mheidat, "Single-carrier frequency domain equalization," *Signal Processing Magazine, IEEE*, vol. 25, pp. 37 –56, Sep. 2008. 15, 112

[13] F. Horlin and A. Bourdoux, "Comparison of the sensitivity of OFDM and SC-FDE to CFO, SCO and IQ imbalance," in *Communications, Control and Signal Processing, 2008. ISCCSP 2008. 3rd International Symposium on*, pp. 111–116, 2008. 15

[14] J. Zamorano, J. Nsenga, W. Van Thillo, A. Bourdoux, and F. Horlin, "Impact of Phase Noise on OFDM and SC-CP," in *Global Telecommunications Conference, 2007. GLOBECOM '07. IEEE*, pp. 3822 –3825, 2007. 16, 112, 117

[15] B. Razavi, "Design considerations for direct-conversion receivers," *Circuits and Systems II: Analog and Digital Signal Processing, IEEE Transactions on*, vol. 44, no. 6, pp. 428–435, 1997. 18, 34

[16] V. Syrjala and M. Valkama, "Receiver DSP for OFDM Systems Impaired by Transmitter and Receiver Phase Noise," in *Communications (ICC), 2011 IEEE International Conference on*, pp. 1–6, 2011. 18

[17] P. Robertson and S. Kaiser, "Analysis of the effects of phase-noise in orthogonal frequency division multiplex (OFDM) systems," in *Communications, 1995. ICC '95 Seattle, 'Gateway to Globalization', 1995 IEEE International Conference on*, vol. 3, pp. 1652 –1657 vol.3, Jun. 1995. 19, 37, 116

[18] Q. Zou, A. Tarighat, and A. Sayed, "Joint compensation of IQ imbalance and phase noise in OFDM wireless systems," *Communications, IEEE Transactions on*, vol. 57, no. 2, pp. 404 –414, 2009. 20, 38, 60, 69, 82, 89, 112, 115, 116

[19] A. Demir, A. Mehrotra, and J. Roychowdhury, "Phase noise in oscillators: a unifying theory and numerical methods for characterisation," in *Design Automation Conference, 1998. Proceedings*, pp. 26 – 31, Jun. 1998. 20

[20] W. Robins, *Phase Noise in Signal Sources: (Theory and Applications)*. IEE Telecommunications Series, Peregrinus, 1982. 20

[21] E. Rubiola, *Phase Noise and Frequency Stability in Oscillators*. Cambridge books online, Cambridge University Press, 2009. 20

[22] A. Garcia Armada and M. Calvo Ramon, "Rapid prototyping of a test modem for terrestrial broadcasting of digital television," *Consumer Electronics, IEEE Transactions on*, vol. 43, pp. 1100 –1109, Nov. 1997. 21, 37

[23] Q. Zou, A. Tarighat, and A. Sayed, "Compensation of Phase Noise in OFDM Wireless Systems," *Signal Processing, IEEE Transactions on*, vol. 55, no. 11, pp. 5407–5424, 2007. 22

[24] P. Rabiei, W. Namgoong, and N. Al-Dhahir, "Efficient Pilot-Aided Digital Baseband Compensation of Phase Noise ICI in OFDM Receivers," pp. 1 –5, Nov. 2009. 22

[25] P. Rabiei, W. Namgoong, and N. Al-Dhahir, "A Non-Iterative Technique for Phase Noise ICI Mitigation in Packet-Based OFDM Systems," *Signal Processing, IEEE Transactions on*, vol. 58, pp. 5945 –5950, Nov. 2010. 22, 100, 113, 115, 116

[26] P. Horlin and A. Bourdoux, *Digital Compensation for Analog Front-Ends: A New Approach to Wireless Transceiver Design*. Wiley, 2008. 24, 45, 56, 80, 112

[27] E. Tsui and J. Lin, "Adaptive IQ imbalance correction for OFDM systems with frequency and timing offsets," in *Global Telecommunications Conference, 2004. GLOBECOM '04. IEEE*, vol. 6, pp. 4004 – 4010 Vol.6, Nov. 2004. 24, 28, 35, 36, 44, 54, 78

[28] G. Xing, M. Shen, and H. Liu, "Frequency offset and I/Q imbalance compensation for direct-conversion receivers," *Wireless Communications, IEEE Transactions on*, vol. 4, pp. 673 – 680, Mar. 2005. 24, 36, 54, 58, 68, 80

[29] T. Schenk, P. Smulders, and E. Fledderus, "Estimation and compensation of TX and RX IQ imbalance in OFDM-based MIMO systems," in *Radio and Wireless Symposium, 2006 IEEE*, pp. 215 – 218, Jan. 2006. 24, 28, 35, 36

[30] C.-J. Hsu, R. Cheng, and W.-H. Sheen, "Joint Least Squares Estimation of Frequency, DC Offset, I-Q Imbalance, and Channel in MIMO Receivers," *Vehicular Technology, IEEE Transactions on*, vol. 58, pp. 2201 –2213, Jun. 2009. 28

[31] E. Lopez-Estraviz, S. De Rore, F. Horlin, and L. Van der Perre, "Optimal training sequences for joint channel and frequency-dependent IQ imbalance estimation in OFDM-based receivers," in *Communications, 2006. ICC '06. IEEE International Conference on*, vol. 10, pp. 4595 –4600, Jun. 2006. 28, 36, 45, 51, 54, 68, 80, 89

[32] D. Tandur and M. Moonen, "Digital Compensation of RF Imperfections for Broadband Wireless Systems," in *Communications and Vehicular Technology in the Benelux, 2007 14th IEEE Symposium on*, pp. 1 –5, Nov. 2007. 28, 35, 36, 44, 54, 63, 68, 69, 78, 80

[33] X. Cai, Y.-C. Wu, H. Lin, and K. Yamashita, "Estimation and Compensation of CFO and I/Q Imbalance in OFDM Systems Under Timing Ambiguity," *Vehicular Technology, IEEE Transactions on*, vol. 60, no. 3, pp. 1200–1205, 2011. 28, 37

[34] E. Lopez-Estraviz, S. De Rore, F. Horlin, and A. Bourdoux, "Pilot design for Joint Channel and Frequency-Dependent Transmit/Receive IQ Imbalance Estimation and Compensation in OFDM-Based Transceivers," in *Communications, 2007. ICC '07. IEEE International Conference on*, pp. 4861–4866, 2007. 28, 36, 45, 51, 80

[35] I.-H. Sohn, E.-R. Jeong, and Y. H. Lee, "Data-aided approach to I/Q mismatch and DC offset compensation in communication receivers," *Communications Letters, IEEE*, vol. 6, no. 12, pp. 547–549, 2002. 31, 36, 55, 68

[36] G.-T. Gil, I.-H. Sohn, J.-K. Park, and Y. H. Lee, "Joint ML estimation of carrier frequency, channel, I/Q mismatch, and DC offset in communication receivers," *Vehicular Technology, IEEE Transactions on*, vol. 54, no. 1, pp. 338–349, 2005. 31, 36

[37] H.-Y. Tseng, W.-J. Cho, T.-K. Chang, S.-M. Phoong, and Y.-P. Lin, "Compensation of IQ Imbalance and DC Offset for OFDM Transmission over Frequency Selective Channels," in *Communications, 2008. ICC '08. IEEE International Conference on*, pp. 641–645, 2008. 31, 36, 55, 68

[38] C. Rapp., "Effects of HPA-nonlinearity on a 4-DPSK/OFDM-signal for a digitial sound broadcasting system," in *Proceedings of the Second European Conference on Satellite Communications , Liege, Belgium*, pp. 179-184, Oct. 1991. 32, 98

[39] A. Saleh, "Frequency-Independent and Frequency-Dependent Nonlinear Models of TWT Amplifiers," *Communications, IEEE Transactions on*, vol. 29, pp. 1715 – 1720, Nov. 1981. 32, 98

[40] D. Schreurs, *RF Power Amplifier Behavioral Modeling*. The Cambridge RF and Microwave Engineering Series, Cambridge University Press, 2008. 32

[41] H. Shafiee and S. Fouladifard, "Calibration of IQ imbalance in OFDM transceivers," in *Communications, 2003. ICC '03. IEEE International Conference on*, vol. 3, pp. 2081 – 2085 vol.3, May 2003. 35, 44

[42] Y. Egashira, Y. Tanabe, and K. Sato, "A Novel IQ Imbalance Compensation Method with Pilot-Signals for OFDM System," in *Vehicular Technology Conference, 2006. VTC-2006 Fall. 2006 IEEE 64th*, pp. 1–5, 2006. 35

[43] A. Tarighat, R. Bagheri, and A. Sayed, "Compensation schemes and performance analysis of IQ imbalances in OFDM receivers," *Signal Processing, IEEE Transactions on*, vol. 53, pp. 3257 – 3268, Aug. 2005. 35, 44, 54, 56, 63, 69

[44] A. Tarighat and A. Sayed, "Joint compensation of transmitter and receiver impairments in OFDM systems," *Wireless Communications, IEEE Transactions on*, vol. 6, no. 1, pp. 240–247, 2007. 35, 36, 44, 51, 78, 89

[45] R. K. McPherson and J. Schroeder, "Frequency-selective I/Q imbalance compensation for OFDM receivers using decision-feedback adaptive filtering," in *Signals, Systems and Computers (ASILOMAR), 2012 Conference Record of the Forty Sixth Asilomar Conference on*, pp. 188–192, IEEE, 2012. 35

[46] D. Tandur and M. Moonen, "Joint adaptive compensation of transmitter and receiver IQ imbalance Under Carrier Frequency Offset in OFDM-Based Systems," *Signal Processing, IEEE Transactions on*, vol. 55, no. 11, pp. 5246–5252, Nov. 35, 37

[47] S. Fouladifard and H. Shafiee, "Frequency offset estimation in OFDM systems in the presence of IQ imbalance," in *Communications, 2003. ICC '03. IEEE International Conference on*, vol. 3, pp. 2071–2075 vol.3, 2003. 36, 78

[48] J. Tubbax, A. Fort, L. Van der Perre, S. Donnay, M. Engels, M. Moonen, and H. De Man, "Joint compensation of IQ imbalance and frequency offset in OFDM systems," in *Global Telecommunications Conference, 2003. GLOBECOM '03. IEEE*, vol. 4, pp. 2365 – 2369 vol.4, Dec. 2003. 36, 62, 78

[49] Y.-H. Chung, K.-D. Wu, and S.-M. Phoong, "Joint estimation of I/Q imbalance, CFO and channel response for OFDM systems," in *Acoustics, Speech and Signal Processing, 2009. ICASSP 2009. IEEE International Conference on*, pp. 2573–2576, 2009. 36, 62, 72

[50] Y. Chung and S. Phoong, "Joint estimation of I/Q imbalance, CFO and channel response for MIMO OFDM systems," *Communications, IEEE Transactions on*, vol. 58, pp. 1485 –1492, May 2010. 36, 37, 54, 62, 69, 79

[51] D. Tandur, C.-Y. Lee, and M. Moonen, "Efficient compensation of RF impairments for OFDM systems," in *Wireless Communications and Networking Conference, 2009. WCNC 2009. IEEE*, pp. 1 –6, Apr. 2009. 37

[52] S. De Rore, E. Lopez-Estraviz, F. Horlin, and L. Van der Perre, "Joint estimation of carrier frequency offset and IQ imbalance for 4G mobile wireless systems," in *Communications, 2006. ICC '06. IEEE International Conference on*, vol. 5, pp. 2066–2071, 2006. 37

[53] J. Luo, W. Keusgen, and A. Kortke, "Preamble Based Joint CFO, Frequency-Selective I/Q-Imbalance and Channel Estimation and Compensation in MIMO OFDM Systems," in *Vehicular Technology Conference (VTC Fall), 2011 IEEE*, pp. 1–5, 2011. 37

[54] M. Morelli and M. Moretti, "Carrier Frequency Offset Estimation for OFDM Direct-Conversion Receivers," *Wireless Communications, IEEE Transactions on*, vol. 11, no. 7, pp. 2670–2679, 2012. 37

[55] M. Valkama, M. Renfors, and V. Koivunen, "Compensation of frequency-selective i/q imbalances in wideband receivers: models and algorithms," in *Wireless Communications, 2001.(SPAWC'01). 2001 IEEE Third Workshop on Signal Processing Advances in*, pp. 42–45, IEEE, 2001. 37

[56] M. Valkama, M. Renfors, and V. Koivunen, "Blind signal estimation in conjugate signal models with application to I/Q imbalance compensation," *Signal Processing Letters, IEEE*, vol. 12, no. 11, pp. 733–736, 2005. 37

[57] L. Anttila, M. Valkama, and M. Renfors, "Circularity-Based I/Q Imbalance Compensation in Wideband Direct-Conversion Receivers," *Vehicular Technology, IEEE Transactions on*, vol. 57, no. 4, pp. 2099–2113, 2008. 37, 45, 79

[58] J. de Witt and G.-J. Van Rooyen, "A Blind I/Q Imbalance Compensation Technique for Direct-Conversion Digital Radio Transceivers," *Vehicular Technology, IEEE Transactions on*, vol. 58, no. 4, pp. 2077–2082, 2009. 37, 45, 79

[59] H. Steendam, M. Moeneclaey, and H. Sari, "The effect of carrier phase jitter on the performance of orthogonal frequency-division multiple-access systems," *Communications, IEEE Transactions on*, vol. 46, pp. 456 –459, Apr. 1998. 37

[60] S. Wu and Y. Bar-Ness, "A phase noise suppression algorithm for OFDM-based WLANs," *Communications Letters, IEEE*, vol. 6, pp. 535 – 537, Dec. 2002. 37

[61] D. Petrovic, W. Rave, and G. Fettweis, "Performance degradation of coded-OFDM due to phase noise," in *Vehicular Technology Conference, 2003. VTC 2003-Spring. The 57th IEEE Semiannual*, vol. 2, pp. 1168 – 1172 vol.2, Apr. 2003. 37

[62] D. Petrovic, W. Rave, and G. Fettweis, "Effects of Phase Noise on OFDM Systems With and Without PLL: Characterization and Compensation," *Communications, IEEE Transactions on*, vol. 55, pp. 1607 –1616, Aug. 2007. 37

[63] D. Petrovic, W. Rave, and G. Fettweis, "Limits of Phase Noise Suppression in OFDM," in *Wireless Conference 2005 - Next Generation Wireless and Mobile Communications and Services (European Wireless), 11th European*, pp. 1–6, 2005. 38

[64] S. Bittner, A. Frotzscher, G. Fettweis, and E. Deng, "Oscillator Phase Noise compensation using Kalman tracking," in *Acoustics, Speech and Signal Processing, 2009. ICASSP 2009. IEEE International Conference on*, pp. 2529–2532, 2009. 38

[65] G. Fettweis, M. Lohning, D. Petrovic, M. Windisch, P. Zillmann, and W. Rave, "Dirty RF: a new paradigm," in *Personal, Indoor and Mobile Radio Communications, 2005. PIMRC 2005. IEEE 16th International Symposium on*, vol. 4, pp. 2347–2355 Vol. 4, 2005. 38

[66] P. Rabiei, W. Namgoong, and N. Al-Dhahir, "Reduced-Complexity Joint Baseband Compensation of Phase Noise and I/Q Imbalance for MIMO-OFDM Systems," *Wireless Communications, IEEE Transactions on*, vol. 9, pp. 3450 –3460, Nov. 2010. 38

[67] P. Rabiei, W. Namgoong, and N. Al-Dhahir, "A Non-Iterative Technique for Phase Noise ICI Mitigation in Packet-Based OFDM Systems," *Signal Processing, IEEE Transactions on*, vol. 58, pp. 5945 –5950, Nov. 2010. 38

[68] J. Tellado, L. Hoo, and J. Cioffi, "Maximum-likelihood detection of nonlinearly distorted multicarrier symbols by iterative decoding," *Communications, IEEE Transactions on*, vol. 51, pp. 218 – 228, Feb. 2003. 38, 39, 96, 97

[69] D. Kim and G. Stuber, "Clipping noise mitigation for OFDM by decision-aided reconstruction ," *Communications Letters, IEEE*, vol. 3, pp. 4 –6, jan 1999. 38, 96, 97

[70] Y. Xiao, S. Li, X. Lei, and Y. Tang, "Clipping noise mitigation for channel estimation in OFDM systems," *Communications Letters, IEEE*, vol. 10, no. 6, pp. 474–476, 2006. 38, 39

[71] K. Wesolowski and J. Pochmara, "Efficient algorithm for adjustment of adaptive predistorter in OFDM transmitter," in *Vehicular Technology Conference, 2000. IEEE-VTS Fall VTC 2000. 52nd*, vol. 5, pp. 2491–2496 vol.5, 2000. 39

[72] A. Saleh and J. Salz, "Adaptive linearization of power amplifiers in digital radio systems," *The Bell System Technical Journal*, vol. 62, no. 4, pp. 1019–1033, 1983. 39

[73] G. Karam and H. Sari, "A data predistortion technique with memory for QAM radio systems," *Communications, IEEE Transactions on*, vol. 39, no. 2, pp. 336–344, 1991. 39

[74] A. D'Andrea, V. Lottici, and R. Reggiannini, "RF power amplifier linearization through amplitude and phase predistortion," *Communications, IEEE Transactions on*, vol. 44, pp. 1477 –1484, Nov. 1996. 39

[75] H. Chen and A. Haimovich, "Iterative estimation and cancellation of clipping noise for ofdm signals," *Communications Letters, IEEE*, vol. 7, no. 7, pp. 305–307, 2003. 39

[76] F. Peng and W. Ryan, "New approaches to clipped OFDM channels: modeling and receiver design," in *Global Telecommunications Conference, 2005. GLOBECOM '05. IEEE*, vol. 3, pp. 5 pp.–, 2005. 39

[77] J. Tubbax, B. Come, L. Van der Perre, S. Donnay, M. Engles, and C. Desset, "Joint compensation of IQ imbalance and phase noise," in *Vehicular Technology Conference, 2003. VTC 2003-Spring. The 57th IEEE Semiannual*, vol. 3, pp. 1605 – 1609 vol.3, Apr. 2003. 44

[78] P. H. Moose, "A technique for orthogonal frequency division multiplexing frequency offset correction," *Communications, IEEE Transactions on*, vol. 42, no. 10, pp. 2908–2914, Oct 1994. 59, 71, 81, 89, 90

[79] H. Zhou, A. Malipatil, and Y.-F. Huang, "OFDM Carrier Synchronization Based on Time-Domain Channel Estimates," *Wireless Communications, IEEE Transactions on*, vol. 7, no. 8, pp. 2988–2999, Aug. 2008. 69, 71, 73, 90

[80] S. M. Kay, *Fundamentals of Statistical signal processing, Volume 2: Detection theory*. Prentice Hall PTR, 1998. 70, 73, 89, 91, 92, 93

[81] I. Barhumi, G. Leus, and M. Moonen, "Optimal training design for MIMO OFDM systems in mobile wireless channels," *Signal Processing, IEEE Transactions on*, vol. 51, no. 6, pp. 1615–1624, 2003. 69

[82] H. Minn and N. Al-Dhahir, "Optimal training signals for MIMO OFDM channel estimation," *Wireless Communications, IEEE Transactions on*, vol. 5, no. 5, pp. 1158–1168, 2006. 69

[83] Y. Chung and S. Phoong, "OFDM channel estimation in the presence of transmitter and receiver I/Q imbalance," in *European Signal Processing Conference*, 2008. 79

[84] Y. Chung and S. Phoong, "Estimation of Frequency Selective I/Q Imbalance and CFO for OFDM Systems," in *Asia-Pacific Signal and Information Processing Association, Annual Summit and Conference*, pp. 692 – 695, Oct. 2009. 79

[85] J. Feigin and D. Brady, "Joint Transmitter/Receiver I/Q Imbalance Compensation for Direct Conversion OFDM in Packet-Switched Multipath Environments," *Signal Processing, IEEE Transactions on*, vol. 57, no. 11, pp. 4588–4593, 2009. 79

[86] S. Narayanan, B. Narasimhan, and N. Al-Dhahir, "Baseband estimation and compensation of joint TX/RX I/Q imbalance in SC-FDE transceivers," in *Information Sciences and Systems, 2009. CISS 2009. 43rd Annual Conference on*, pp. 551–556, 2009. 89, 127

[87] A. D'Andrea, V. Lottici, and R. Reggiannini, "Nonlinear predistortion of OFDM signals over frequency-selective fading channels," *Communications, IEEE Transactions on*, vol. 49, pp. 837 –843, May 2001. 96

[88] T. Jiang and Y. Wu, "An Overview: Peak-to-Average Power Ratio Reduction Techniques for OFDM Signals," *Broadcasting, IEEE Transactions on*, vol. 54, pp. 257 –268, Jun. 2008. 96

[89] N. Ermolova and O. Tirkkonen, "Analysis of joint effect of nonlinear amplification and I/Q imbalance in OFDM transmission," in *Personal Indoor and Mobile Radio Communications (PIMRC), 2010 IEEE 21st International Symposium on*, pp. 656 –661, Sept. 2010. 96

[90] D. D. Lin, R. Pacheco, T. J. Lim, and D. Hatzinakos, "Joint estimation of channel response, frequency offset, and phase noise in OFDM," *Signal Processing, IEEE Transactions on*, vol. 54, pp. 3542 –3554, Sept. 2006. 100, 112, 115

[91] C. Dehos and T. Schenk, "Digital Compensation of Amplifier Nonlinearities in the Receiver of a Wireless System," in *Communications and Vehicular Technology in the Benelux, 2007 14th IEEE Symposium on*, pp. 1 –6, Nov. 2007. 102

[92] N. Benvenuto, R. Dinis, D. Falconer, and S. Tomasin, "Single Carrier Modulation With Nonlinear Frequency Domain Equalization: An Idea Whose Time Has Come Again," *Proceedings of the IEEE*, vol. 98, pp. 69 –96, Jan. 2010. 112

[93] M. Ghogho, V. Gil-Jimenez, and A. Swami, "Multipath Diversity and Coding Gains of Cyclic-prefixed Single Carrier Systems," in *Acoustics, Speech and Signal Processing, 2009. ICASSP 2009. IEEE International Conference on*, pp. 2837 –2840, Apr. 2009. 112

[94] M. Huemer, H. Witschnig, and J. Hausner, "Unique Word based Phase Tracking Algorithms for SC/FDE-systems," in *Global Telecommunications Conference, 2003. GLOBECOM '03. IEEE*, vol. 1, pp. 70 – 74, Dec. 2003. 112

[95] L. Deneire, B. Gyselinckx, and M. Engels, "Training sequence versus cyclic prefix-a new look on single carrier communication," *Communications Letters, IEEE*, vol. 5, pp. 292 –294, Jul. 2001. 112

[96] B. Narasimhan, D. Wang, S. Narayanan, H. Minn, and N. Al-Dhahir, "Digital Compensation of Frequency-Dependent Joint Tx/Rx I/Q Imbalance in OFDM Systems Under High Mobility," *Selected Topics in Signal Processing, IEEE Journal of*, vol. 3, no. 3, pp. 405–417, 2009. 127